

**NPS ARCHIVE**  
**1969**  
**DAVIS, G.**

MEASUREMENT OF AIR TEMPERATURE AND WIND VE-  
LOCITY FROM ONE TO EIGHTY CENTIMETERS ABOVE  
THE SEA SURFACE

by

Gary Malcolm Davis



# United States Naval Postgraduate School



## THE SIS

MEASUREMENT OF AIR TEMPERATURE AND WIND VELOCITY  
FROM  
ONE TO EIGHTY CENTIMETERS ABOVE THE SEA SURFACE

by

Gary Malcolm Davis

T132716

October 1969

*This document has been approved for public re-  
lease and sale; its distribution is unlimited.*

LIBRARY  
NAVAL POSTGRADUATE SCHOOL  
MONTEREY, CALIF. 93940

Measurement of Air Temperature and Wind Velocity  
from  
One to Eighty Centimeters Above the Sea Surface

by

Gary Malcolm Davis  
Lieutenant (junior grade), United States Navy  
B.M.E., Auburn University, 1968

Submitted in partial fulfillment of the  
requirements for the degree of

MASTER OF SCIENCE IN OCEANOGRAPHY

from the

NAVAL POSTGRADUATE SCHOOL  
October 1969

NPS 11/11/58  
1969  
DAVIS, G

ABSTRACT

A wave following mechanism was designed and tested at the field station operated by the Institute of Oceanography of the University of British Columbia.

Separate measurements were made of temperature and velocity fluctuations by sensors attached to the vertically moving follower arm at heights of 1 cm, 5 cm, 24 cm, and 78 cm above the sea surface. These data were analyzed both by analog and digital methods. While the data generally follow the  $-5/3$  power law proposed by Kolmogorov, there are significant departures from existing theories which could prove important.

Since most air-sea interactions take place below 30 cm and few measurements have been made below this level, the wave follower could be a useful tool in investigating near surface phenomena.

# TABLE OF CONTENTS

DUDLEY KNOX LIBRARY  
NAVAL POSTGRADUATE SCHOOL  
MONTEREY, CA 93943-5101

I.	INTRODUCTION-----	9
II.	REVIEW OF PREVIOUS WORK-----	10
III.	OBJECT-----	14
IV.	THE FIELD SITE-----	15
V.	WAVE FOLLOWING MECHANISM-----	21
	A. WAVE SENSOR DESIGN-----	22
	B. ARM ASSEMBLY-----	25
	C. SERVO MOTOR AND AMPLIFIER-----	28
	D. TESTING-----	30
VI.	SENSOR MECHANISM-----	35
	A. TEMPERATURE SENSORS-----	35
	B. VELOCITY SENSORS-----	42
	C. RECORDING-----	43
VII.	STATISTICAL ANALYSIS-----	45
	A. DIGITAL ANALYSIS-----	45
	B. ANALOG ANALYSIS-----	48
VIII.	DATA-----	51
	A. CASE 1-----	51
	B. CASE 2-----	57
	C. CASE 3-----	61
	D. CASE 4-----	64
	E. CASE 5-----	64
	F. CASE 6-----	74
	G. CASE 7-----	82

H. CASE 8----- 83

I. CASE 9----- 94

IX. CONCLUSIONS AND AREAS FOR FUTURE WORK----- 101

BIBLIOGRAPHY----- 104

INITIAL DISTRIBUTION LIST----- 106

FORM DD 1473----- 109



## LIST OF FIGURES

Figure	Page
1. Streamline Configurations	12
2. Location of Site	16
3a. Instrumentation Mast - Front View	17
3b. Instrumentation Mast - Side View	18
4. Experimentation Site	20
5. Wave Potentiometer Circuit	23
6a. Follower Probe and Support	24
6b. Follower Error Circuit	26
7. Wave Follower - Mast Assembly	27
8. Servo-Amplifier	29
9. Simulator Test of Follower	32
10. Strobe Analysis of Follower	34
11. Sensor Placement	36
12. Thermistors	37
13. Thermistor Response Characteristics	39
14. Thermistor Circuit	40
15. Thermistor Calibration	41
16. Hot-Film Anemometer Calibration	44
17. Flow Chart - Analog/Digital Method	47
18. Flow Chart - Analog Method	49
19. Case 1 - Sample Record	53
20. Case 1 - Sea Surface Elevation Spectrum	54
21. Case 1 - High Floating Thermistor Spectrum	55

Figure	Page
22. Case 1 - High Fixed Thermistor Spectrum	56
23. Case 1 - Coherence Between Waves and High Floating Thermistors	58
24. Case 1 - Coherence Between Waves and High Fixed Thermistors	59
25. Case 1 - Coherence Between High Floating and High Fixed Thermistors	60
26. Case 2 - Sample Record	62
27. Case 3 - Sample Record	63
28. Case 4 - Sample Record	65
29. Case 5 - Sample Record	67
30. Case 5 - Sea Surface Elevation Spectrum	68
31. Case 5 - High Floating Velocity Spectrum	69
32. Case 5 - High Fixed Velocity Spectrum	70
33. Case 5 - Coherence Between Waves and High Floating Velocity	71
34. Case 5 - Coherence Between Waves and High Fixed Velocity	72
35. Case 5 - Coherence Between High Fixed and High Floating Velocity	73
36. Case 6 - Sample Record	75
37. Case 6 - Sea Surface Elevation Spectrum	76
38. Case 6 - High Floating Velocity Spectrum	77
39. Case 6 - Intermediate Floating Velocity Spectrum	78
40. Case 6 - Coherence Between Waves and High Floating Velocity	79
41. Case 6 - Coherence Between Waves and Intermediate Floating Velocity	80
42. Case 6 - Coherence Between High Floating and Intermediate Floating Velocity	81

Figure	Page
43. Case 7 - Sample Record	84
44. Case 7a - Sea Surface Elevation Spectrum	85
45. Case 7a - Intermediate Floating Velocity Spectrum	86
46. Case 7a - Coherence Between Waves and Intermediate Floating Velocity	87
47. Case 7b - Sea Surface Elevation Spectrum	88
48. Case 7b - Intermediate Floating Velocity Spectrum	89
49. Case 7b - Coherence Between Waves and Intermediate Floating Velocity	90
50. Case 7c - Sea Surface Elevation Spectrum	91
51. Case 7c - Intermediate Floating Velocity Spectrum	92
52. Case 7c - Coherence Between Waves and Intermediate Floating Velocity	93
53. Case 8 - Sample Record	95
54. Case 8 - Sea Surface Elevation Spectrum	96
55. Case 8 - Low Floating Velocity Spectrum	97
56. Case 8 - Coherence Between Waves and Low Floating Velocity	98
57. Case 9 - Sample Record	100

## ACKNOWLEDGEMENTS

The author gratefully wishes to express his appreciation to his two thesis advisors, Professor Noel E. J. Boston and Professor Theodore Green, III. Professor Green originally conceived the idea of the wave follower mechanism and presented the problem to the author. Professor Boston assisted in all phases of research both in Monterey, California, and in Vancouver, British Columbia, Canada. Professor Warren Denner was responsible for acquiring much of the instrumentation required for these measurements and logistic support.

The author would also like to thank Professor R. W. Burling and the staff of the Institute of Oceanography, University of British Columbia, for their assistance in the field.

The author could not have completed this project without a great deal of technical assistance from Mr. David Lindquist and Mr. F. E. Jerome of the University of British Columbia, and from Mr. Allen White of the Naval Postgraduate School.

The author would like to acknowledge the support provided by the Naval Ordnance Systems Command under NAVORD CONTRACT ORD TASK-03C-005/551-1/UR104-03-01. Lacking this support, this study would not have been possible.

## I. INTRODUCTION

Knowledge of the velocity and temperature fields above the sea surface is necessary to understand the wind generation of waves and heat, energy, and momentum transfers across the air-sea interface.

A significant missing link in this knowledge is a lack of definitive measurements near the sea surface. Measurement of wind velocity and temperature near the air-sea interface is complicated by the need for support mechanisms that will not obstruct the flow. If measurements are to be made closer to the instantaneous sea surface than the wave height, then the sensor must move up and down with the sea surface.

Sensors can be placed on floats, but floats have disadvantages such as response, stability, size, and support limitations. They tend to damp out small waves, oscillate about their vertical axes, and in general, introduce extraneous movements in sensors mounted on them.

An alternative method is to use a device that actively follows the sea surface. This thesis represents an attempt to obtain turbulent temperature and velocity measurements near the sea surface using such a device.

## II. REVIEW OF PREVIOUS WORK

Until about twelve years ago, the most significant theory of wave generation was that proposed by Jeffreys (1924). Jeffreys predicted a minimum wind for the growth of waves of about 1.1 m/sec. This corresponds to a phase speed of .35 m/sec, a wavelength of .08 m, and a period of .22 sec. Jeffreys stated that as a wind blows over a wave of this size the streamlines separate at the crest sheltering the trough. Jeffreys neglected tangential stresses so that the energy transfer to the waves must take place by normal stresses. While other important works also appeared, this model remained unchallenged for thirty years until Ursell pointed out the inadequacies of the Jeffreys' sheltering theory. Then followed a series of papers by Miles and Phillips.

Miles (1957) and Phillips (1957) presented theoretical models for wave generation. These have been altered to a considerable extent by Miles (1959, 1960, 1962, 1967) and Stewart (1967). In Miles' theory, the air flow is regarded as quasi-laminar with the atmospheric turbulence neglected except for its effect upon the mean vertical profile. The air flow is considered over a sinusoidal water surface about which the actual surface fluctuates randomly due to the presence of other wave components. The critical height is defined as the height ( $Z_c$ ) above the instantaneous surface where the phase speed is equal to the wind speed. In Miles' theory, momentum is transferred downward across the critical height and is shown to be an important part of the wave generating mechanism. Air moving upward through the critical height

transports more negative vorticity than air moving downward. The flow as pictured by Phillips is shown in figure 1a.

Stewart (1967), after observing that the region of separation is much closer to the sea surface than Miles indicated, revised Miles' streamline pattern as shown in figure 1b. Above this critical height, the streamlines are horizontal and eddies occur in the trough leaving a "cats-eye" close to the surface in the trough.

Pond, Stewart, and Burling (1963), reported results of measurements obtained with hot wire anemometers mounted 1 m to 3 m above the surface. These data gave strong support to the Kolmogorov theory that the energy spectrum of the turbulent velocity fluctuations is a function of the wave number to the  $-5/3$  power. This power law extends to wave numbers as low as  $.005 \text{ cm}^{-1}$ .

V. I. Makova (1963), performed a similar type of experiment with a thermocouple. He measured the temperature at positions greater than 2 m above the sea surface. He concluded that the Kolmogorow-like hypothesis holds in the temperature regime. Makova did not attempt to correlate his data with wave data.

The more recent measurements by Pond, Smith, Hamblin, and Burling (1966) also support the validity of the Kolmogorov hypothesis and yield a value for the Kolmogorov constant. All of these measurements were made from fixed heights more than 1 m above the sea surface.

One of the first published attempts to establish the relationship between the sea surface and velocity fluctuations was made by Seesholtz (1968). He mounted cup anemometers at heights greater than 30 cm on a buoy in Buzzards Bay, Massachusetts. These measurements were still well above the critical height, and the limitations of buoy mounted sensors

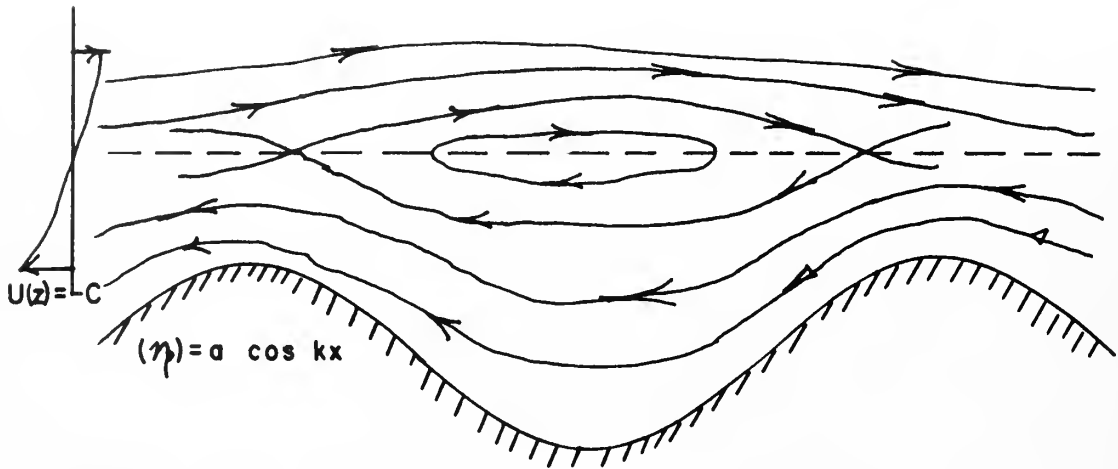


**FIGURE -1A.** Main streamlines in turbulent flow above waves as seen in reference system moving with the wave profile. Lighthill (1962) shows the closed streamlines centered directly over the trough and others show them elsewhere. The critical height is shown as dotted line.

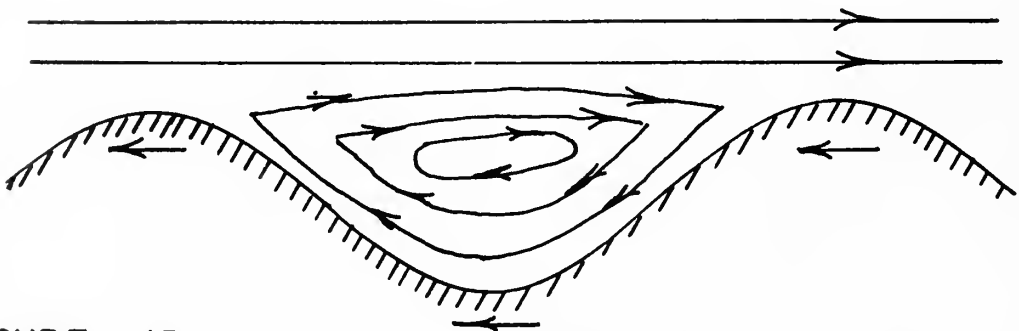


**FIGURE -1B.** This possible configuration of streamlines, with the same co-ordinate system as 1A, accounts for Stewart's observation that the air flow does not appear wave-like a short distance from the sea surface. The rightward acceleration at the left side of the figure would be produced by a shear stress gradient, the leftward acceleration on the right side by a horizontal pressure gradient. (from Stewart, 1967)



must be considered. He did, however, attempt to directly correlate his wind data to the sea surface elevation.

Ramzy and Young (1968) mounted thermistors on small floats approximately 3 cm above the water surface. This work was done in a small lake where the air temperature was greatly different from the water temperature. The wind generated waves were very small, on the order of 1.5 cm. Under these conditions, the critical height is very close to the water surface. This work cannot be accurately scaled up since the surface tension for waves of this size is important whereas it can be neglected in gravity waves.

### III. OBJECT

The objectives of this research were threefold:

1. To develop an instrument which would maintain a constant height with respect to an undulating sea water surface.

This follower should be able to maintain this position in waves whose height is less than one meter and cause little disturbance to the air flow or water flow at the point of measurement.

2. To make simultaneous measurements of the temperature, sea surface elevation, and instantaneous velocity.

These measurements were fixed with respect to the earth and fixed with respect to the sea surface at heights from 1 cm to 78 cm above the sea surface.

3. To analyze the data statistically to determine the possible correlation between temperatures, velocity, and the sea surface elevation.

Attempts were made to determine if a separation exists between the air flow and the sea surface.

#### IV. THE FIELD SITE

Measurements were made at the Spanish Banks field station located on the northwest shore of Point Gray near Vancouver. This station is operated by the Institute of Oceanography of the University of British Columbia (IOUBC), Vancouver, British Columbia, Canada. The site consists of a platform and two instrument masts located approximately one-half mile from the high water shoreline on Spanish Banks (figure 2).

The location is exposed to predominantly west and west northwest winds which average about 4 m/sec. The fetch length in these directions is greater than thirty miles. Since Georgia Strait, which lies to the west of the site, is protected by Vancouver Island on the west, there is very little swell observed at the site.

The tides in this area are mixed in nature. The station is dry at lower low water and reaches a depth of 5 m at higher high water. Low tides make it possible to work on the instrument mast, however, currents in these areas are fairly strong during flood or ebb. Deep water wave properties can be assumed for wave periods up to 2.42 sec, a longer period than most of the waves which occur in this area.

The wave follower and sensors were mounted on an aluminum mast of 10 cm in diameter as shown in figure 3a and in figure 3b. The mast is supported by three tubular supports that extend 1.8 m above the low water mark. These supports were underwater when the measurements were made. This mast can be rotated so that the sensors could be aligned with the wind. Due to the large tidal fluctuations, the

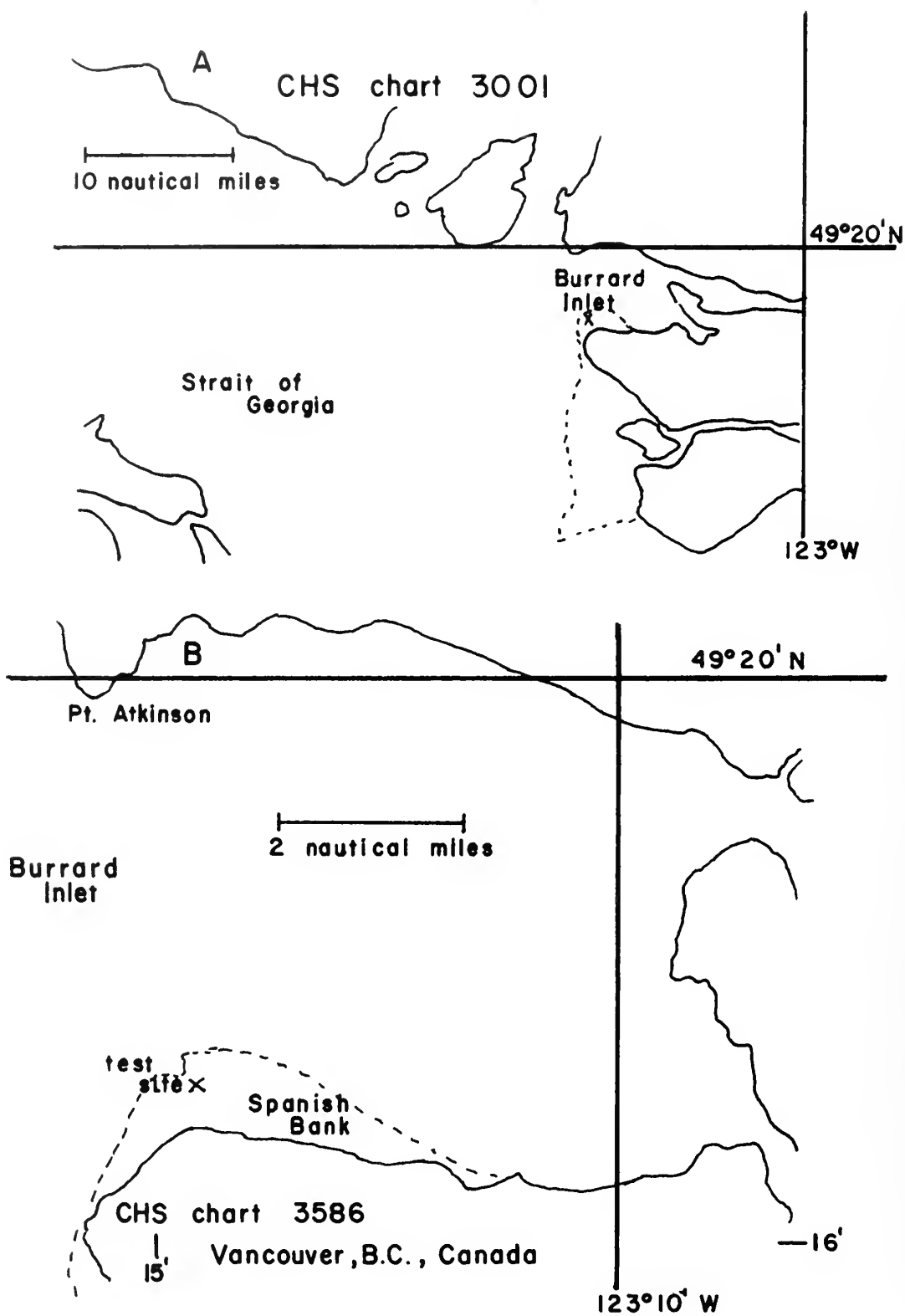


FIGURE 2 - Physical location of experimental site.  
Platform  $49^{\circ}17.1'N$   $123^{\circ}14.4'W$

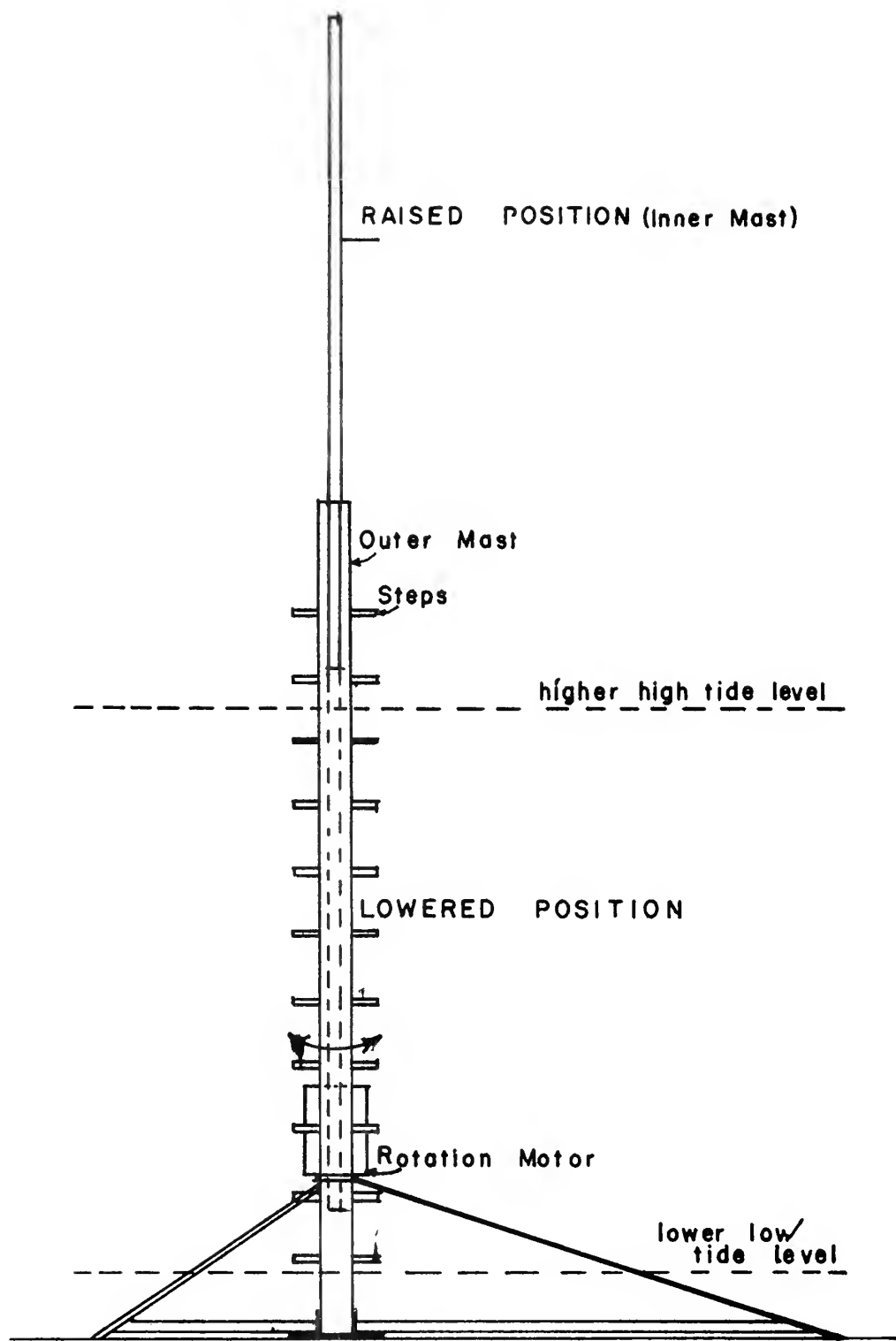


FIGURE 3A - INSTRUMENT MAST - FRONT VIEW

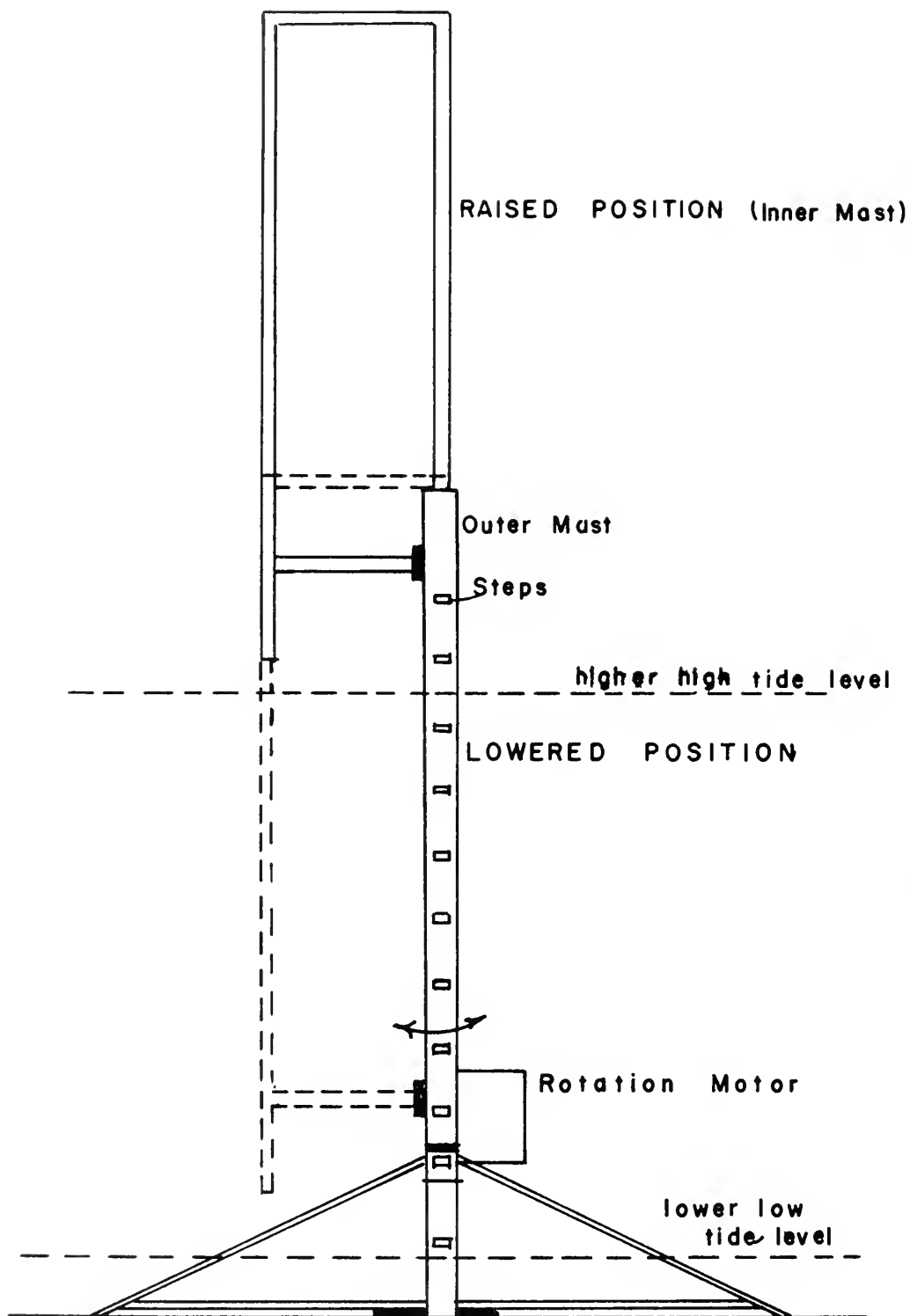
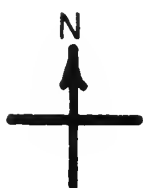
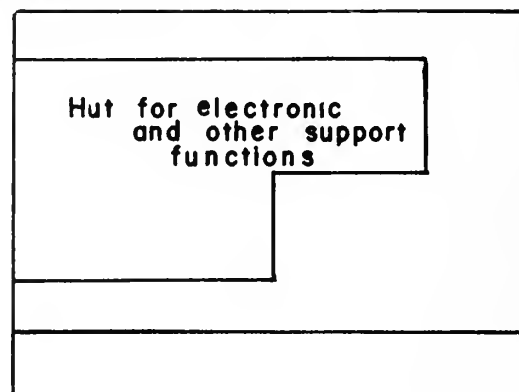


FIGURE 3B - INSTRUMENT MAST - SIDE VIEW

follower and sensors could be raised so that the follower could be positioned at any stage of the tide except at lower low water. Adjustments could be made remotely from a hut located on a platform approximately 40 m to the southeast. All of the electronics for the wave follower and sensors were located in the hut and connected by cables to the instrumentation mast. The hut arrangement is shown in figure 4.



Plan View



## ELEVATION

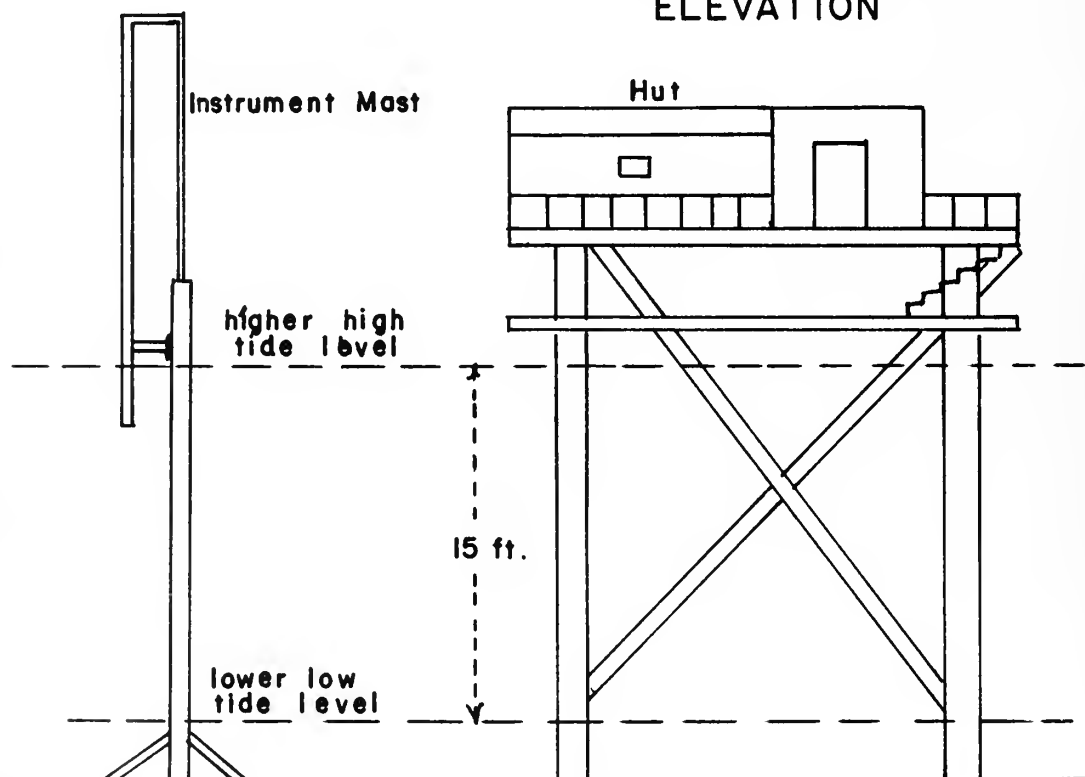


FIGURE 4 EXPERIMENTAL SITE



## V. WAVE FOLLOWING MECHANISM

The measurement of small-scale air-sea parameters requires measurements to be made very close to the sea surface. Often sensors must be placed closer to the sea surface than the height of the waves. This requires a vehicle that will maintain a constant height relationship with respect to sea surface.

The vehicle should not interfere with ocean processes such as the waves, the velocity field above the waves, and the heat transfer across the interface. The vehicle should be small in cross-section in the region close to the air-sea interface. The frequency response is also important. Any vehicle used to place the sensors a constant distance from the air-sea surface should give a flat response for the wave and turbulence frequencies of interest, and should remain vertical at all times.

The wave follower operates on the same principle as a resistance wave gage. When two wires are placed in a conducting fluid, the resistance varies, among other things, with the spacing between the wires and their depth of immersion. In a resistance wave gage, the probes are placed as one leg of a bridge, changing the resistance fluctuation to a voltage fluctuation. The wave follower operates similarly. The probes are placed on the end of an arm connected to a servo motor. The voltage fluctuations from the bridge act as the error signal to the servo amplifier. The servo amplifier drives the servo motor in such a manner that the error signal remains zero, thus the depth of immersion remains constant. The cross-sectional area of

the arm is very small so the interference with the air-sea processes is small. A potentiometer can be placed in the mechanical linkage which accurately reproduces the wave profile. This potentiometer circuit (figure 5) is independent of the servo circuit. Because the arm extends from the sea surface to approximately four feet above the wave crest, the sensors can be placed at varying distances from the sea surface.

#### A. WAVE SENSOR DESIGN

In order for this type of wave follower to operate properly, the sensor must be stable such that the resistance across the probes at a given point is constant for a constant depth of immersion. Since a DC current must be placed across the probes, corrosion of the probes can occur. Twenty-two gage platinum iridium was used for the probes. Since the probe support can be no closer than three inches from the waves, the platinum required stiffening. A stainless steel sleeve was placed over the platinum so that it would not vibrate. The electrode and sleeve were then cast into a plastic block or module so they could be interchanged easily.

Servo amplifiers require an amplitude error signal to create enough driving force to move the arm. This gives rise to a dead space above and below the center resistance. A slanted probe was used to make this dead space small with respect to the vertical, and to keep the probe support behind the point of water contact.

The support provides a moving mast so that probes can be mounted and then attached to the follower arm. The probe and support is shown in figure 6a.

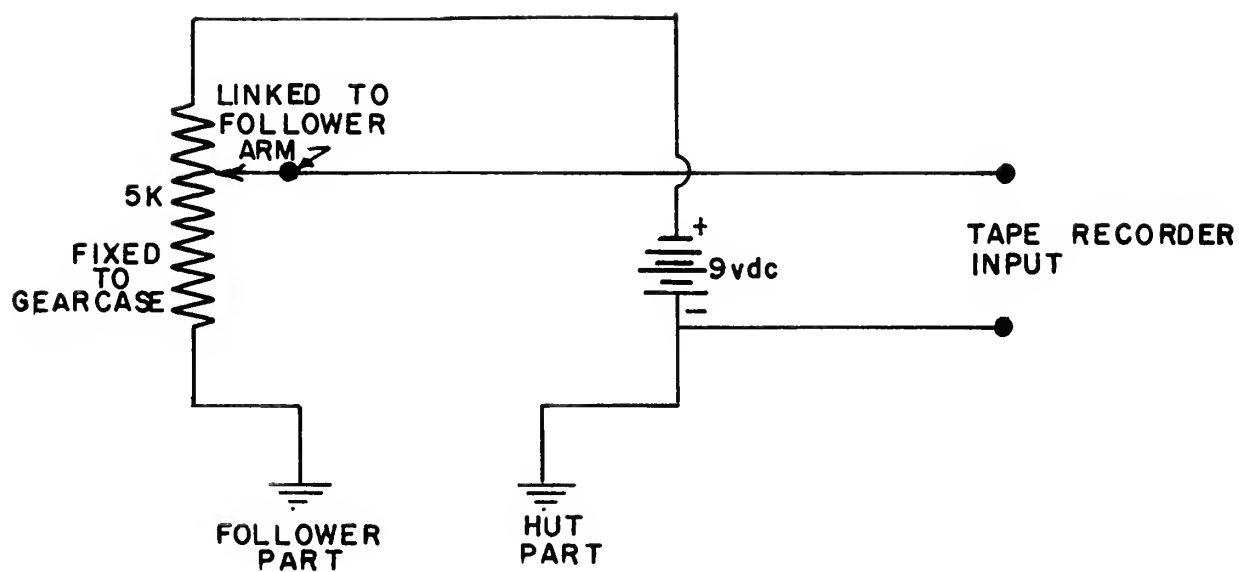
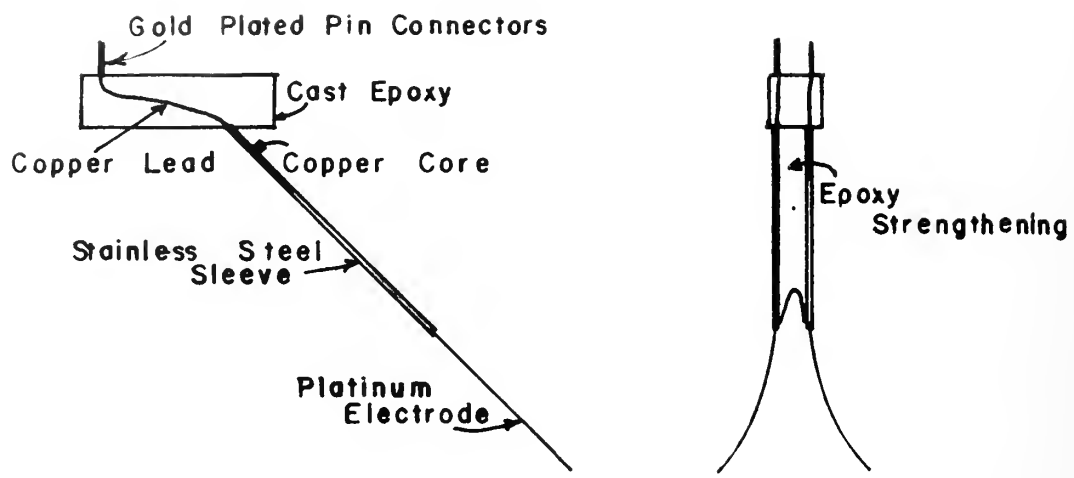
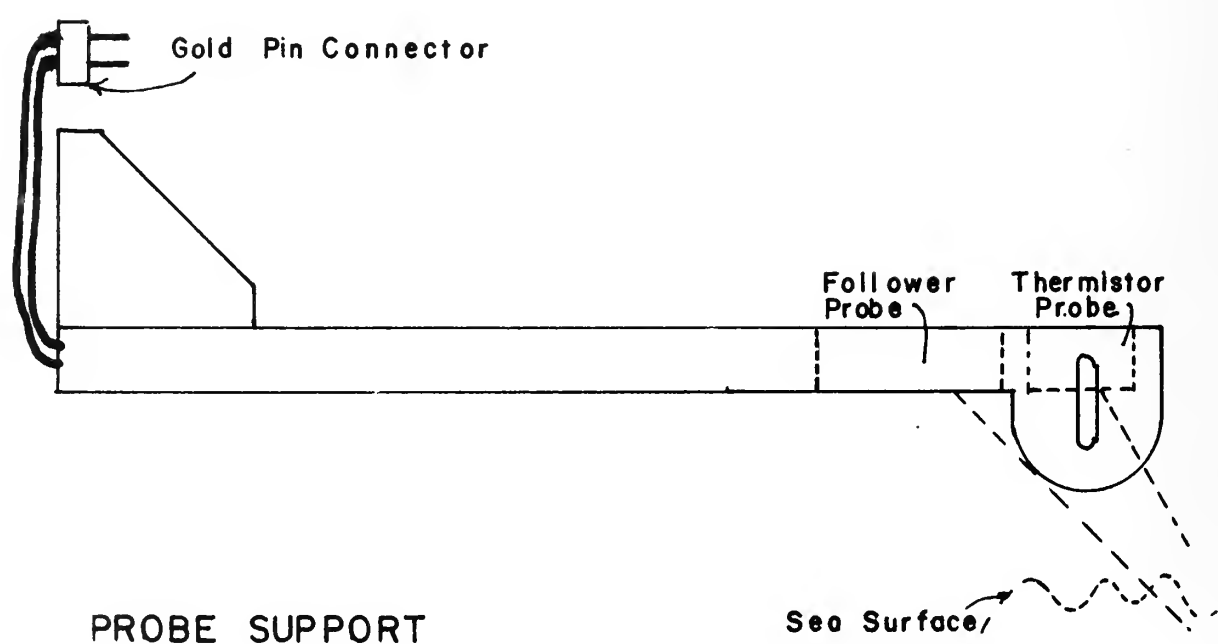


FIGURE 5 - WAVE POTENTIOMETER CIRCUIT



### FOLLOWER PROBE DETAIL



### PROBE SUPPORT

FIGURE 6A —FOLLOWER PROBE AND SUPPORT

The error circuit is basically a Wheatstone bridge with a potentiometer placed in series with the wave probe and a 5 volt zener diode placed in parallel to control the maximum output voltage. This apparatus was designed to operate in both fresh and salt water. The resistance across the probes can vary with the salinity as much as 14,000 ohms. The error circuit is shown in figure 6b.

#### B. ARM ASSEMBLY

The arm assembly consists of two parts; the arm and track (figure 7) travel up and down the slide and transmit the rotational movement of the servo motor to vertical motions of the sensor arm. Two tracks are welded back to back and the slide consists of two four-wheeled sleds attached to the arm. The sleds interlock to reduce movement in the plane of the arm. The arm is driven up and down the track by means of a nickel steel wire attached to the arm and frictionally secured to the upper drive pulley and around a lower follower pulley.

Two arms were manufactured. The shorter (9 in) arm has a travel of about ten inches, and this is lighter and more accurate than the longer (4 ft) arm. The shorter arm is used for laboratory work where the waves are very small, and the longer arm is used in the field where the peak to peak wave height is greater than nine inches. Both arms are completely interchangeable with the same gearing and motor.

The gearing system consists of five shafts with a mechanical advantage of about 2.5 to 1. A potentiometer wiper is geared into the second or third shaft, depending on whether the short or long arm is used. The potentiometer can be adjusted so that the wiper can have

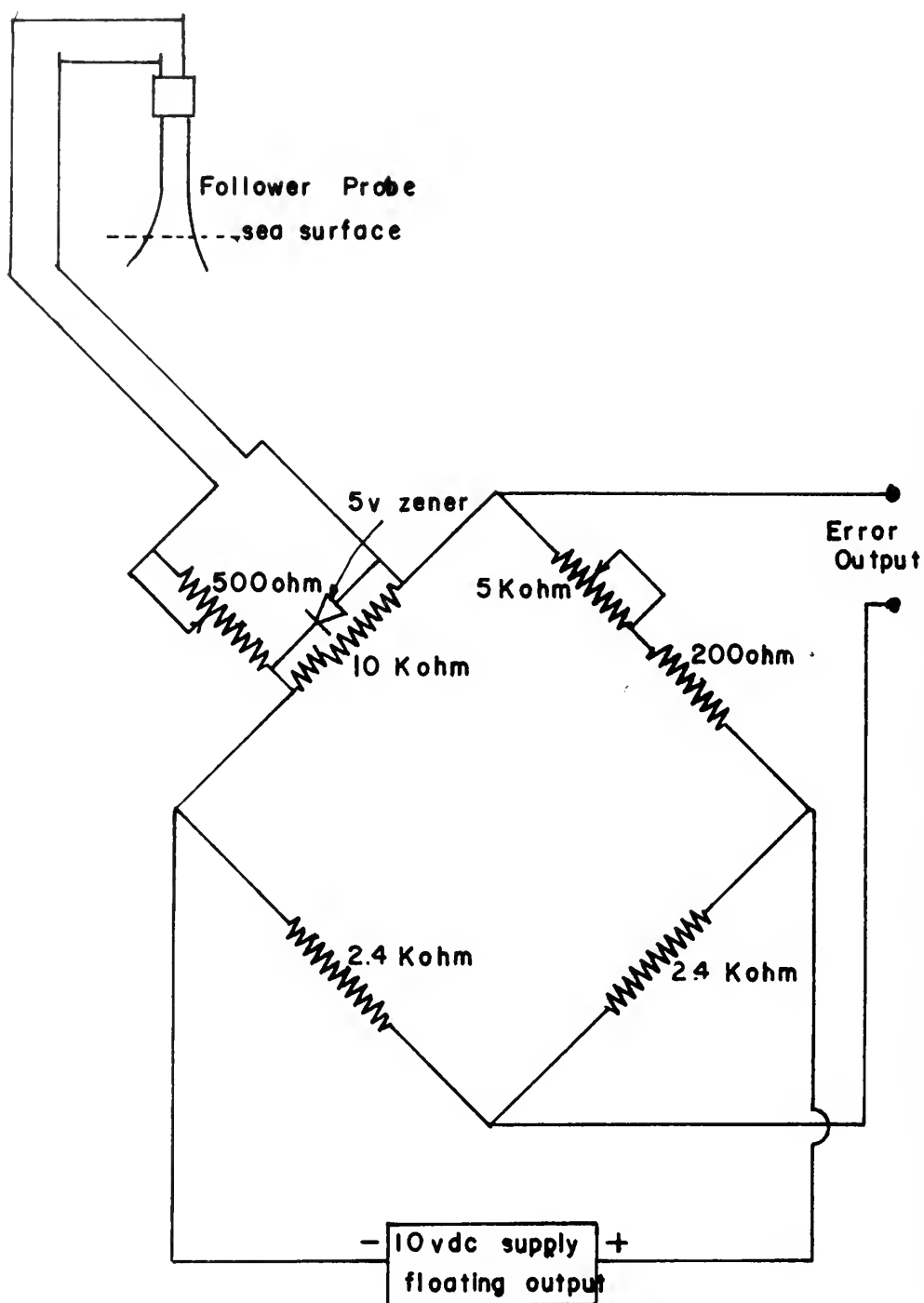


FIGURE 6B — FOLLOWER ERROR CIRCUIT

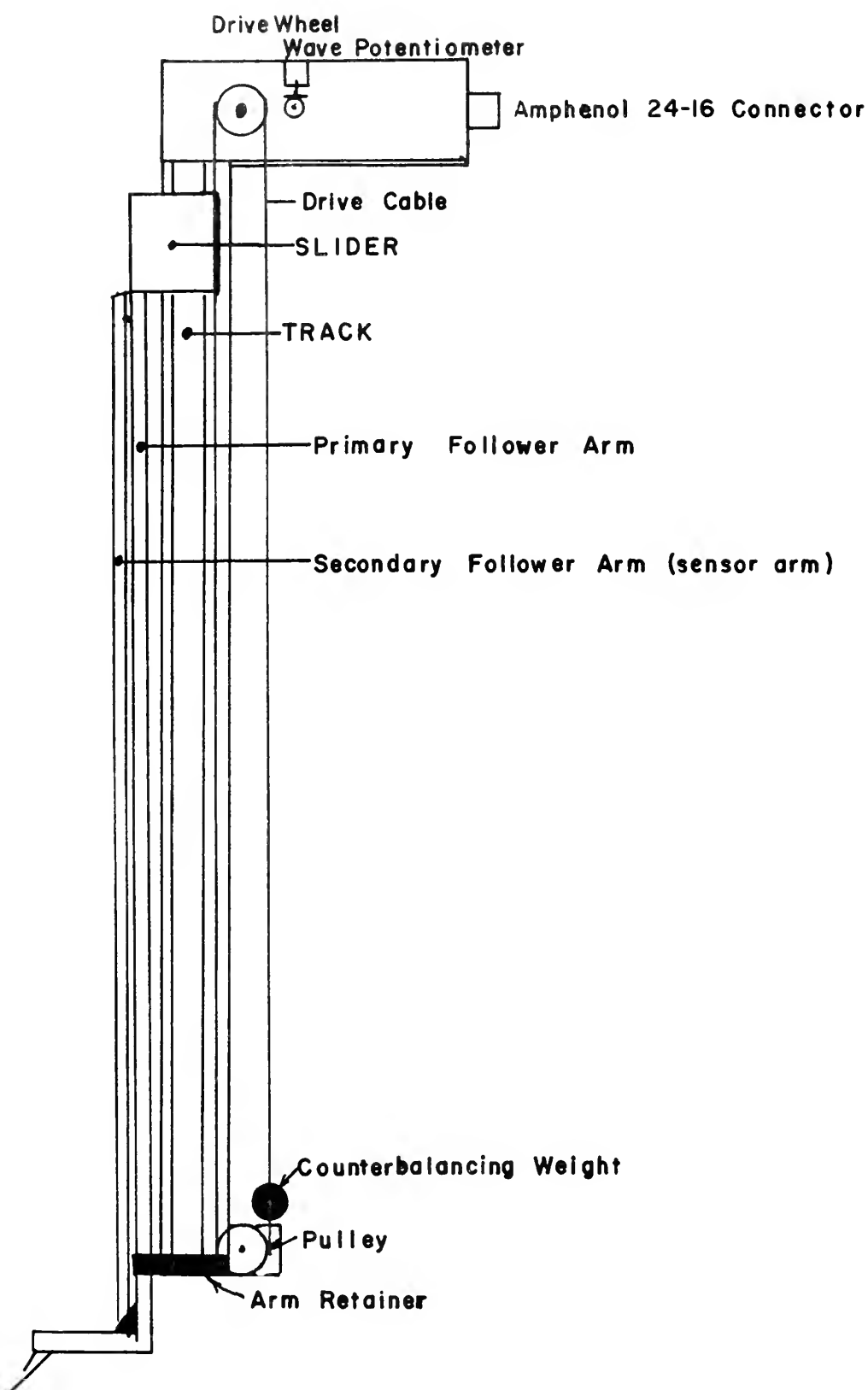


FIGURE 7- WAVE FOLLOWER- MAST ASSEMBLY

a maximum swing when the slide is moved. While this mechanical advantage reduces the frequency response of the follower arm, the response is still greater than necessary.

The response is based on the supposition that the torque required from the motor should remain constant. Unless the arm is dynamically balanced, the torque required to drive the arm up is greater than the torque that is required to drive the arm down. The imbalance, if it exists, forces the servo to overdrive the error signal. The arm is balanced by clamping a 24 oz. weight to the nickel steel wire opposite to where the wire attaches to the arm. This corrects the imbalance, but still allows full swing. A strap placed around the arm at the base of the slide further limits the arm to vertical motions (figure 7).

#### C. SERVO MOTOR AND AMPLIFIER

The arm and sensors are driven by a permanent magnet DC motor capable of delivering at least 60 watts. This motor satisfies the requirement of small size, high torque, and low cost.

The servo amplifier drives the motor until the error signal has been nulled. The speed is controlled by a rate generator that adjusts the speed of the motor proportional to the amplitude of the error signal. The servo amplifier used in this work was a modified Inland model 150A amplifier (figure 8). This amplifier is capable of delivering five amperes at 28 volts DC.

The cable connecting the amplifier and motor is a 16 line cable with eight shielded pairs. In order to deliver five amperes to the



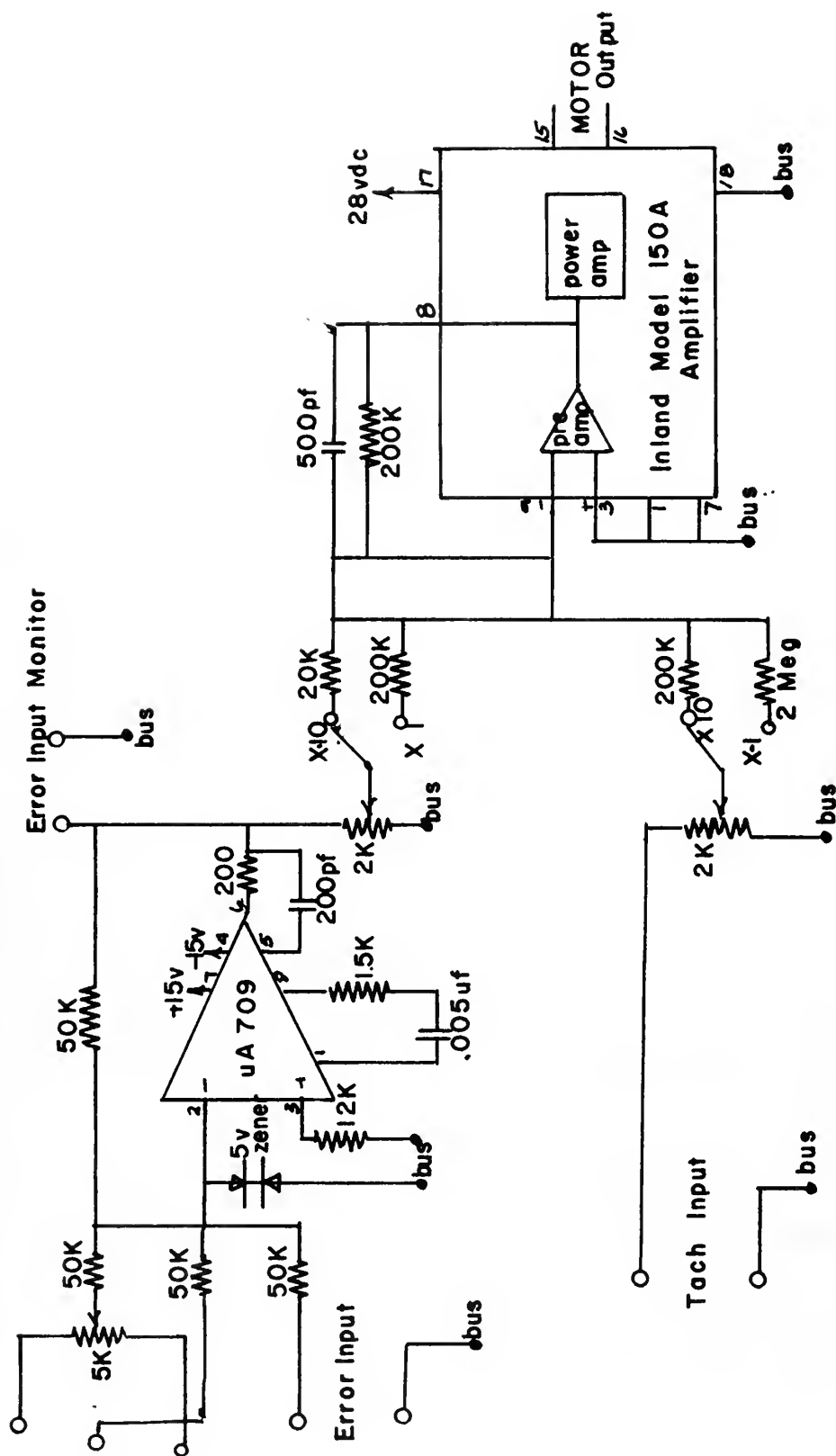


FIGURE 8 SERVO AMPLIFIER

motor, each of the motor connections use two of the 20 gage wires. The error tachometer and motor use this cable to consolidate the wires to the motor arm assembly. The cable is joined to the motor unit and control box by two amphenol 62-16 connectors.

#### D. TESTING

Testing fell into two categories: static testing and dynamic testing. In each of these areas there are two phases. The first is the relative ability with which the probe remains at constant depth. The second is the ability of the follower to follow the movements of the waves.

Static testing consists of measurement of the drift of the wave follower in still water and the calibration of the wave record output. The wave probe was allowed to warm up and the probe depth set. The wave potentiometer output, recorded on a Brush recorder, indicated arm fluctuations. Since the follower was operating in still water, any fluctuation in the output could be considered drift. This test showed that for fresh water (15 ohms across the probes) the maximum drift was 1 mm after three hours operation, which was entirely adequate for the intended uses.

A scale was placed beside the arm and the arm was moved between set marks along the slide. The wave output was then recorded for movements between these marks to determine the reliability of the follower potentiometer linkage. In all tests the output signals varied by no more than 1 mm. This is at least two orders of magnitude smaller than the intended waves.

Three methods were used to determine the dynamic characteristics of the wave follower. The first used a mechanical wave simulator, consisting of a variable speed motor which turned a 24 cm diameter gear through a linkage. On this gear, a worm gear was placed such that the worm follower could be adjusted to any distance from the center of the gear. The slide arm was attached to this worm follower. This slider is held on a track so that the slider can only move vertically when the large gear is rotated. A small beaker was attached to the slider. With this arrangement, the water-filled beaker moves sinusoidally with variable period and amplitude. A potentiometer was geared to the slider so the exact movement of the slide could be recorded. The wave follower was then fixed above the beaker so that the probes could make free contact with the water. The output of the wave follower was then recorded on a Brush recorder along with the generator input. Results are shown in figure 9.

First, a curve of maximum waves is plotted using the generally accepted formulae  $\frac{H}{L} = \frac{1}{7}$  and  $L = \frac{gT^2}{2\pi}$ . Then the wave length, L, and period, T, is varied corresponding to points above the curve of maximum speed of the motor. This testing shows in all cases that the follower is accurate to  $\pm 0.8$  mm for all the periods of interest. While the range of frequencies is limited, it is expected that lower frequencies would place less demands on the follower than higher frequency oscillations.

The second type of dynamic testing used strobe photography. The wave follower is placed above a wave tank which mechanically produced a regular train of waves that proceed down the tank. A strobe light was flashed at the probes and water. This operation was photographed

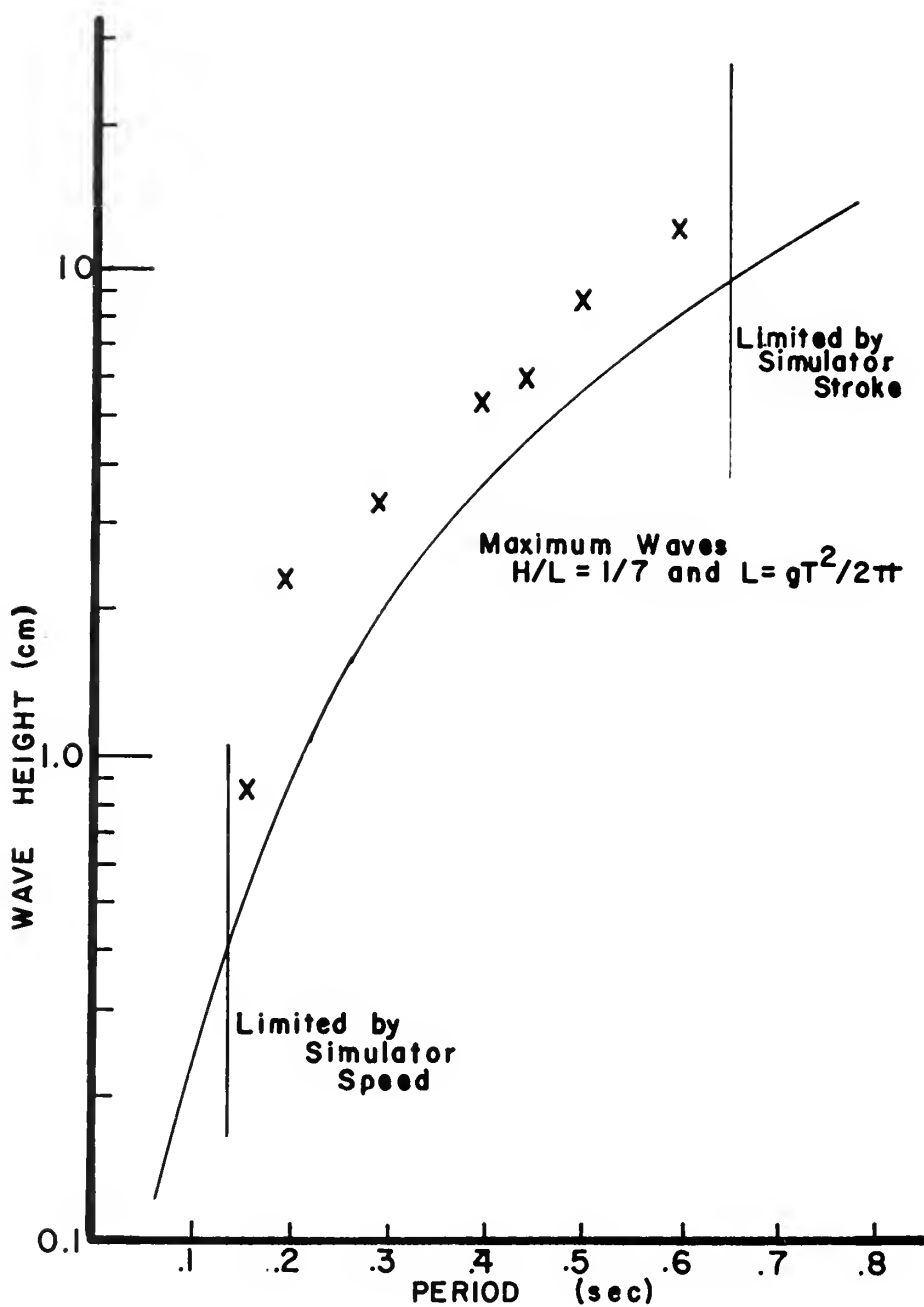


FIGURE 9- SIMULATOR TEST OF FOLLOWER

at several different wave periods and on different parts of the individual wave trough, leading side, crest, and trailing side. The pictures allow the distance between the probe support and the point the probes entered the water to be measured. In all cases, the maximum difference in these measurements was never greater than 0.8 mm. This also shows that the follower is accurate to 0.8 mm. Results of this are shown in figure 10.

The third, and least efficient method of dynamic testing, consists of subjecting the follower to wind generated capillary waves. A resistance wave gage was placed close to the follower probes. Both outputs were recorded and analyzed. As nearly as it could be determined, the follower can follow a fairly random sea, as well as regular waves within the limits previously stated.

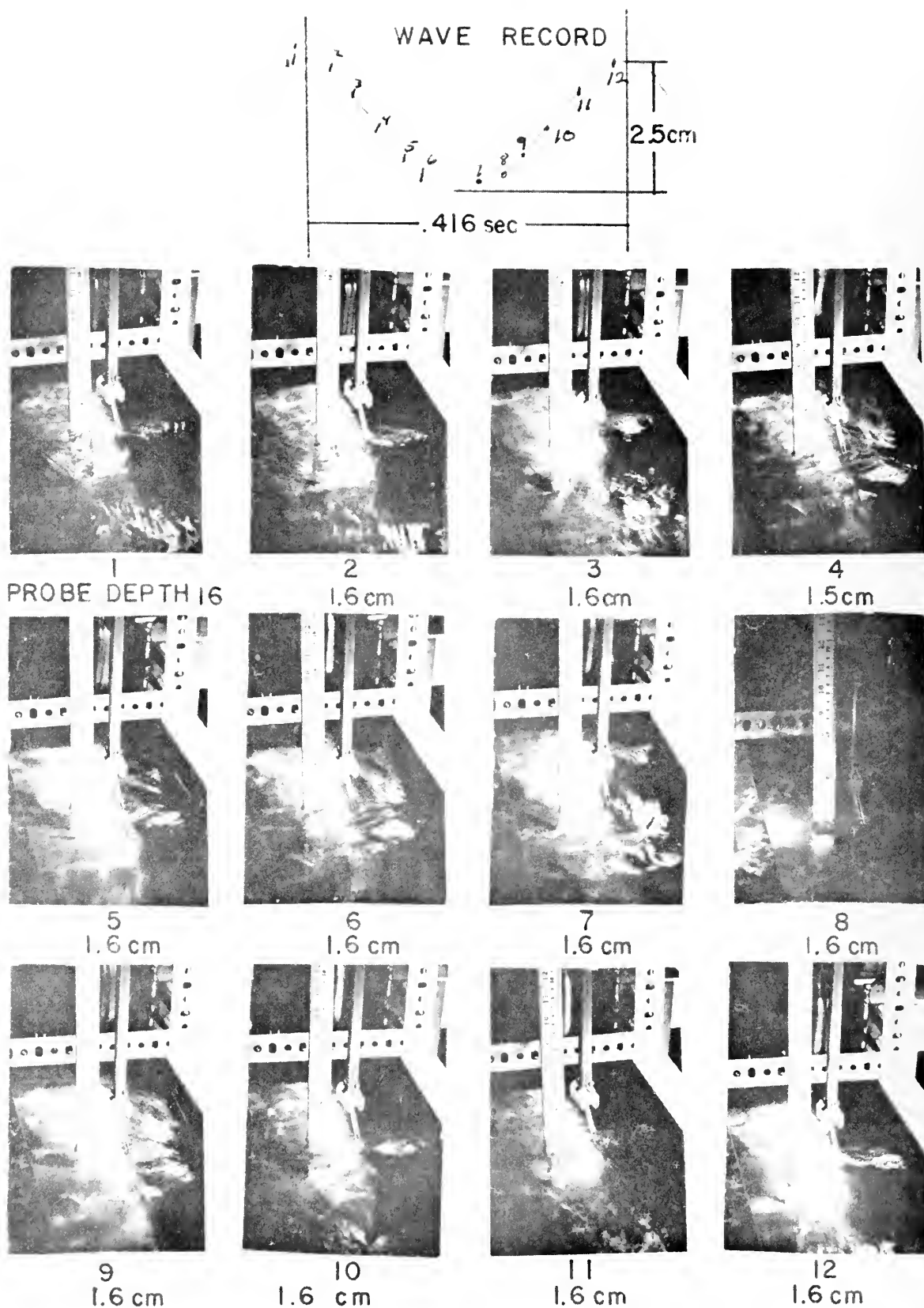


FIGURE 10-- STROBE ANALYSIS OF FOLLOWER OPERATION

## VI. SENSOR MECHANISMS

The wave follower was designed for a wide range of experimentation of the parameters above and below the air-sea interface. The parameters velocity, temperature, and pressure must be measured from the sea surface to several meters above the surface. This instrument deals with the critical first meter above the interface. In the series of experiments conducted at this time, the velocity and temperature at varying distances above the sea surface have been investigated. The total velocity and temperature sensor arrangement is shown in figure 11.

### A. TEMPERATURE SENSORS

Victor Engineering (VECO 41A401A and 32A50) thermistors were used to measure temperature and are shown in figures 12a and 12b. The thermistors were mounted on individual modules and calibrated. These modules could be changed easily if a malfunction occurred.

The physical specifications for each of these thermistors were:

	41A401A	32A50
Bead diameter	.005 in.	.010
Lead diameter	.0007 in.	.001 in.
Resistance at 25°C	10,000 ohms	2,000 ohms
Time constant (dry air)	0.1 sec $\pm$ 0.01 as advertised by vendor	0.5 sec $\pm$ 0.05 $\pm$ 10%
Time constant (humid air)	.0505 sec. as determined experimentally	0.25 sec.
Resistance change at 25 C	-3.6%/°C	-3.4%/°C

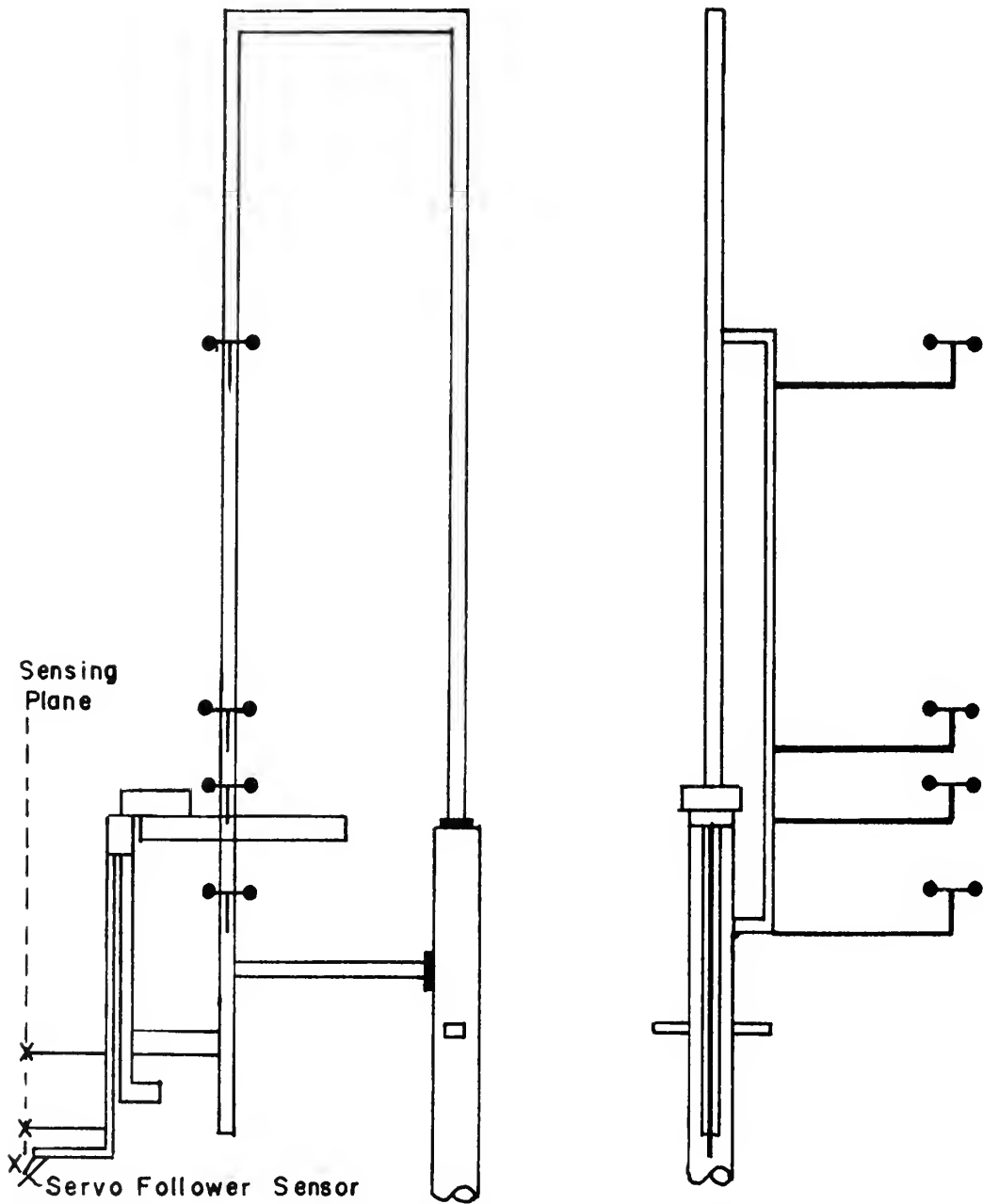
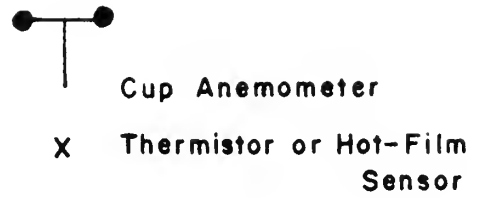
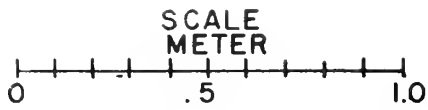


FIGURE II — SENSOR PLACEMENT



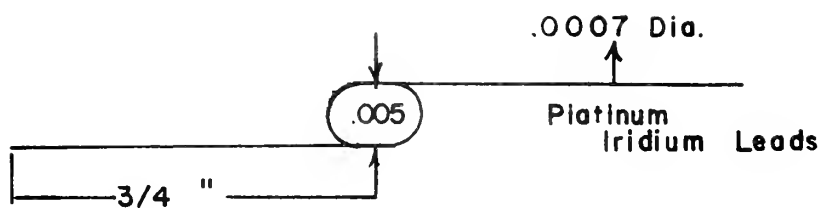


FIGURE 12A - VECO 41A401A MICRO-BEAD THERMISTOR

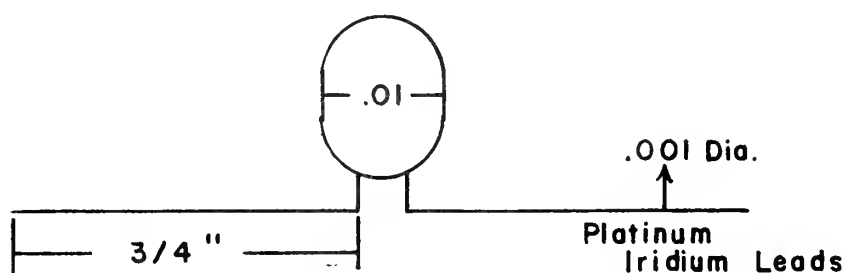


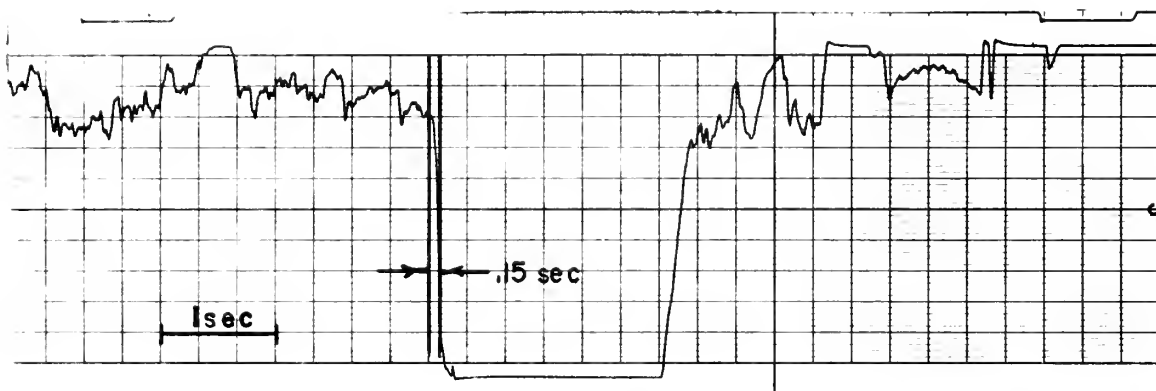
FIGURE 12B - VECO 32A50 ULTRA-SMALL THERMISTOR

The change in resistance can be considered linear for the temperature range in question. The time constant determination was carried out by Ramzy and Young (1968) for the 41A401A thermistor. The humid air time constant was determined in the field for the 32A50 thermistor, when the thermistor was placed very close to the sea surface and wetting was encountered (figure 13). The time constant can be determined by taking 63% of the time for the final temperature change to take place.

Ramzy and Young (1968), showed that velocity and humidity changes could be neglected for these thermistors in this application.

The modified bridge circuit used to change the resistance fluctuation to a voltage fluctuation is shown in figure 14. The modifications are necessary to compensate for the difference in the nominal resistances of the two thermistors (2K and 10K) and to provide the 100 ohm steps for the calibration of the instrument. The potentiometer allows the mean of the temperature fluctuations to be zeroed for ease in recording and accuracy. Furthermore, the standard bridge circuit had to be modified in the field to eliminate an induced potential resulting from the long thermistor leads. The operational amplifier as shown in figure 14 eliminated this potential.

During laboratory calibration each thermistor module is individually taped to a precision thermometer in a water bath, and as the water bath cools, the voltage output and temperature are recorded. These tests show that between 20°C and 30°C the temperature-voltage curve and temperature-resistance curve are linear. The slope of the curve allows conversion from resistance to temperature (figure 15). A second calibration takes place in the field after the instrument has warmed up. One hundred ohm steps are placed in the



DATA FROM CASE 3 LOW FLOATING THERMISTOR

FIGURE 13— THERMISTOR RESPONSE CHARACTERISTICS

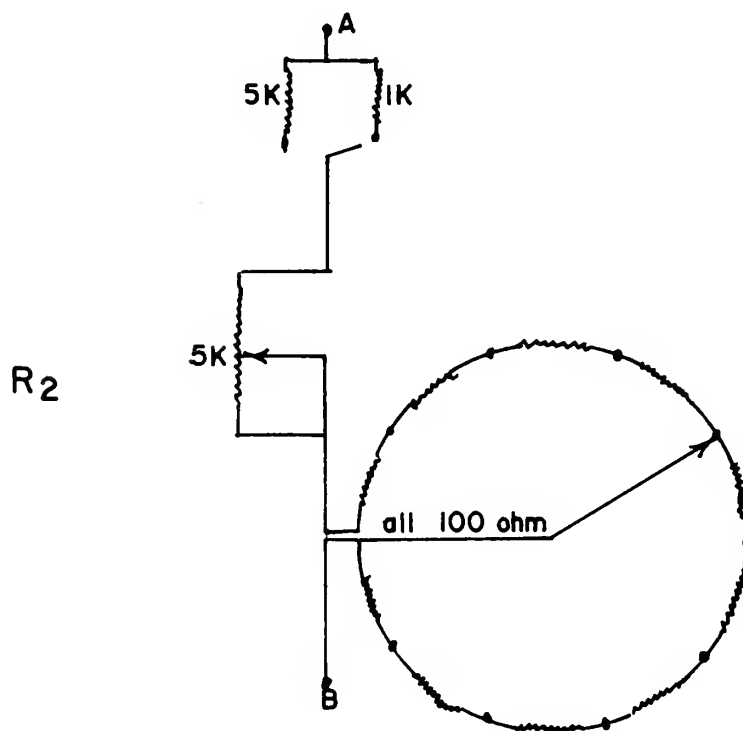
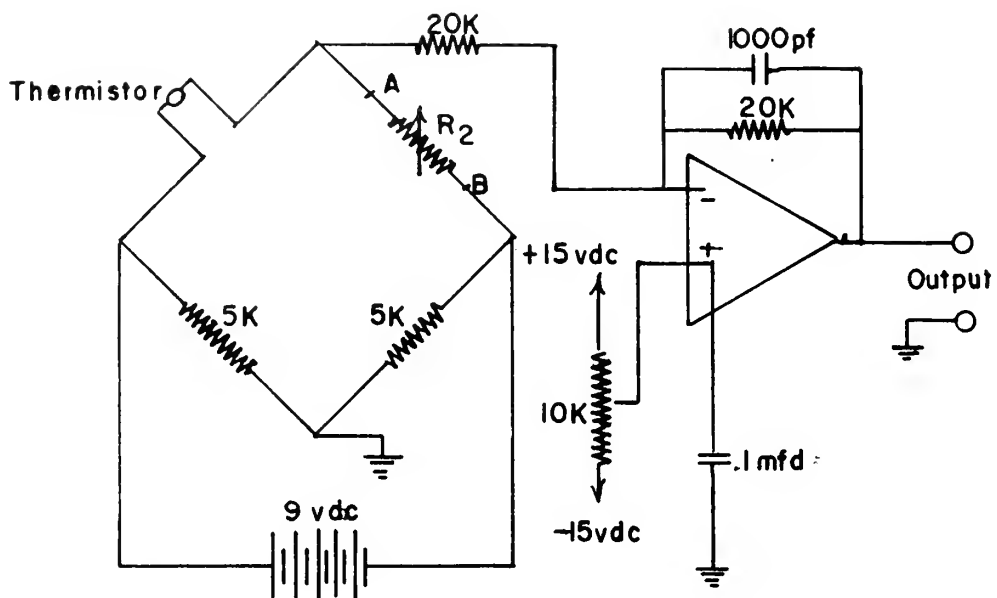


FIGURE 14 THERMISTOR CIRCUIT

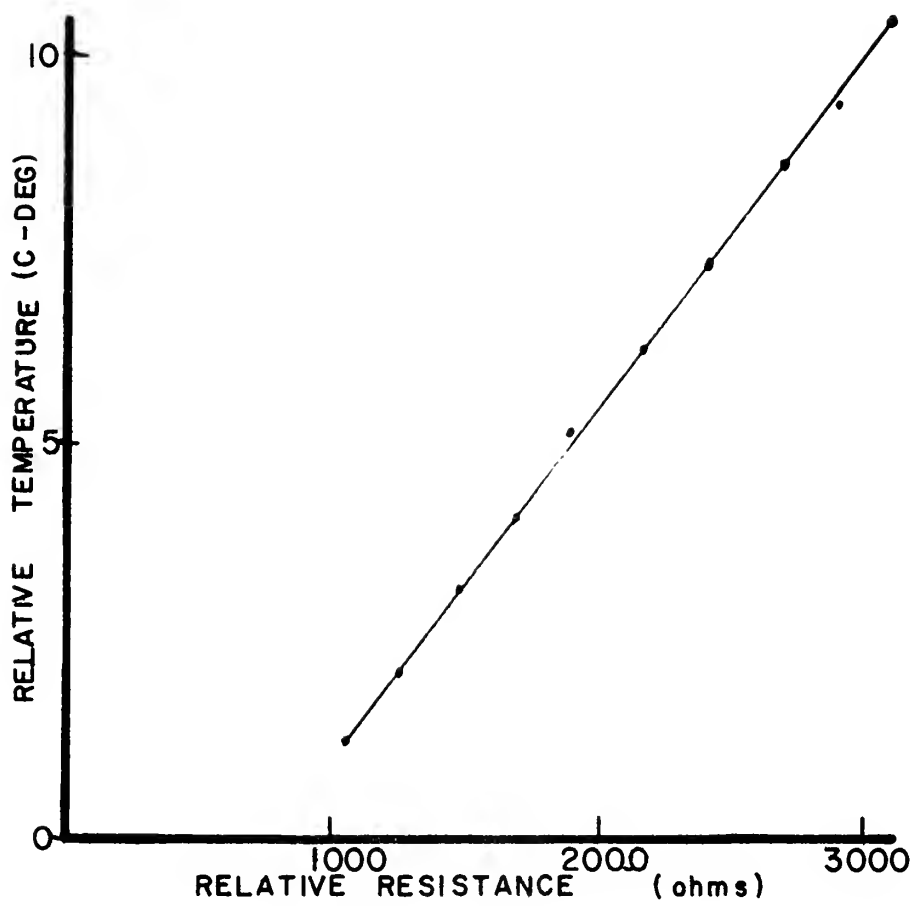


FIGURE 15 - THERMISTOR CALIBRATION

record allowing calibration of the final output record in ohms rather than volts. Division by the thermal coefficient of resistance allows the final temperature to be determined. Confidence limits are difficult to determine for measurements of this nature, but these measurements are probably good within  $\pm .01$  C.

## B. VELOCITY SENSORS

Two velocity sensing devices were used in this experimentation. During the time the data were taken, the mean wind speed was recorded by four Thornthwaite cup anemometers located at distances of 1.80, 1.95, 2.29, and 3.29 meters above the mean sea surface (figure 11). The axis of these cups was 65.8 cm to the right of the wave follower arm and 43 cm behind it.

Turbulent velocity measurements were made with a Thermo-Systems hot-film anemometer model 1054 B. The sensors were quartz coated cylindrical hot-film (model 1210-20). The characteristics were: (Thermo-Systems 1969)

Diameter of film	.002 in.
Length of sensing area	.04 in.
Frequency response (in air at 300 ft/sec)	40,000 K Hz
Nominal resistance	4 to 8 ohms

These 1210-20 probes were selected because of their lower end loss and high frequency response over wedges, single-ended, or the other types of probes. The probe had to be quartz coated because of the humid atmosphere in which the probe would be operating. With this probe, the 1054B anemometer had a frequency response of DC to 5,000 Hz and an output level of noise of less than 0.03%.

The 1054B anemometer has both linearized and non-linearized outputs. If the linearized function is used, the anemometer must be calibrated before use. Since this could not be done in the field, the non-linear output was used. This anemometer allowed adjustment of the overheat ratio of the probe, and when the sensor was placed above 5 cm from the sea surface, the splash was considered minor so the normal 5 to 1 overheat ratio was used. However, below this level a 2.5 to 1 overheat ratio was used. These sensors were calibrated after the fact in a wind tunnel at the Department of Mechanical Engineering, University of British Columbia. These calibrations are shown in figure 16.

Because the recorder would not accept the DC level corresponding to the mean wind velocity, an operational amplifier was used, which is similar to the amplifier used for the thermistor data. This amplifier eliminated the DC level from the recorder input as shown in figure 14. However, because the anemometer output is non-linear, the mean voltage must be recorded for each run. This gives a point along the curve to which a tangent can be drawn and the true calibration determined.

#### C. RECORDING

All data was recorded on an Ampex FR1300 14 channel tape recorder at 7.5 ips using FM electronics. While the signals were being recorded, the channels were being monitored on an oscilloscope and a Brush strip chart recorder.

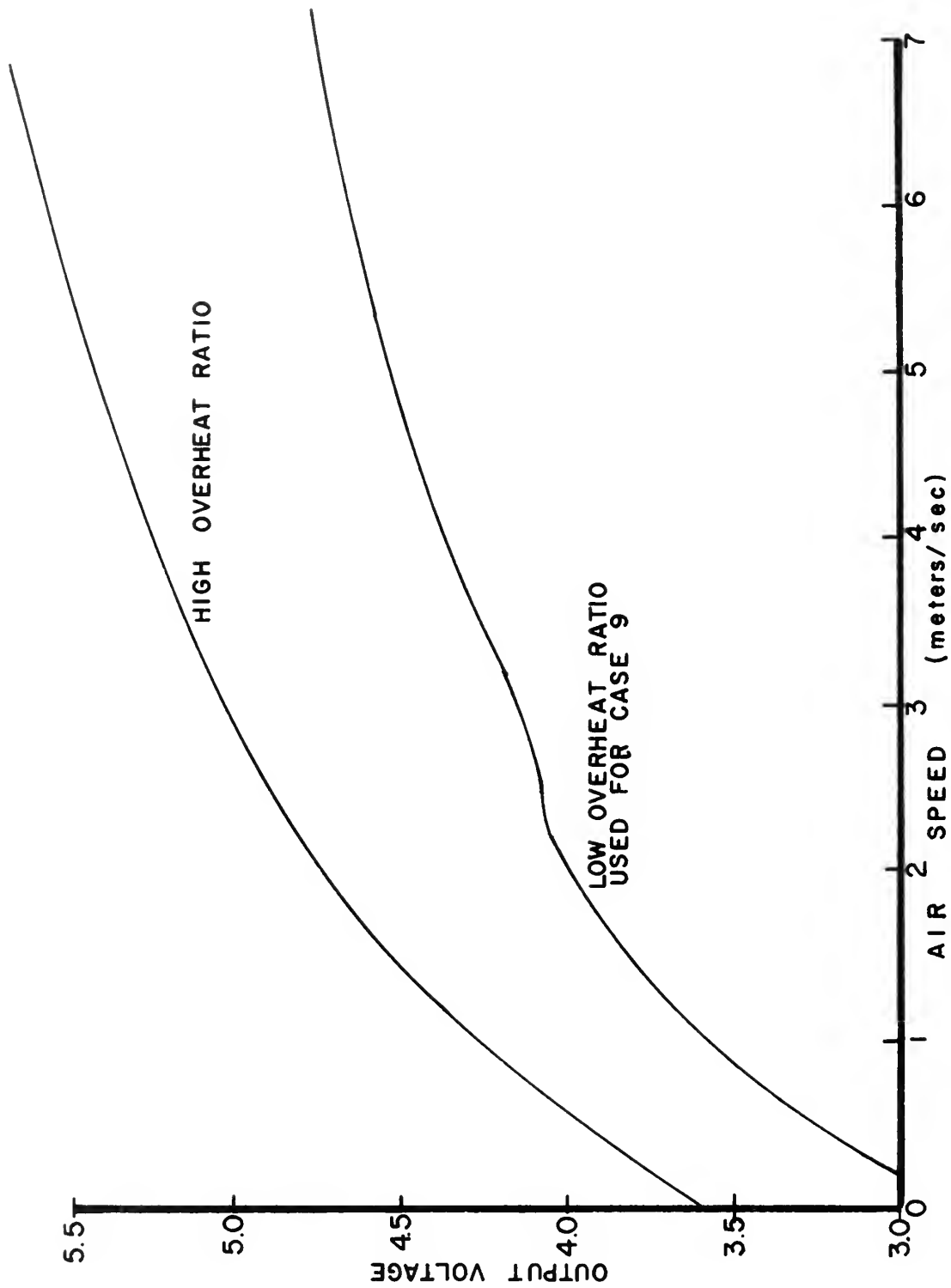


FIGURE 16 - HOT FILM ANEMOMETER CALIBRATION DATA



## VII. STATISTICAL ANALYSIS

Three primary statistical relations have been calculated; power spectral density of wind velocity, temperature, and wave height, the coherence among these quantities and the phase between these quantities. The coherence requires the computation of the co- and quadrature spectrum, but these spectra have not been examined. Both digital and analog analyses were made of the power spectral density but the analog analyses were unsuccessful.

### A. DIGITAL ANALYSIS

The data collected in this investigation were recorded on an Ampex FR 1300 analog magnetic tape recorder at 7.5 inches per second. For editing, the tapes were replayed at 60 inches per second and the outputs recorded on a Brush strip-chart recorder (vertical scale - 50 mv/mm, and chart speed - 1 mm/sec). A sine wave of 100 Hz was recorded on a vacant channel beginning at the point where digitizing began and ending where digitizing finished. The length of the records digitized was a compromise between the uninterrupted data available and the frequency resolution desired. From the analysis of the strip chart, four records of 16 min. and three records of 4 min. were selected for digitization. Bendat and Piersol (1966) list the following parameters for these records:

$$\text{Sampling rate} = \frac{\text{digitizing rate}}{\text{playback/record speed}} = \frac{1000}{8} = 125 \text{ samples/sec}$$

$$\text{Sample time interval} = h = 1/\text{sampling rate} = \frac{1}{125} = .008 \text{ sec}$$

$$\text{Nyquist frequency} = \frac{1}{2h} = 64 \text{ Hz}$$

$$\begin{aligned} \text{Length of record} \quad 16 \text{ min} &= 960 \text{ sec} \\ &\text{or} \\ &4 \text{ min} = 240 \text{ sec} \end{aligned}$$

$$\begin{aligned} \text{Sampling size} \quad \frac{960}{h} &= 120,000 \text{ samples} \\ &\text{or} \\ \frac{240}{h} &= 30,000 \text{ samples} \end{aligned}$$

Digital analysis was performed using the programs reported by Wilson, Boston, and Denner (1969). These programs analyze blocks of data which each hold  $2^n$  samples where  $n \leq 13$ .  $n=11$  was selected for this study giving the following parameters:

$$\text{Block size (B)} = 2^n = 2^{11} = 2048 \text{ samples/block}$$

$$\text{Number of blocks} = \frac{N}{B} = 120,000/2048 = 58 \text{ blocks}$$

or

$$30,000/2048 = 14 \text{ blocks}$$

$$\begin{aligned} \text{The bandwidth} &= \text{sampling frequency}/2 \times \text{Block size} \\ &= 125/2 \times 2048 = .311 \text{ Hz} \end{aligned}$$

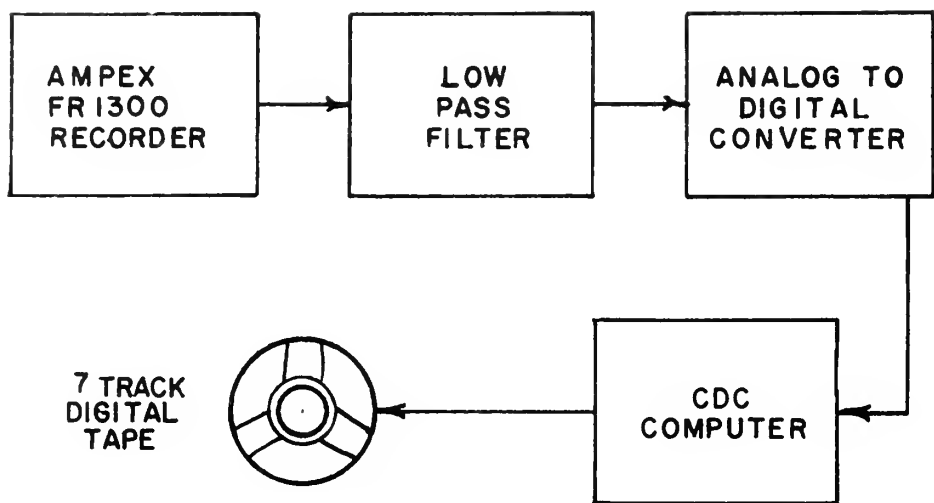
$$\text{Starting frequency} = \text{Bandwidth}/2 = .152 \text{ Hz}$$

$$\begin{aligned} \text{Cutoff frequency for analysis} &= 32 \times \text{Bandwidth} \\ &= 32 \times .311 = 9.75 \text{ Hz} \end{aligned}$$

$$\begin{aligned} \text{Correlation log values} &= m = 1/\text{Bandwidth} \times \text{sampling interval} \\ &= 1/.311 \times .008 = 2.49 \times 10^{-3} \end{aligned}$$

$$\text{Normalized standard error} = \sqrt{m/n} = 1.58 \times 10^{-2} \text{ for the 16 min series}$$

The flow chart for the digital analysis procedures is shown in figure 17. The digital analysis was done at the University of British Columbia.



# ANALOG TO DIGITAL CONVERSION

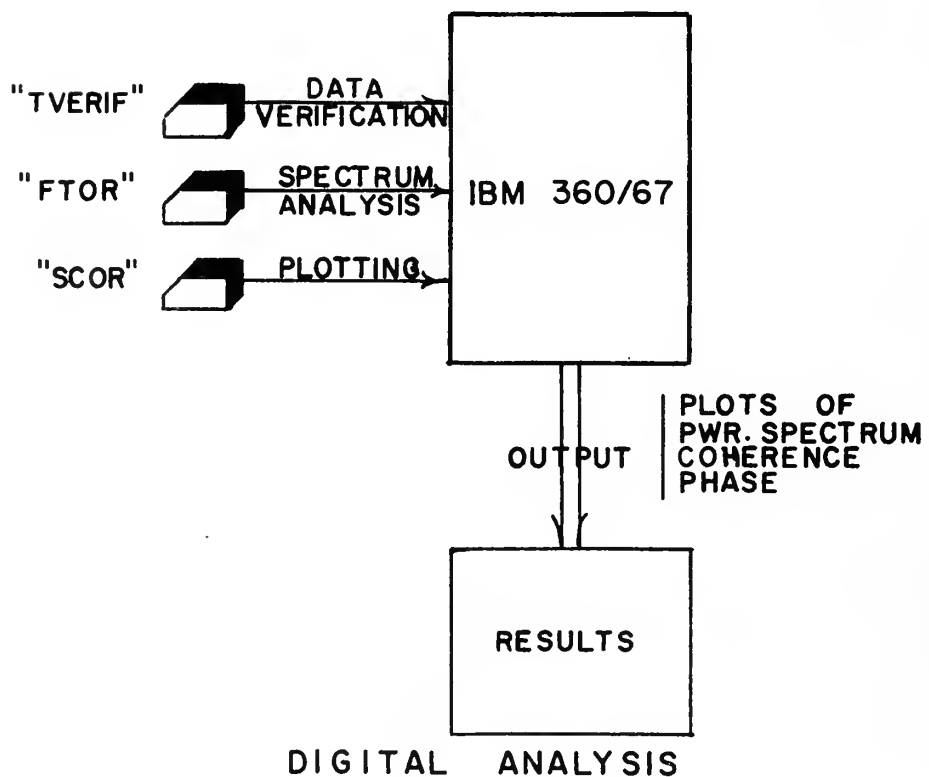


FIGURE 17 -FLOW CHART-ANALOG/DIGITAL METHOD

## B. ANALOG ANALYSIS

Limitations on the digital computer time would not allow processing of all data selected for analysis. Analog methods were employed to process data analyzed digitally as well as the remainder of the selected data. Unfortunately, due to circuit limitations in the analyzer, the spectra produced are not as accurate as those digitally produced.

The original analog tape was played back and re-recorded at 60 inches per second and the signals conditioned by passing them through a bandpass filter (0.01 to 15 Hz). The bandpassing eliminates the DC level at the low end of the spectra and the noise level at the upper end of the spectra. The re-recording was done on a Sangamo Model 3562 tape recorder and analysis was done using an Ampex CP 100 tape recorder.

Analysis was done on a Princeton Applied Research Model 101 Signal Correlator and a Princeton Applied Research Model 102 Fourier Analyzer with the following specifications:

Frequency range: .25 Hz to 5 Hz with 100 points

Frequency resolution: 0.1 Hz

Bandwidth: .0475 Hz

Figure 18 is a flow chart of the analog analysis procedure.

Calibration is done in two steps; the signal output on the analog tape is calibrated in  $^{\circ}\text{C}$  per volt or m/sec per volt, and this factor is then multiplied by the analyzer transfer function. This combined factor is the basis for the output scaling.

The spectra produced by analog methods do not agree with those produced by the digital methods because the power is averaged in the

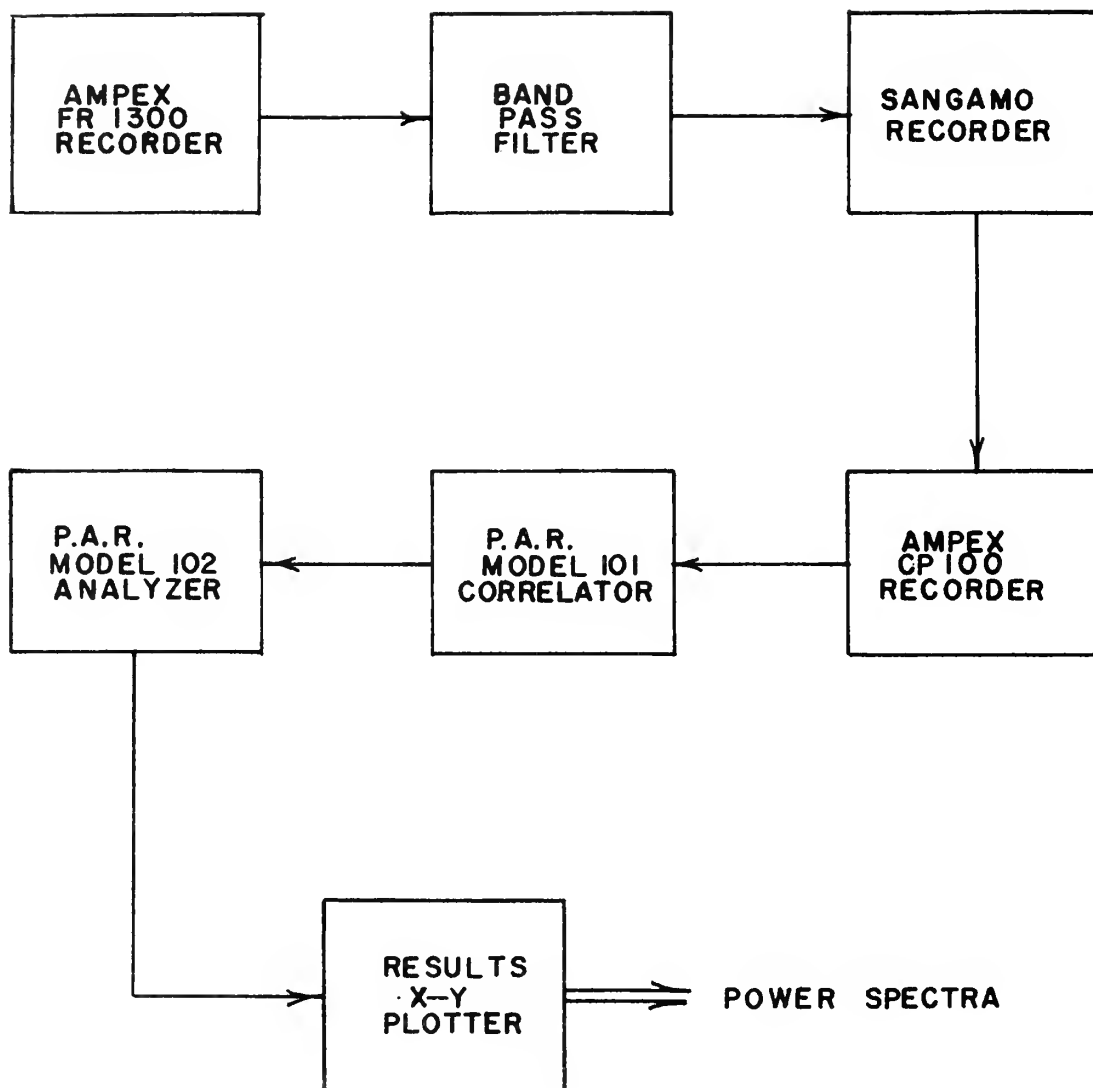


FIGURE 18 - FLOW CHART - ANALOG METHOD

Fourier analyzer over only a 5 Hz bandwidth versus 10 Hz for the digital processing. The spectra produced by analog means were normalized such that full scale is equal to 1.0 extending from a zero value at the origin.

The results of the analog analysis proved to be unsatisfactory. They did not agree with the digital results and physical interpretations proved to be extremely difficult. For these reasons the analog results are not included in this thesis.

## VIII. DATA

The data were taken between 20 July and 25 July 1969, at the Institute of Oceanography, University of British Columbia oceanographic tower. In the first investigation from 20 July to 23 July, the temperature field above the sea surface was measured and compared to the wave fluctuations. This consisted of four cases or thermistor configurations using two thermistor sensors. In the second investigation, the velocity field above the sea surface was measured. Due to breakage of a hot-film sensor, only two of the five velocity runs were obtained. In the other three runs, velocity measurements were made only at one level.

The nine cases presented here are the result of six hours of data collection in the field. After editing, only the best two hours of data were used. Of the nine cases, five were analyzed both digitally and analog, and the other four cases were analyzed by analog techniques only.

The object of this section is to present the analyzed data and to discuss the obvious points of each case. There will be no comparison of the cases. Comparisons and final conclusions are given in section IX.

### A. CASE 1

A micro-bead thermistor was mounted 78 cm above the sea surface on the moving follower arm. Another thermistor was attached to the fixed slide such that the mean position of the follower thermistor coincided

with the height of the fixed thermistor. These measurements were made between 1713 and 1737 on 20 July 1969, but only 16 min of data were used for analysis. The following conditions prevailed:

Wind direction  $270^{\circ}\text{T}$ ; mast aligned with wind

Wave direction  $270^{\circ}\text{T}$

Water temperature  $20.3^{\circ}\text{C}$

Air temperature  $19.5^{\circ}\text{C}$

Mean wind speed

1.2 meters above sea surface = 3.54 m/sec

1.5 meters above sea surface = 3.44 m/sec

1.7 meters above sea surface = 3.58 m/sec

Clear sky

Water depth two meters, flooding tide

Critical height 18 cm - data were obtained above this value

This was obtained by plotting the wave profile and computing the point where the mean wind speed was equal to the dominant wave speed.

Figure 19 shows a representative sample of the data for this run.

The spectrum obtained from the digital analysis of the wave record (figure 20) suffers at the low frequency end due to the limitations imposed by the analog to digital procedure. However, the high frequency end follows the usual energy fall-off with wave-number (slope -5 to -6). Some confidence may be placed in the wave follower's ability to respond correctly.

Both thermistor spectra (figures 21 and 22) show the expected  $-5/3$  dependency of energy on wave-number. Why the floating thermistors should have a more solid  $-5/3$  region than the fixed thermistors is not clear. Further analyses at lower frequencies would be necessary to clear up this point.



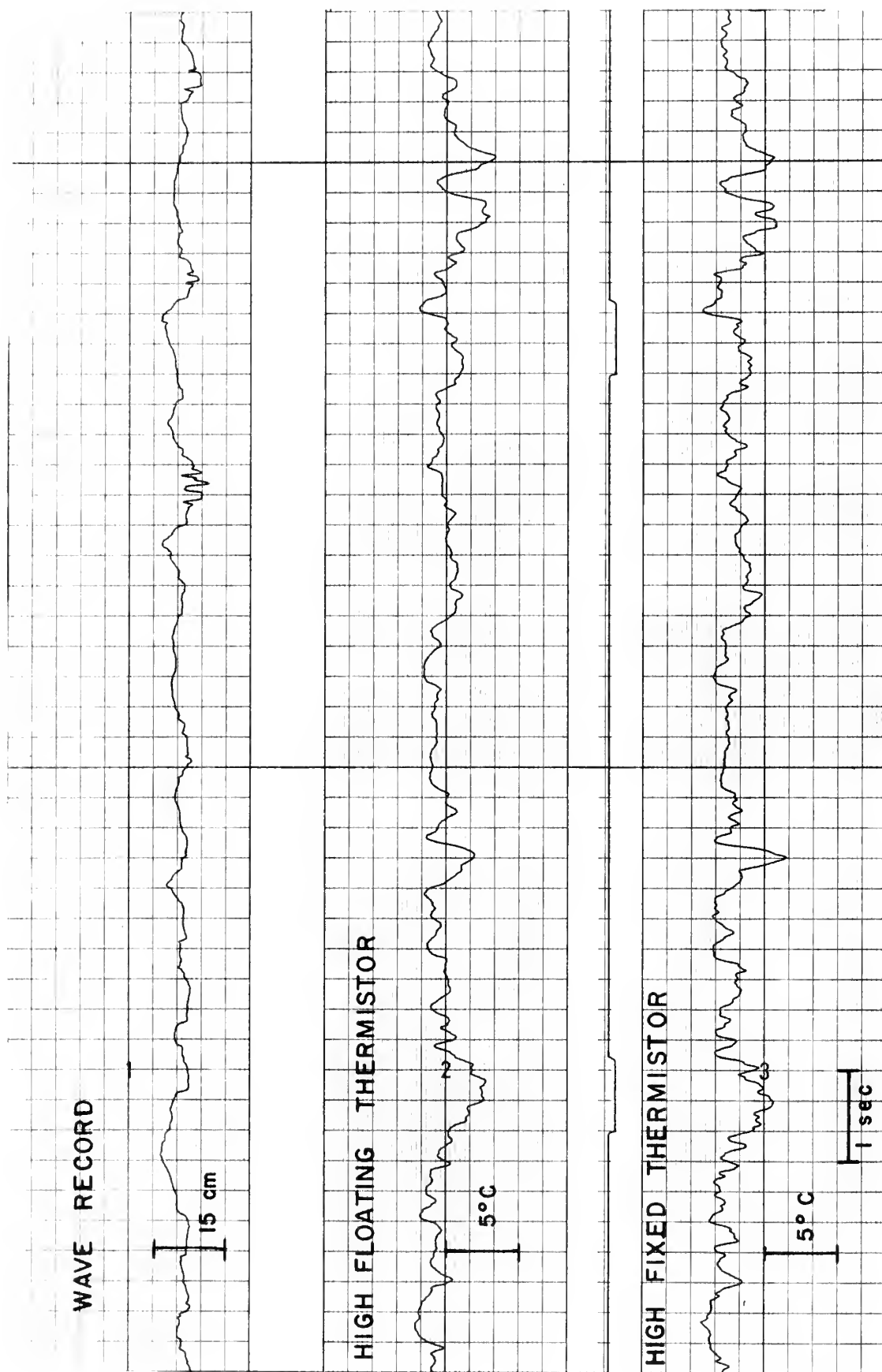


FIGURE 19 SAMPLE RECORD FROM CASE I



FIG. 20-CASE 1 - SEA SURFACE ELEVATION

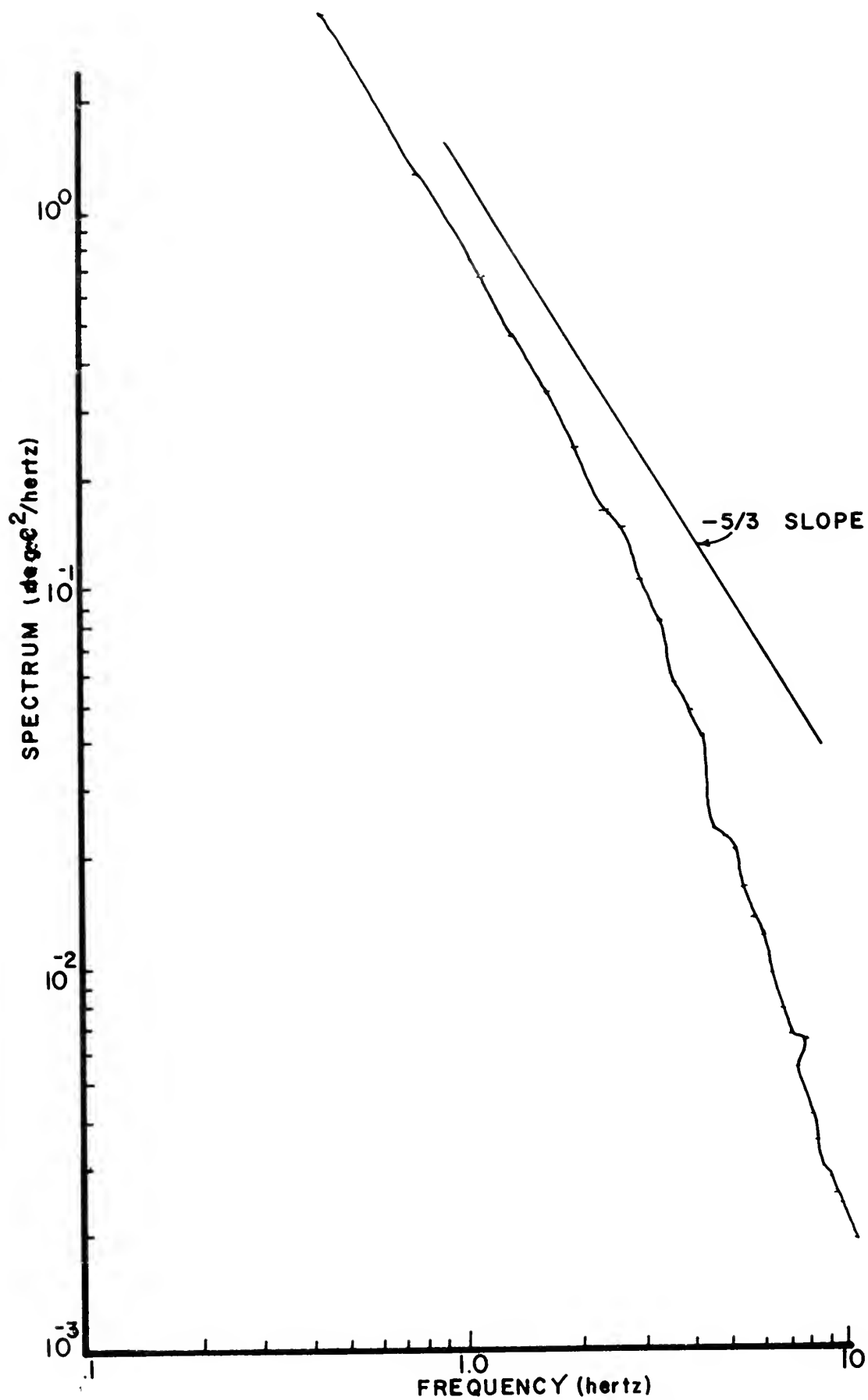


FIG. 21 - CASE 1 - HIGH FLOATING THERMISTOR

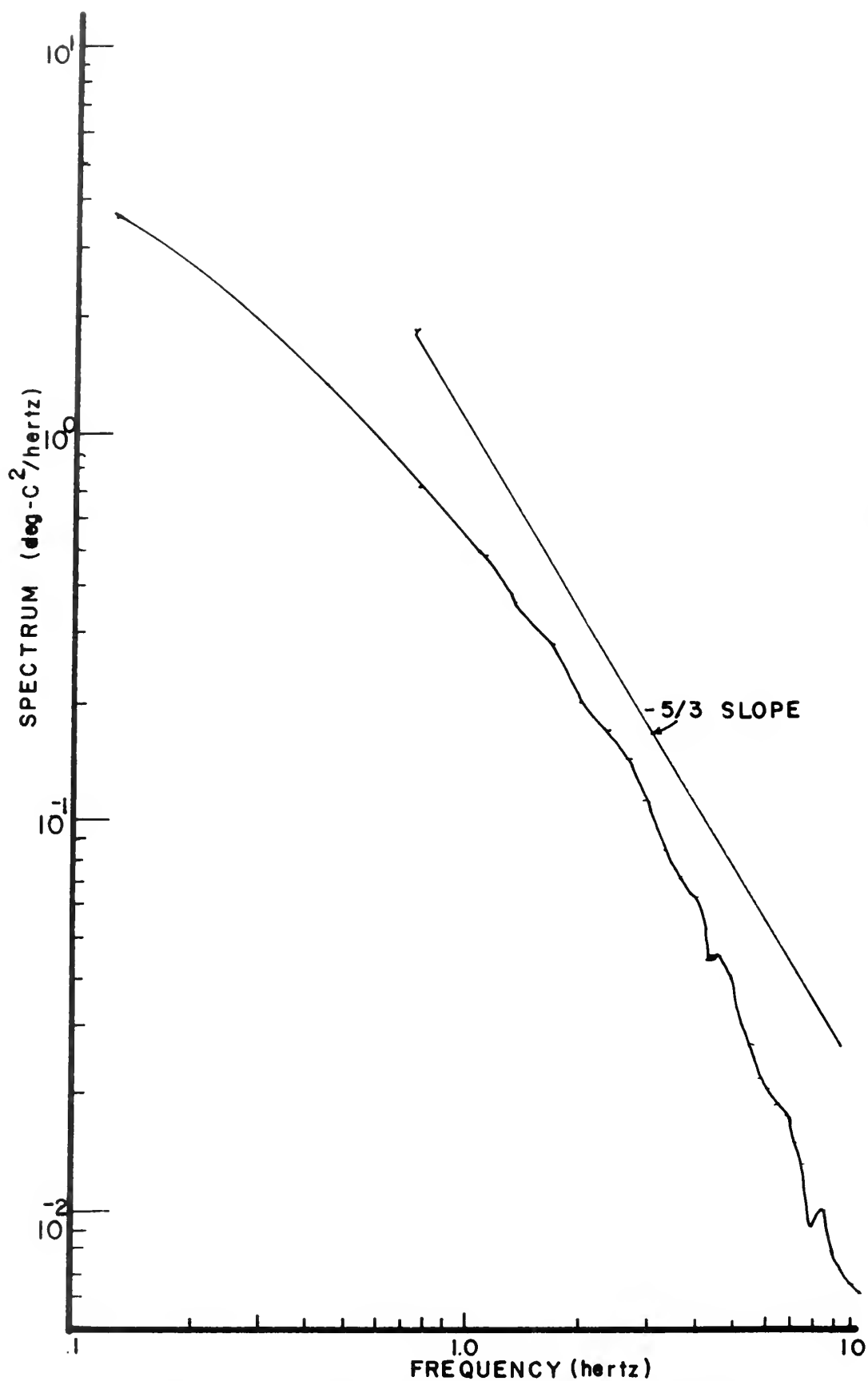


FIG 22 -CASE 1- HIGH FIXED THERMISTOR

Figures 23 and 24 indicate no coherence between the temperatures and wave records. The values obtained are no better than can be expected for random data. This result is not unexpected since the thermistors were more than 50 cm greater than the wave height.

The coherence between the two temperature signals (figure 25), as expected, is excellent at low frequencies and falls off with increasing frequency. The fall-off is remarkably constant ( $-0.07/\text{Hz}$ ). The low value at 0.15 Hz is again probably a function of the analog to digital conversion process. The temperature signal from the floating thermistor seems to lag the fixed thermistor; the lag increases with frequency from 4 to 30 degrees (figure 25).

#### B. CASE 2

A micro-bead thermistor was placed on the follower arm 24.4 cm above the instantaneous sea surface height. A second thermistor was placed on the slide 7.6 cm above mean position of the first thermistor. These measurements were made between 0748 and 0815 on 21 July 1969.

Environmental data were:

Wind direction  $270^{\circ}\text{T}$

Wave direction  $280^{\circ}\text{T}$

Water temperature  $19.8^{\circ}\text{C}$

Air temperature  $19.5^{\circ}\text{C}$

Mean wind speed 1.4 m/sec

Clear morning

Water depth 2.3 meters flooding tide

Critical height could not be determined due to slow wind speed

$\theta$  = PHASE ANGLE (degrees)  
 POSITIVE MEANS THERMISTOR LAGS WAVES

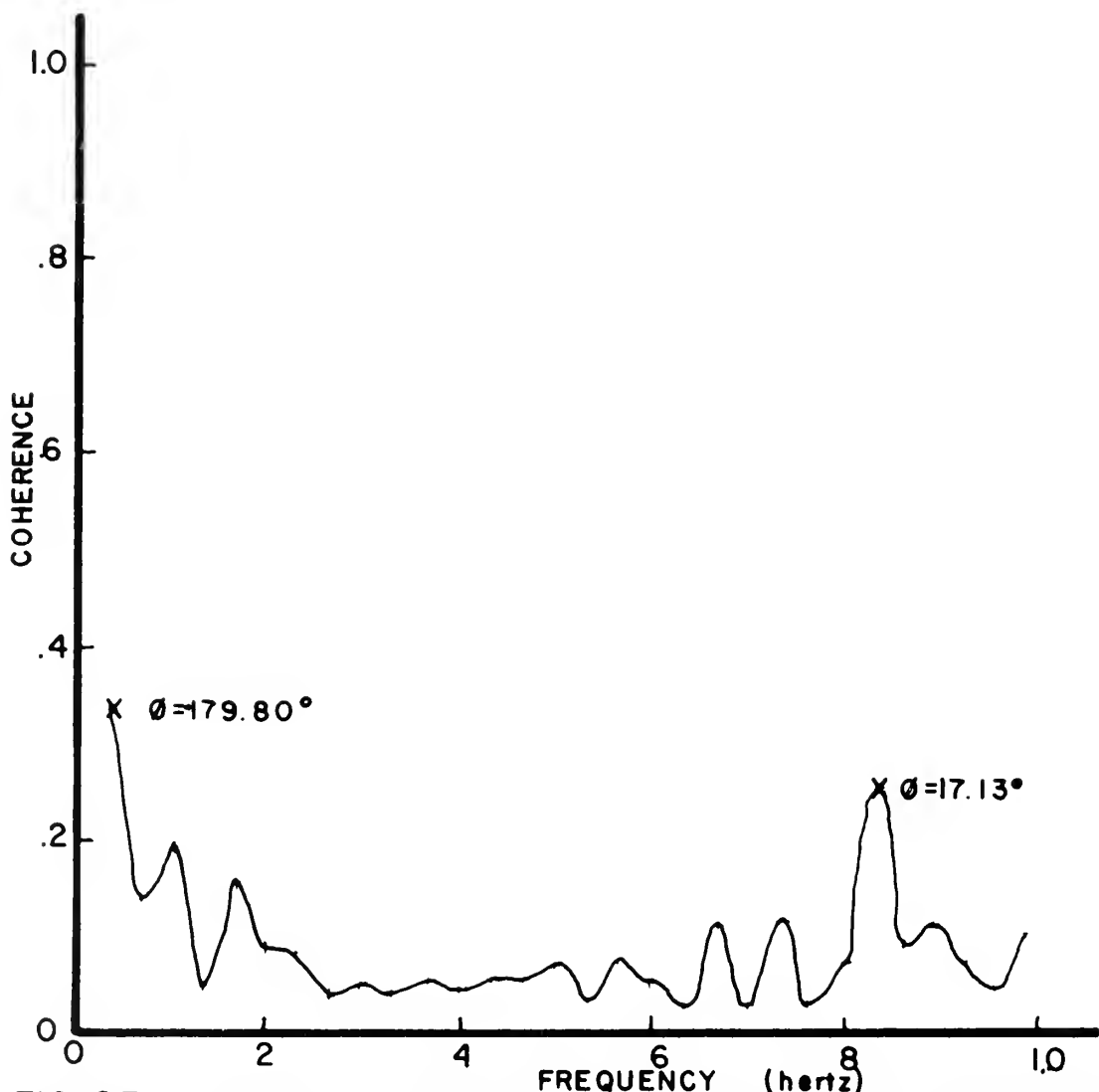


FIG.23 -CASE 1 - COHERENCE BETWEEN WAVES AND HIGH FLOATING THERMISTOR

$\phi$  = PHASE ANGLE(degrees)  
 POSITIVE MEANS THERMISTOR LAGS WAVE

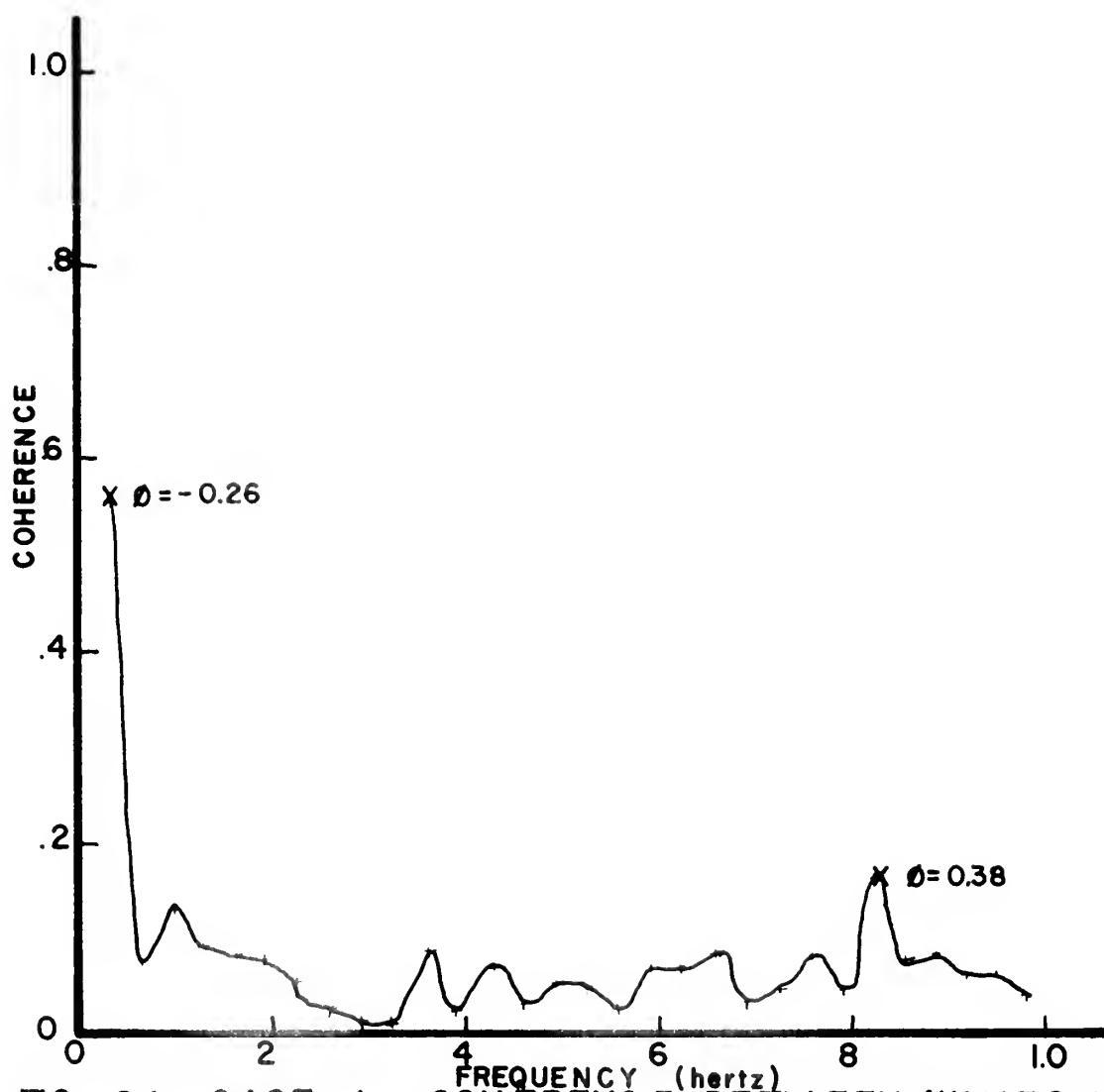


FIG. 24 -CASE 1 - COHERENCE BETWEEN WAVES AND HIGH FIXED THERMISTOR

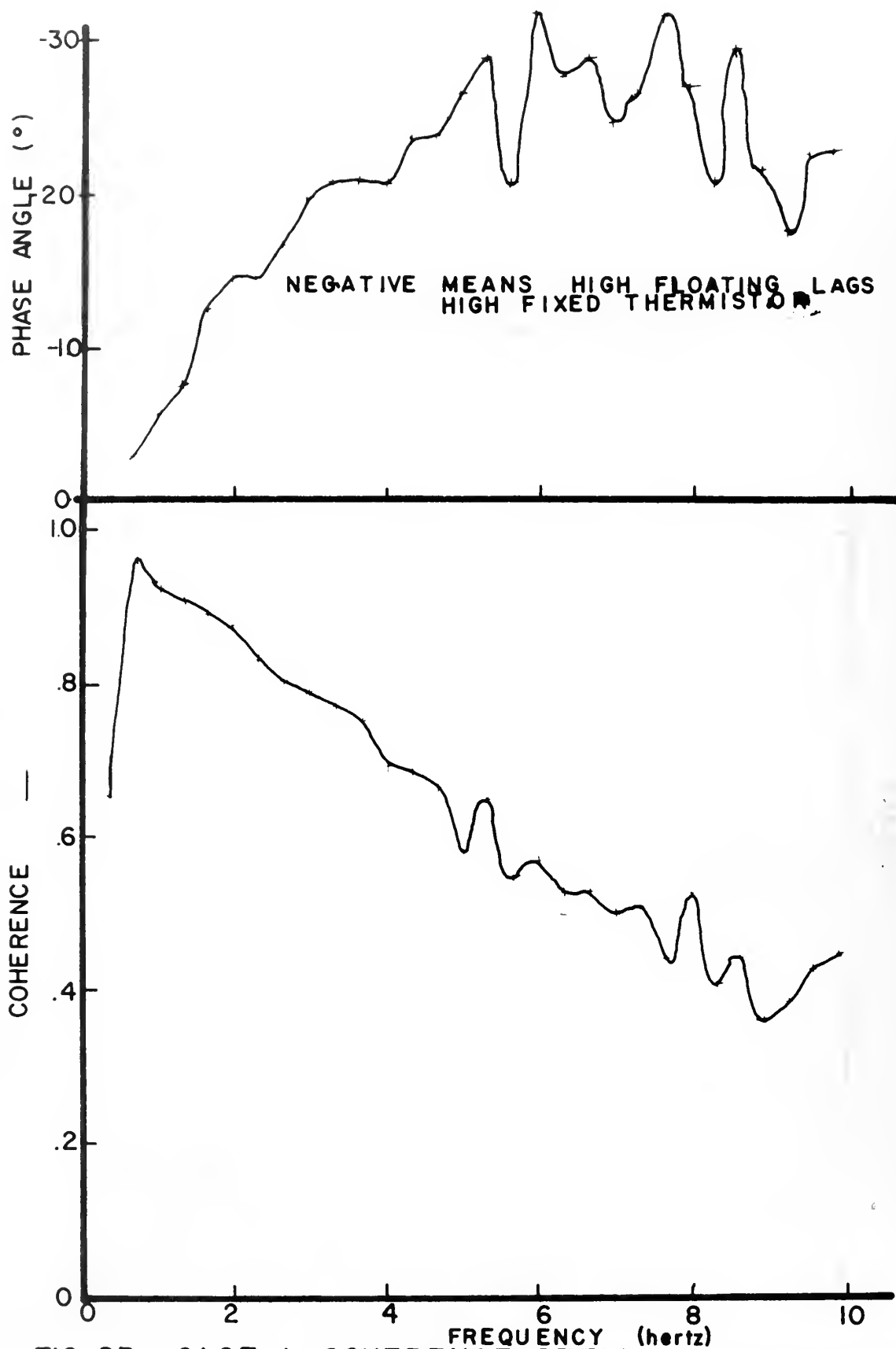


FIG. 25 - CASE 1- COHERENCE BETWEEN HIGH FIXED  
AND HIGH FLOATING THERMISTOR



No digital analysis was done on this data due to a lack of computer time. Several important items can be deduced from figure 26. While the thermistor records are 180 degrees out of phase with the wave record, there is a definite correlation. Since the thermistor signal was inverted during conditioning, the temperature goes up as the wave goes up. The signal from the floating thermistor, a constant distance above the surface, is smaller than the signal from the thermistor attached to the slide.

### C. CASE 3

In this case, two micro-bead thermistors were placed on the follower arm one 24 cm above the sea surface, and the other 7 cm above the surface. The data for this case were taken between 0843 and 0943 and 0913 on 21 July 1969. Environmental data for this run consisted of:

Wind calm (under 1 m/sec)

Air temperature 19.8°C

Critical height could not be determined

Water depth 2.5 meters, flooding tide

Clear sky

This case was presented to determine the response of thermistors under these conditions. No digital analysis was done. While the intermediate thermistor worked well, the lower thermistor was being splashed continuously as shown in figure 27. This splashing caused high frequency spikes in the record. If the spikes are visually removed, some correlation among signals appears.

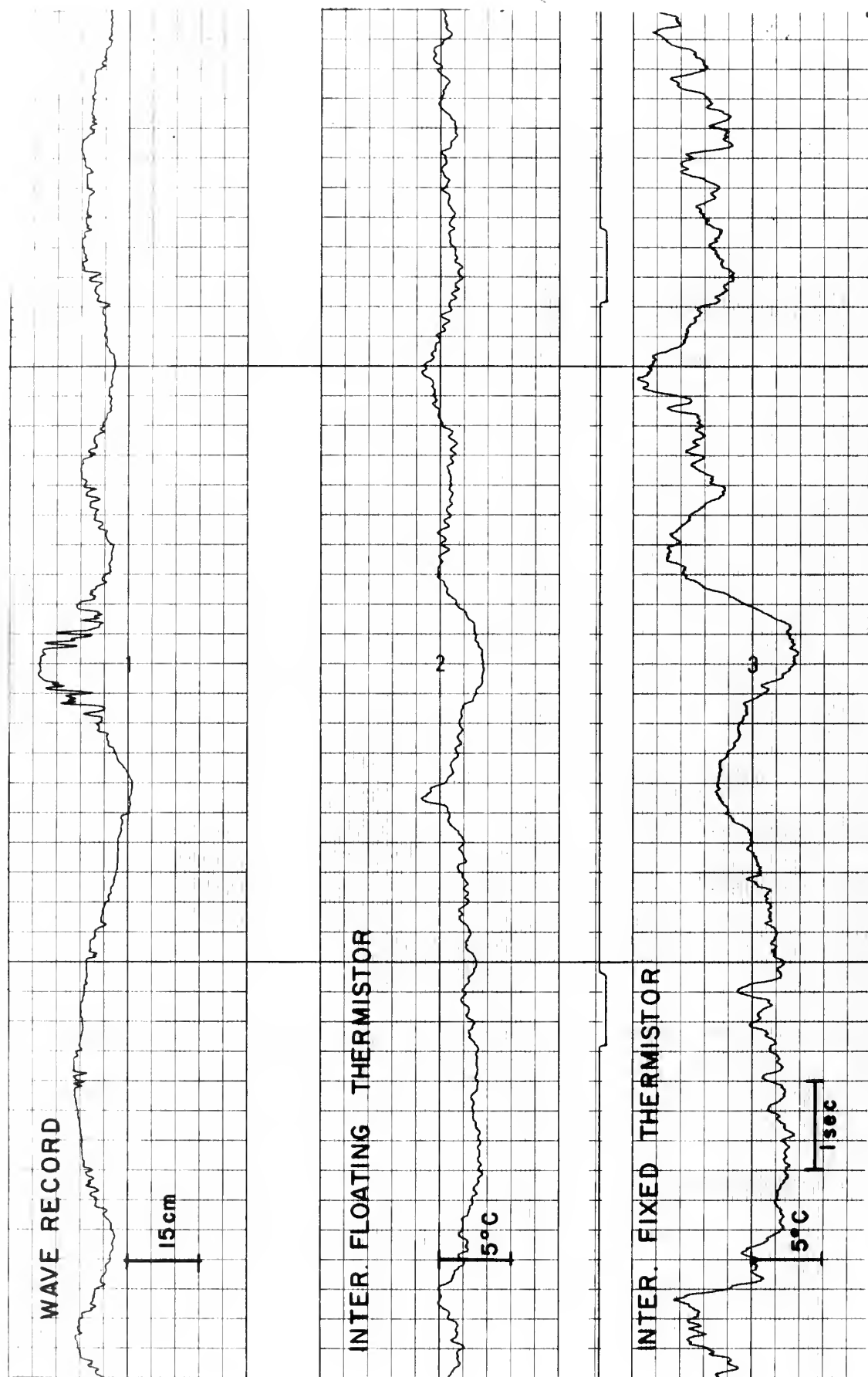


FIGURE 26 SAMPLE RECORD FROM CASE 2

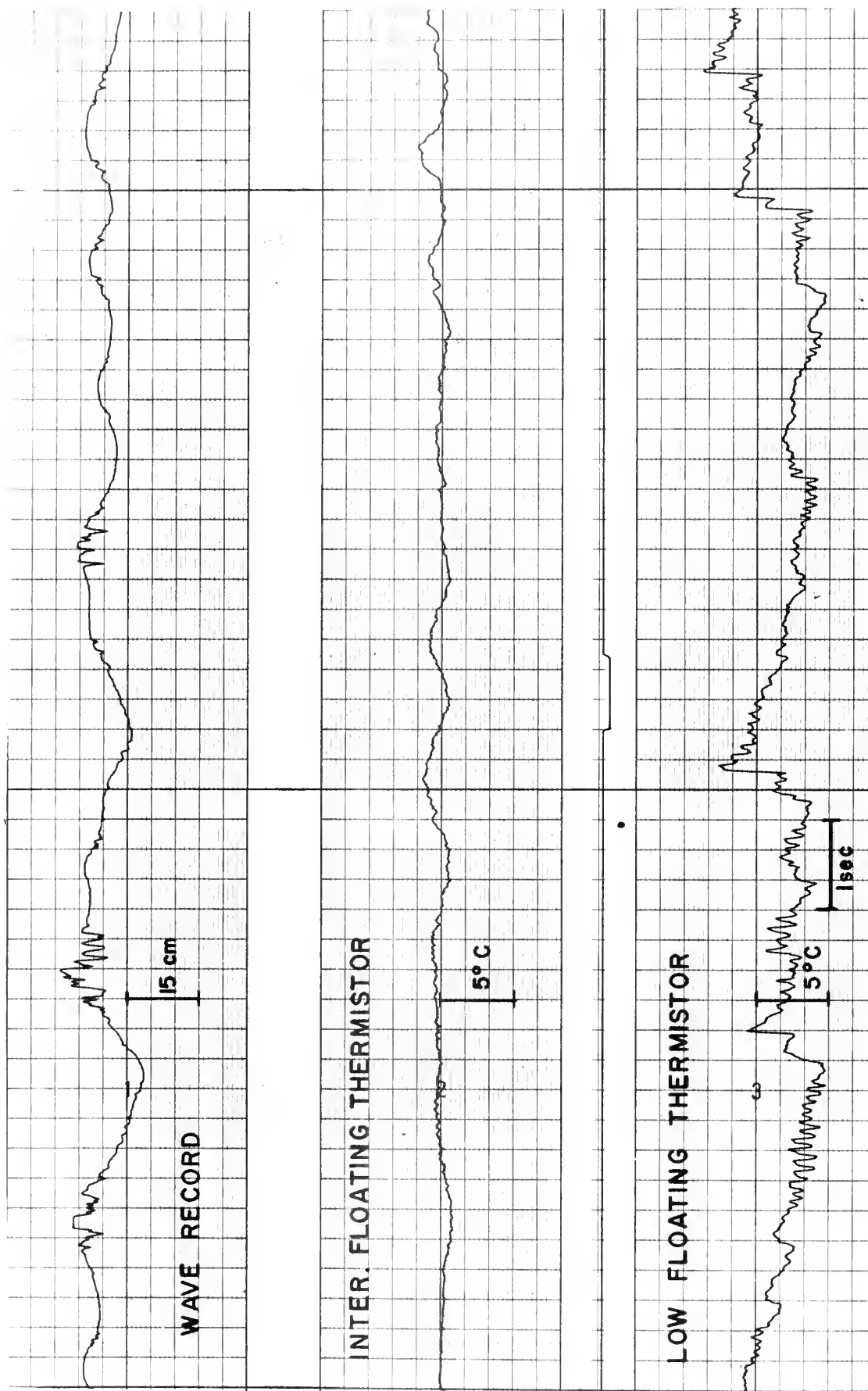


FIGURE 27 SAMPLE RECORD FROM CASE 3

#### D. CASE 4

Two thermistors were placed on the follower arm. One thermistor was attached 7 cm and the other 1 cm above the waves. As in the previous case, problems were encountered with thermistors wetting. While the 7 cm thermistor worked better than in the previous case, the splashing made the 1 cm thermistor record useless (figure 28). The data for this case were taken between 1250 and 1327 on 22 July 1969. No digital analysis was done on this case. Environmental data for this case were:

Mean wind speed

1.2 meters above sea surface = 3.29 m/sec

1.5 meters above sea surface = 3.25 m/sec

1.7 meters above sea surface = 3.40 m/sec

2.7 meters above sea surface = 3.50 m/sec

Wind direction 285°T

Wave direction 280°T

Wet bulb temperature 16.2°C

Dry bulb temperature 18.1°C

Water temperature 19.6°C

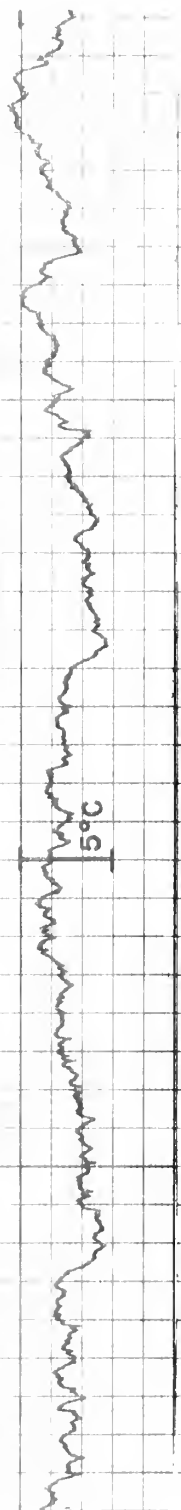
Sky hazy

Critical height could not be determined because the characteristic wave speed, computed by taking the dominant wave period from the record and computing the theoretical wave speed, was 4.68 m/sec.

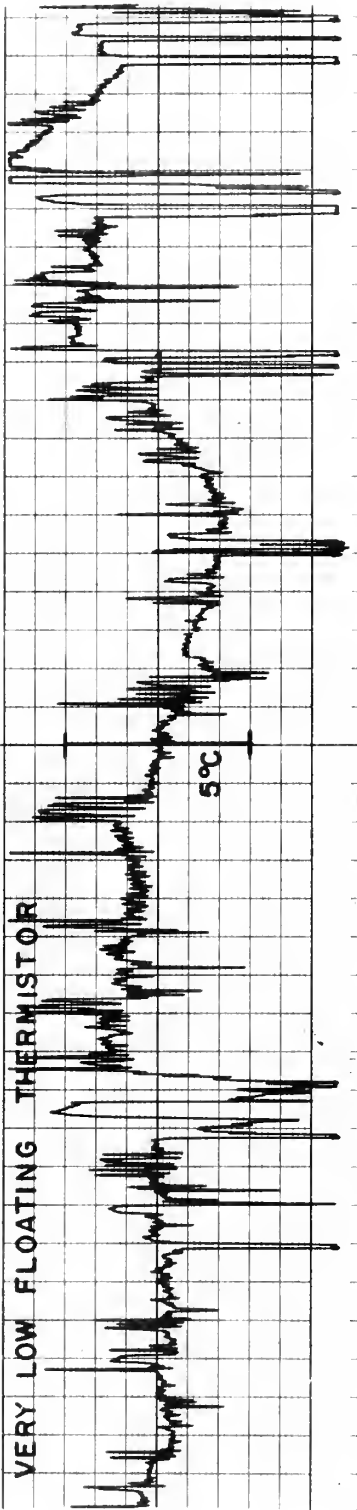
#### E. CASE 5

Case 5 begins velocity measurements in place of the temperature measurements made in the previous four cases. In Case 5, a hot-film

LOW FLOATING THERMISTOR



VERY LOW FLOATING THERMISTOR



WAVE RECORD

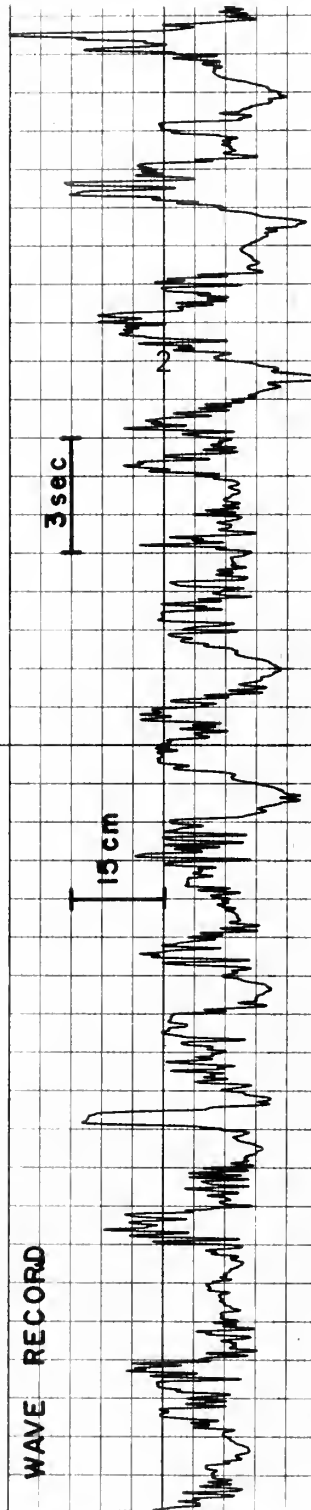


FIGURE 28 SAMPLE RECORD FOR CASE 4

sensor was placed 78 cm above the sea surface and another was fixed to the slide such that the mean position of the sensor following the waves coincides with the sensor following the waves. The data for this case were taken between 1710 and 1740 on 22 July 1969. The environmental information associated with this data were:

Wind direction 275°T

Wave direction 275°T

Wet bulb temperature 17.8°C

Dry bulb temperature 21.3°C

Water temperature 20.8°C

Mean wind speed

1.2 meters above sea surface = 3.91 m/sec

1.5 meters above sea surface = 3.90 m/sec

1.7 meters above sea surface = 4.14 m/sec

2.7 meters above sea surface = 4.26 m/sec

Clear sky

Water depth 2.5 meters, flooding tide

Critical height 88 cm

Since the critical height is above the measurement point by 10 cm, the observed data are quite important and 16 minutes of data were digitally analyzed. Figures 29, 33, and 34 show that in this case there was almost no interaction between the waves and the velocity spectra. This tends to support Stewart's hypothesis (1967) rather than that of Miles (1962). The sea surface spectra (figure 30) tends to show a  $-5/3$  power law only above 1 Hz. Late in the day a swell developed at the site which increased the low frequency part of the spectrum. The spectra of the velocity records (figures 31 and 32) show a strong  $-5/3$  slope. The two velocity records are quite well correlated which was expected (figure 35).

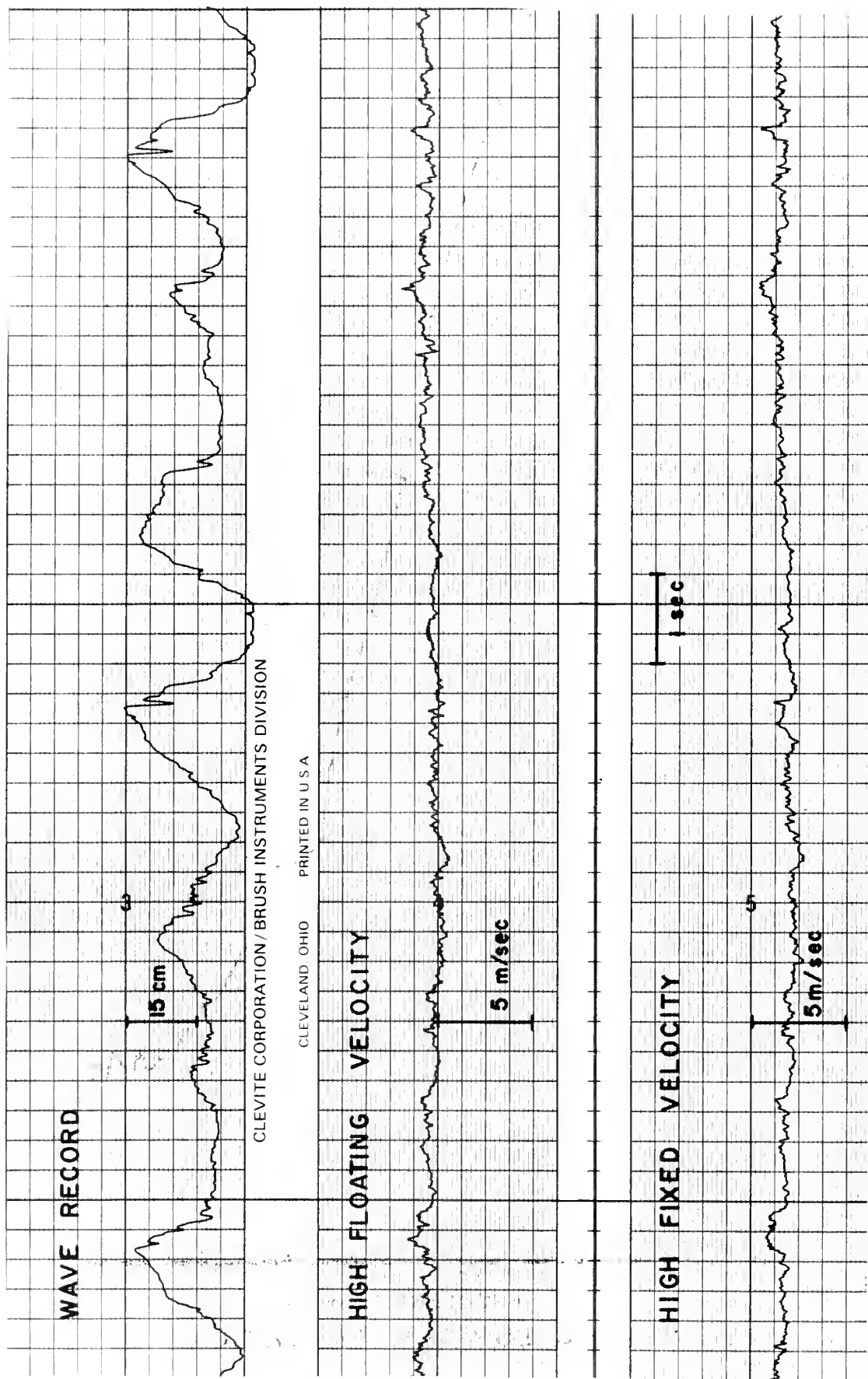


FIGURE 29 SAMPLE RECORD FOR CASE 5

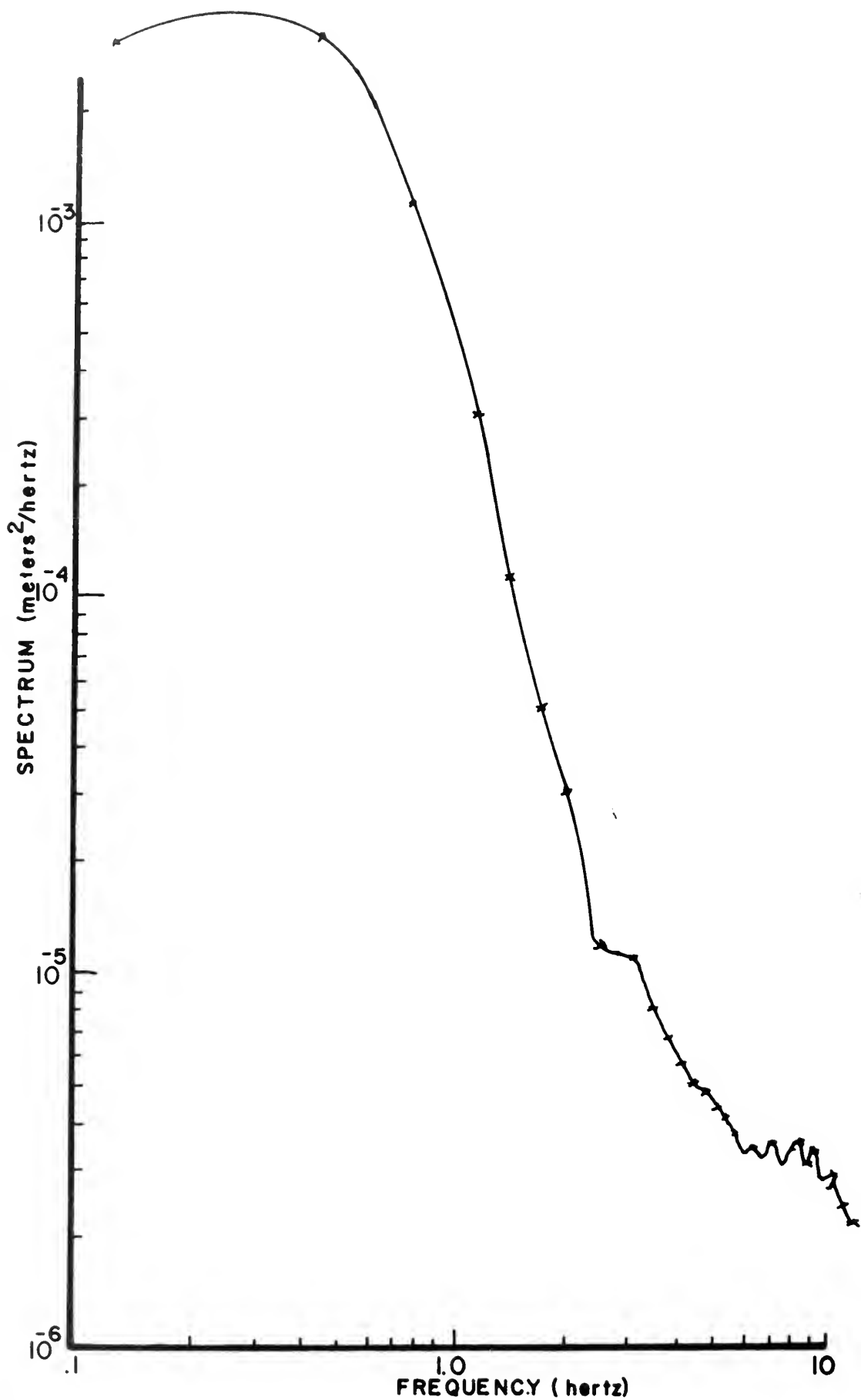


FIG. 30 - CASE 5 - SEA SURFACE ELEVATION



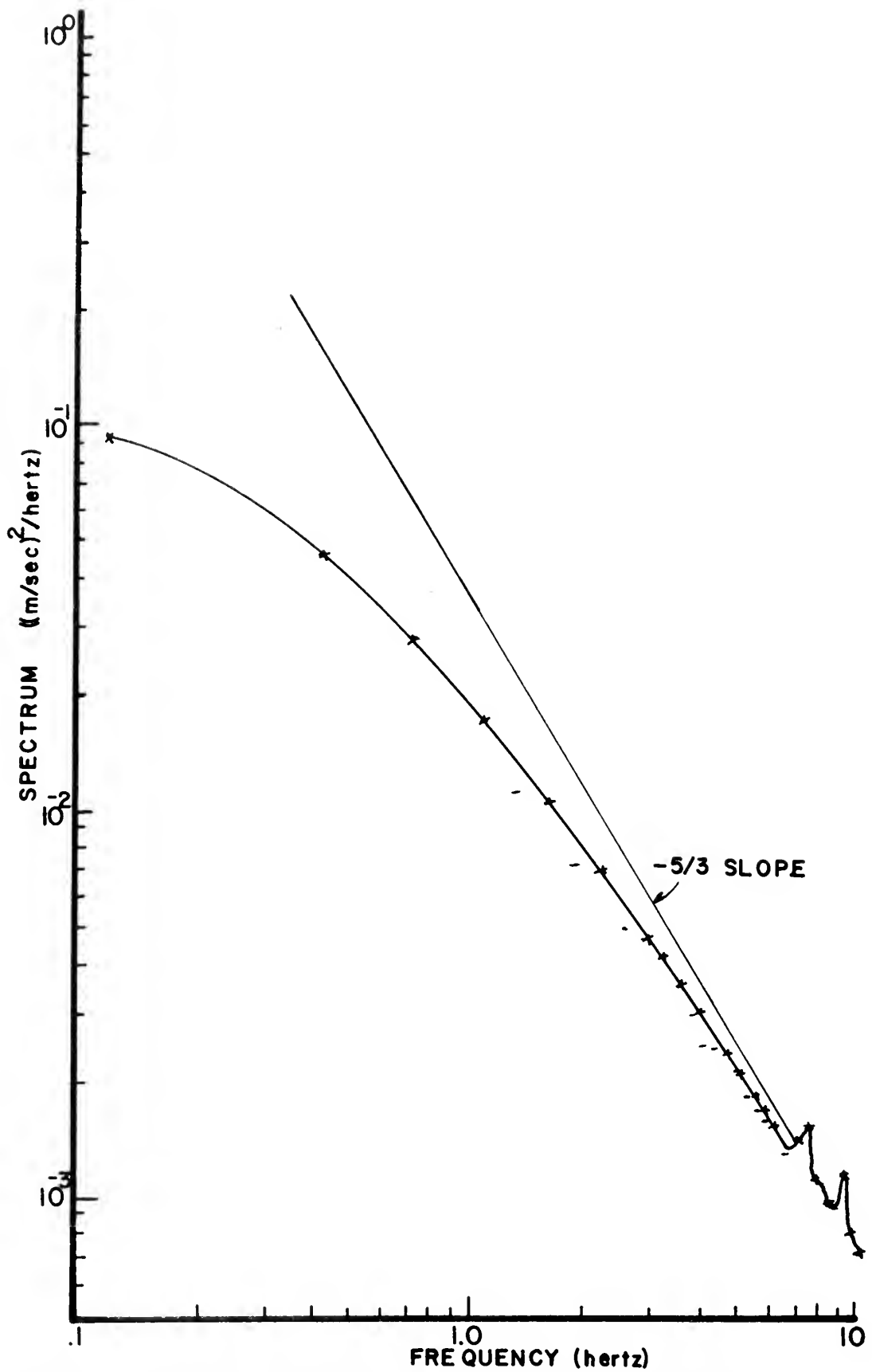


FIG. 31 - CASE 5 - HIGH FLOATING VELOCITY

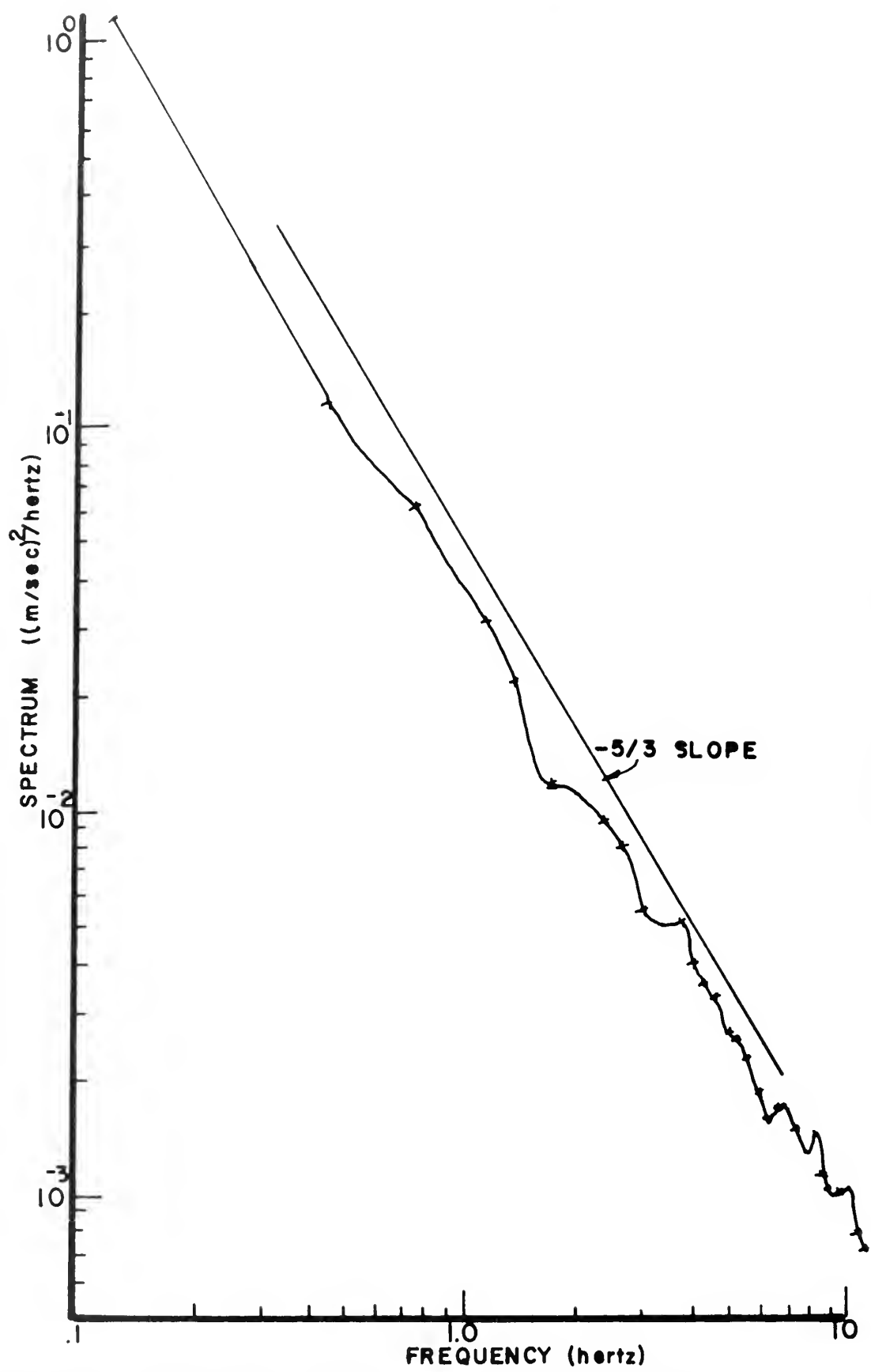


FIG. 32 - CASE 5 - HIGH FIXED VELOCITY

$\theta$  = PHASE ANGLE  
 POSITIVE MEANS VELOCITY LAGS WAVES

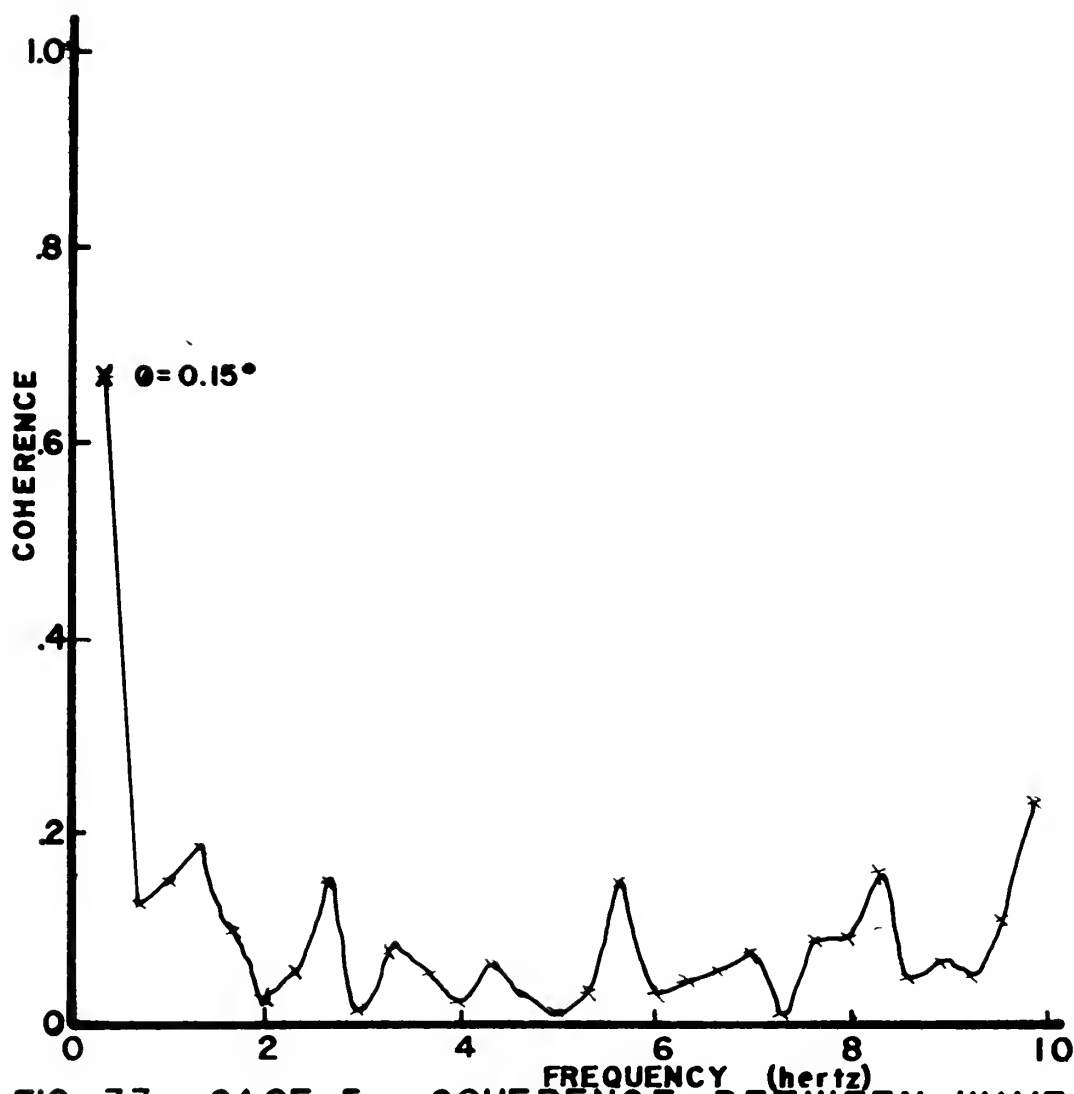


FIG. 33 - CASE 5 - COHERENCE BETWEEN WAVES AND HIGH FLOATING VELOCITY

$\emptyset$  = PHASE ANGLE  
POSITIVE MEANS VELOCITY LAGS WAVES

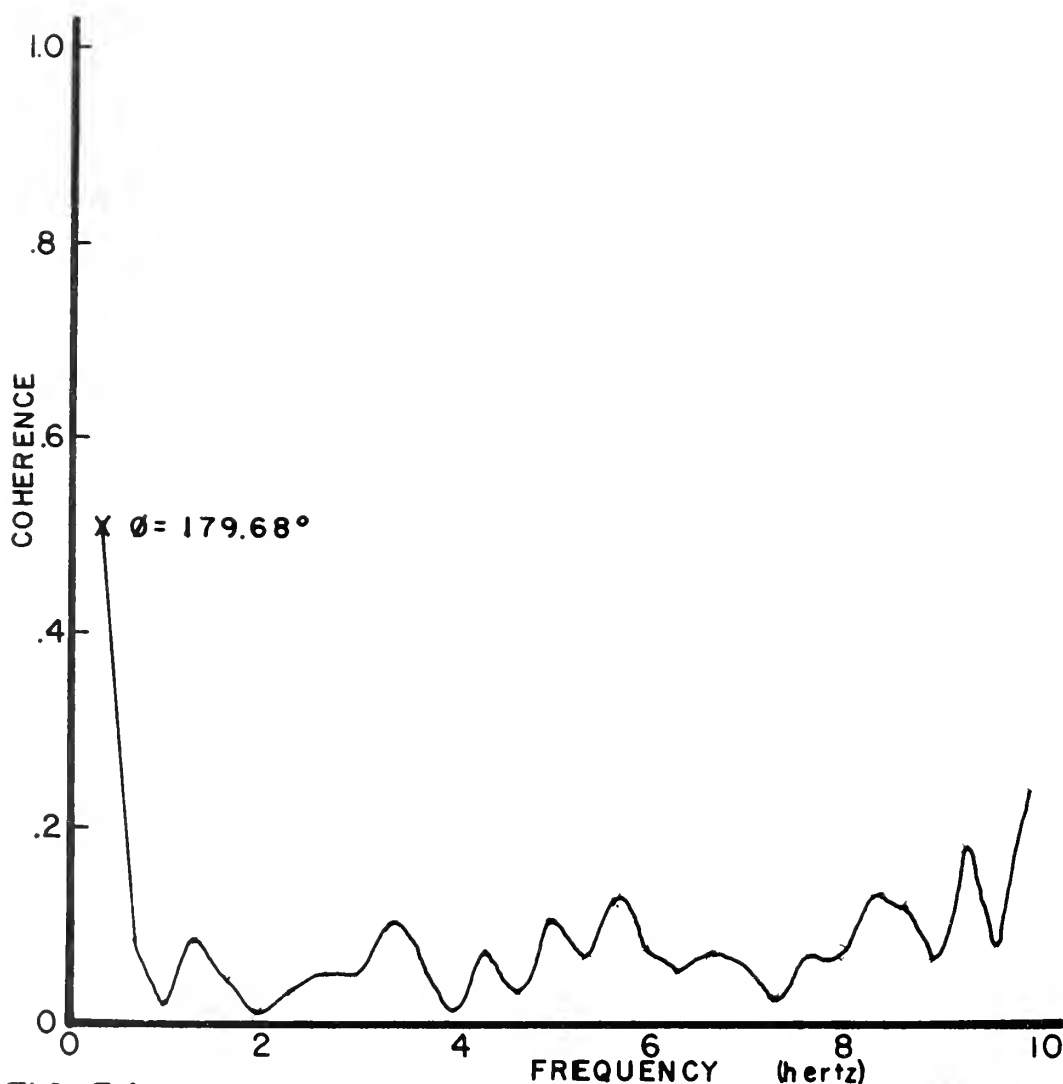


FIG. 34 - CASE 5 - COHERENCE BETWEEN WAVES AND HIGH FIXED VELOCITY

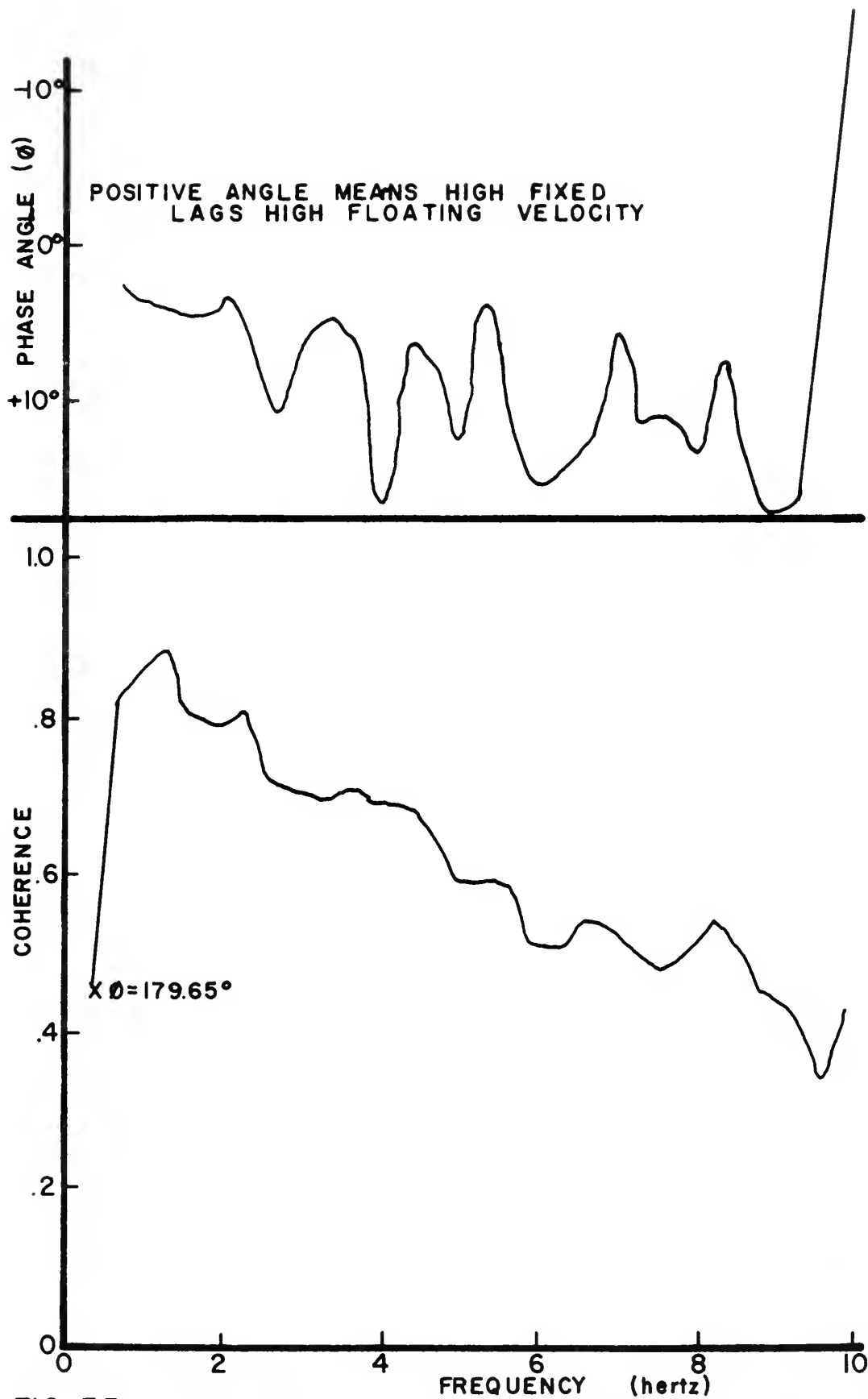


FIG. 35 -CASE 5- COHERENCE BETWEEN HIGH FIXED AND HIGH FLOATING VELOCITY

## F. CASE 6

Two hot-film velocity sensors were placed on the wave follower, one sensor 78 cm above the sea surface, and the other 24 cm above the sea surface. The data were taken from 1812 to 1840 on 22 July 1969. Sixteen minutes of data were analyzed.

The environmental information consisted of:

Wind direction 210°T

Swell direction 260°T; mast aligned with swells

Mean wind speed

1.2 meters above sea surface = 1.37 m/sec

1.5 meters above sea surface = 1.35 m/sec

1.7 meters above sea surface = 1.42 m/sec

2.7 meters above sea surface = 1.46 m/sec

Wet bulb temperature 18.2°C

Dry bulb temperature 20.3°C

Water temperature 21°C

Clear day

Water depth 2.6 meters, flooding tide

Critical height cannot be determined because mean wave speed is 1.5 m/sec

Figures 36-42 point out several things about this non-generating case. First, there is very little correlation among any of the signals. It might be expected that the 24 cm sensor would show more correlation in a generating case. It appears that the 24 cm sensor does tend to follow the wave record better than the 78 cm sensor, but the correlation is still not good. All spectra appear to have some region in which the slope on a log-log plot is  $-5/3$ .

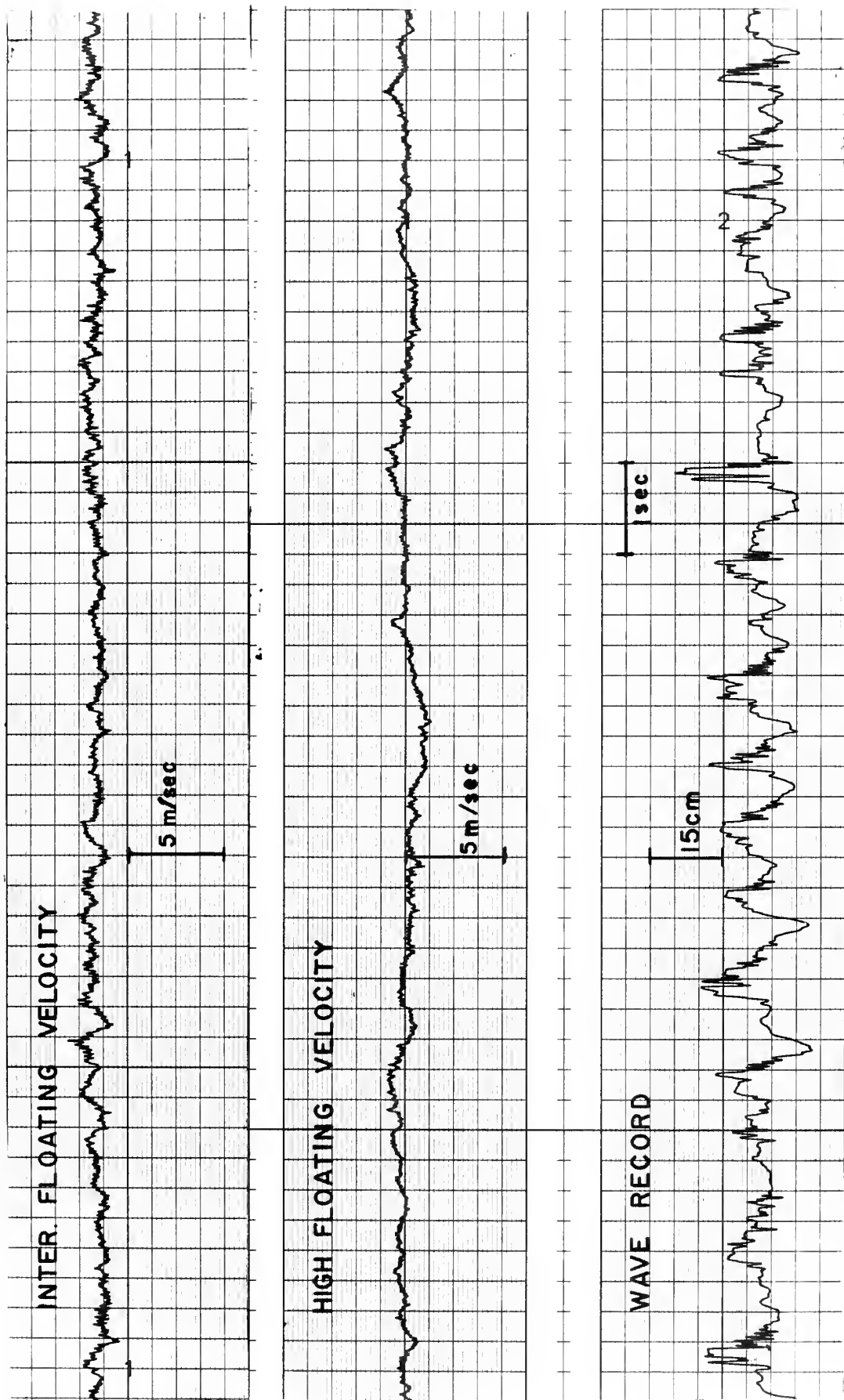


FIGURE-36 SAMPLE RECORD FOR CASE 6

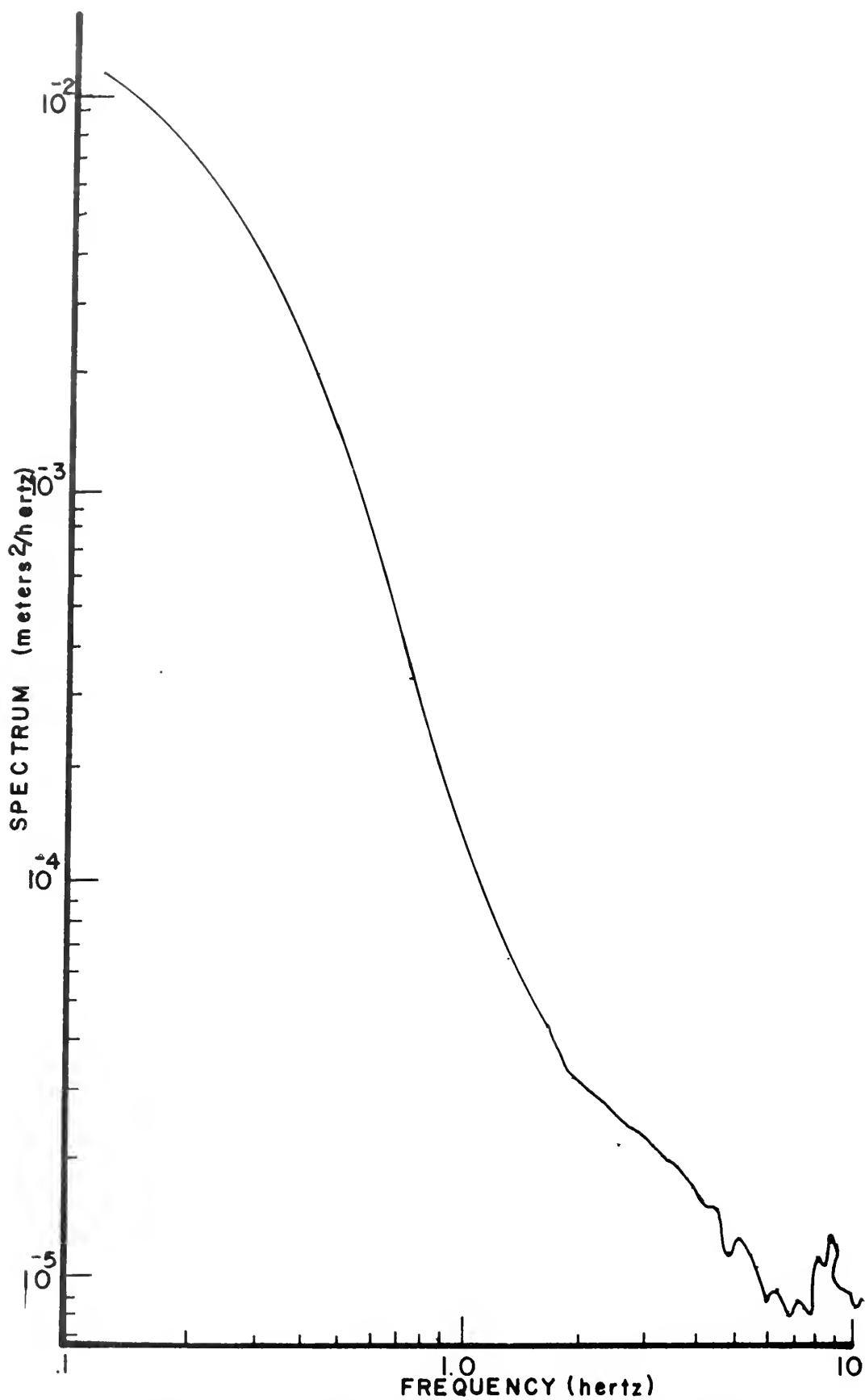


FIG. 37 -CASE 6- SEA SURFACE ELEVATION



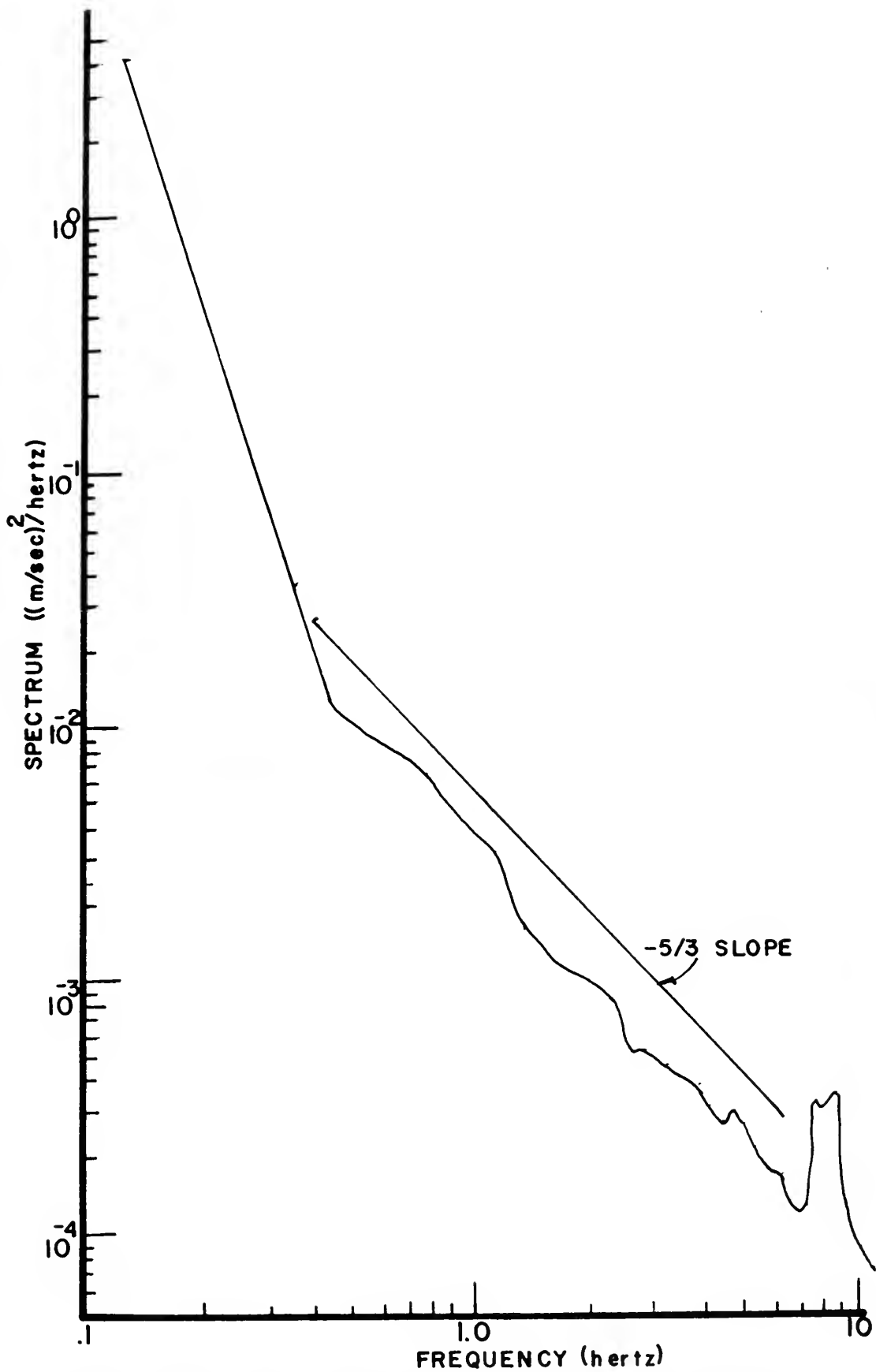


FIG. 38 - CASE 6 - HIGH FLOATING VELOCITY

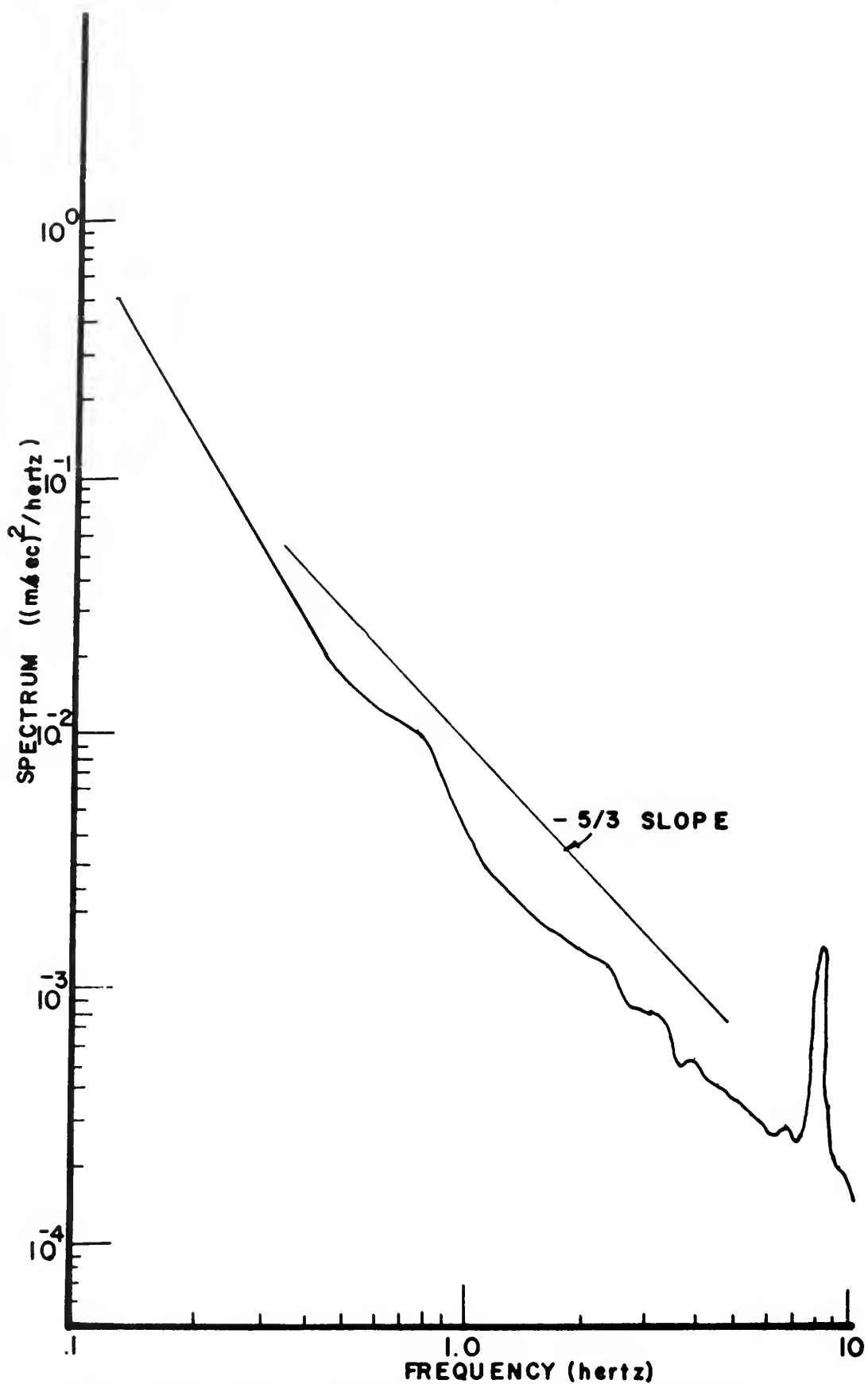


FIG. 39 - CASE 6 - INTER. FLOATING VELOCITY

$\emptyset$  = PHASE ANGLE  
 POSITIVE MEANS HIGH FLOATING VELOCITY  
 LAGS WAVES

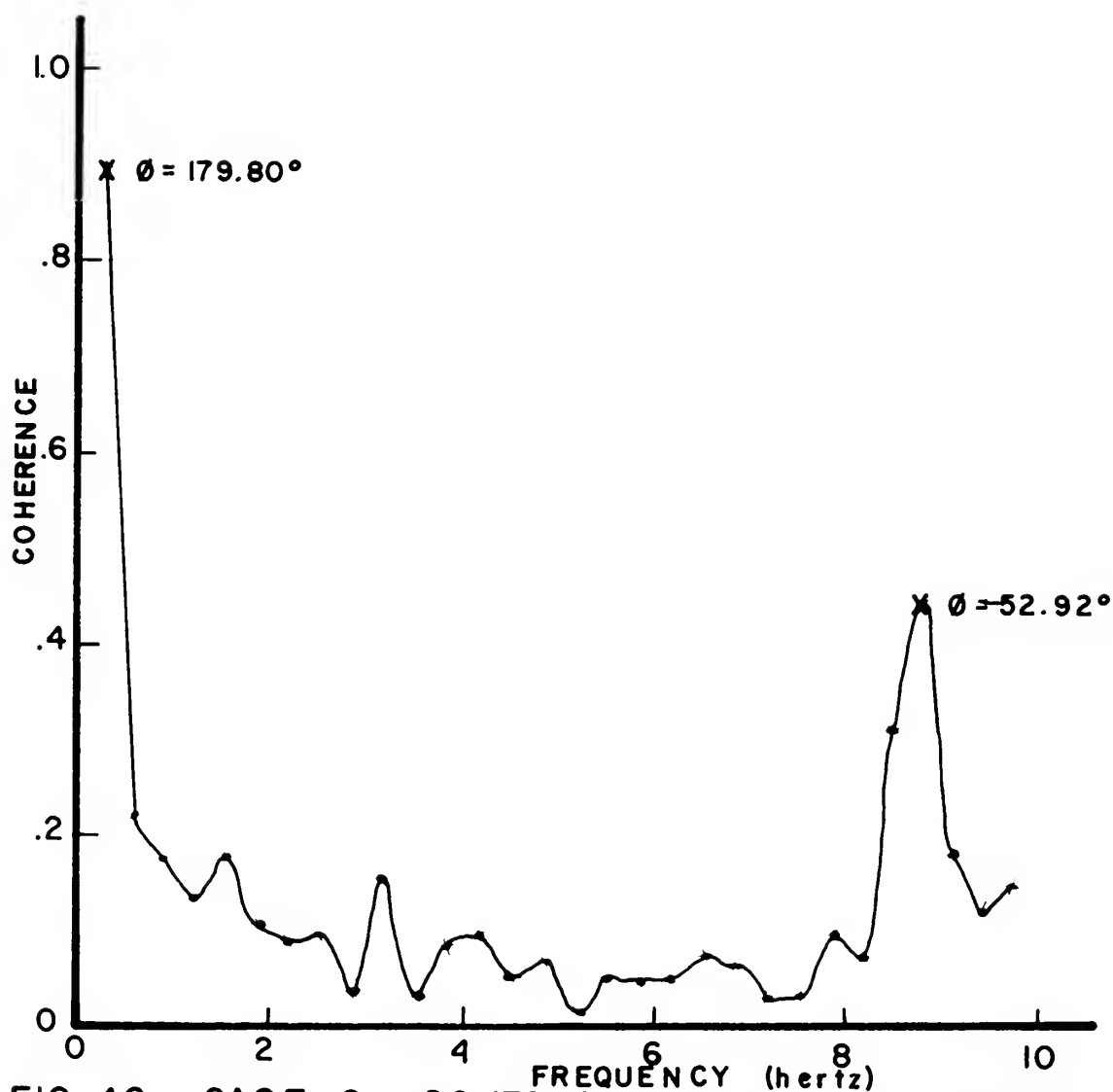


FIG. 40 -CASE 6 - COHERENCE BETWEEN WAVES AND HIGH FLOATING VELOCITY

$\emptyset$  = PHASE ANGLE

POSITIVE MEANS VELOCITY LAGS WAVES

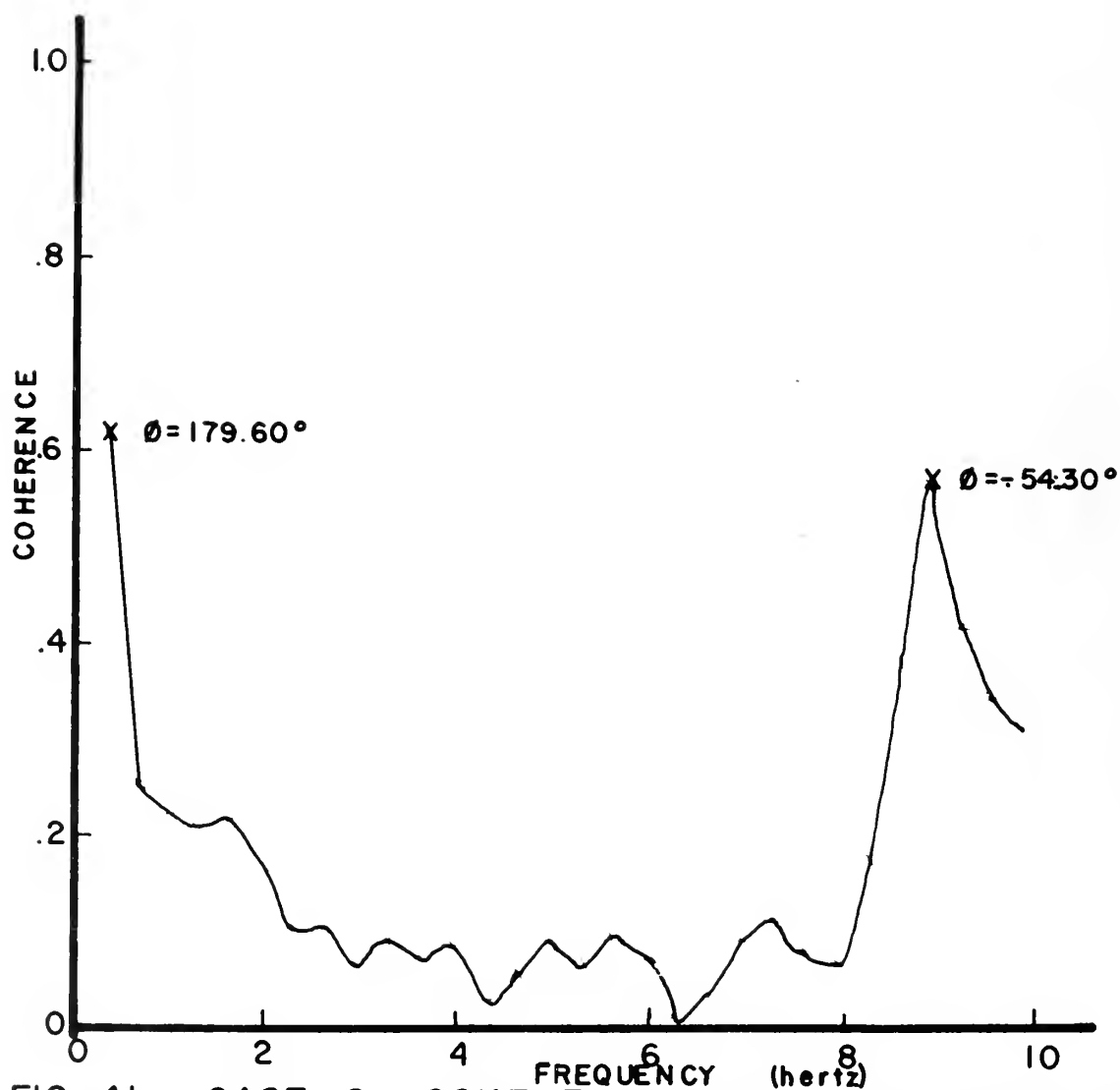


FIG. 41 - CASE 6 - COHERENCE BETWEEN WAVES AND INTER. FLOATING VELOCITY

$\phi$  = PHASE ANGLE  
 POSITIVE MEANS INTER. VELOCITY LAGS HIGH  
 VELOCITY

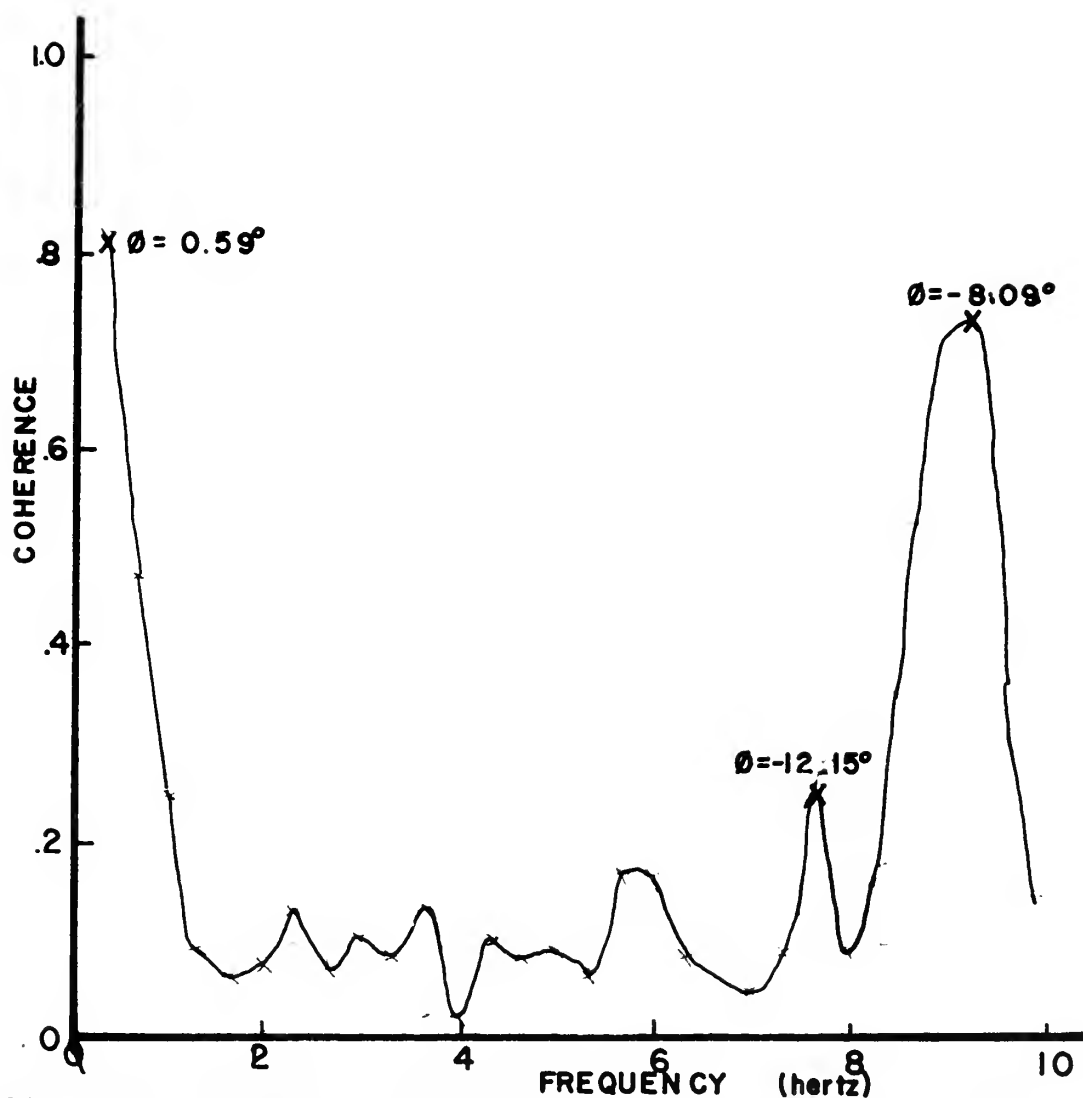


FIG. 42 - CASE 6 - COHERENCE BETWEEN HIGH  
 FLOATING AND INTER. FLOATING VELOCITY

The peaks that occur in the spectra (figures 37, 38, and 39) are a result of the deterioration of the signals. As the wave follower potentiometer deteriorated, due to sea water corrosion, a 9 Hz oscillation occurred whenever the potentiometer changed direction. This signal was imposed on the velocity sensors and becomes evident in their spectra as an energy peak at 9 Hz.

#### G. CASE 7

One velocity sensor was mounted 24 cm above the sea surface on the wave follower arm. The data for this case were taken between 1039 and 1109 on 23 July 1969 and digitally analyzed in three four minute sections since waves were being wind-generated during this run. Environmental information for this run was:

Wind and wave direction 280°T

Mean wind speed

1.2 meters above sea surface = 3.28 m/sec

1.5 meters above sea surface = 3.23 m/sec

1.7 meters above sea surface = 3.37 m/sec

2.7 meters above sea surface = 3.46 m/sec

Wet bulb temperature 16.9°C

Dry bulb temperature 18.0°C

Water temperature 19.8°C

Water depth two meters, flooding tide

Clear sky

Critical height 20 cm for part A, 24 cm for part B, and 28 cm for part C, due to increasing of wave height. This was determined by extrapolating the wind profile on a log profile to the sea surface, determining the wave speed theoretically from the wave record and finding the point where the wind speed equals the wave speed.

The sea surface record was quite noisy (figure 43) due to the deteriorating potentiometer. Attempts were made to filter this out prior to analysis. The remaining noise appears as peaks at the high end of the spectrum (figures 44, 47, and 50). This noise again interferes with the velocity spectra which was discussed in the previous case.

A surprising result is that the wave spectra (figures 44, 47, and 50) closely follow a  $-5/3$  power law dependency. This  $-5/3$  dependency appears to be great when the waves are being strongly generated and measurements taken near the critical height. This should be explored in greater detail. The velocity spectra also show a strong  $-5/3$  dependence, but this is expected. The divergence at the low end of all the digitally produced spectra is due to the short record analyzed (4 min).

The coherence plots (figures 46, 49, and 52) illustrate another feature which deserves further investigating. Superposition of these figures shows that the coherence increases as the sensor passes across the critical height level. While this does not indicate a strong coherence below the critical height plane, it does increase as the distance from the wave surface decreases.

#### H. CASE 8

A hot-film velocity sensor was placed on the wave follower 5 cm above the sea surface. Little trouble was encountered in obtaining measurements this close to the sea surface. This is attributed in part to the low impedance across the sensor (about 5 ohms). The data for this case were obtained between 1128 and 1208 on 23 July 1969. Sixteen minutes of data were digitally analyzed.

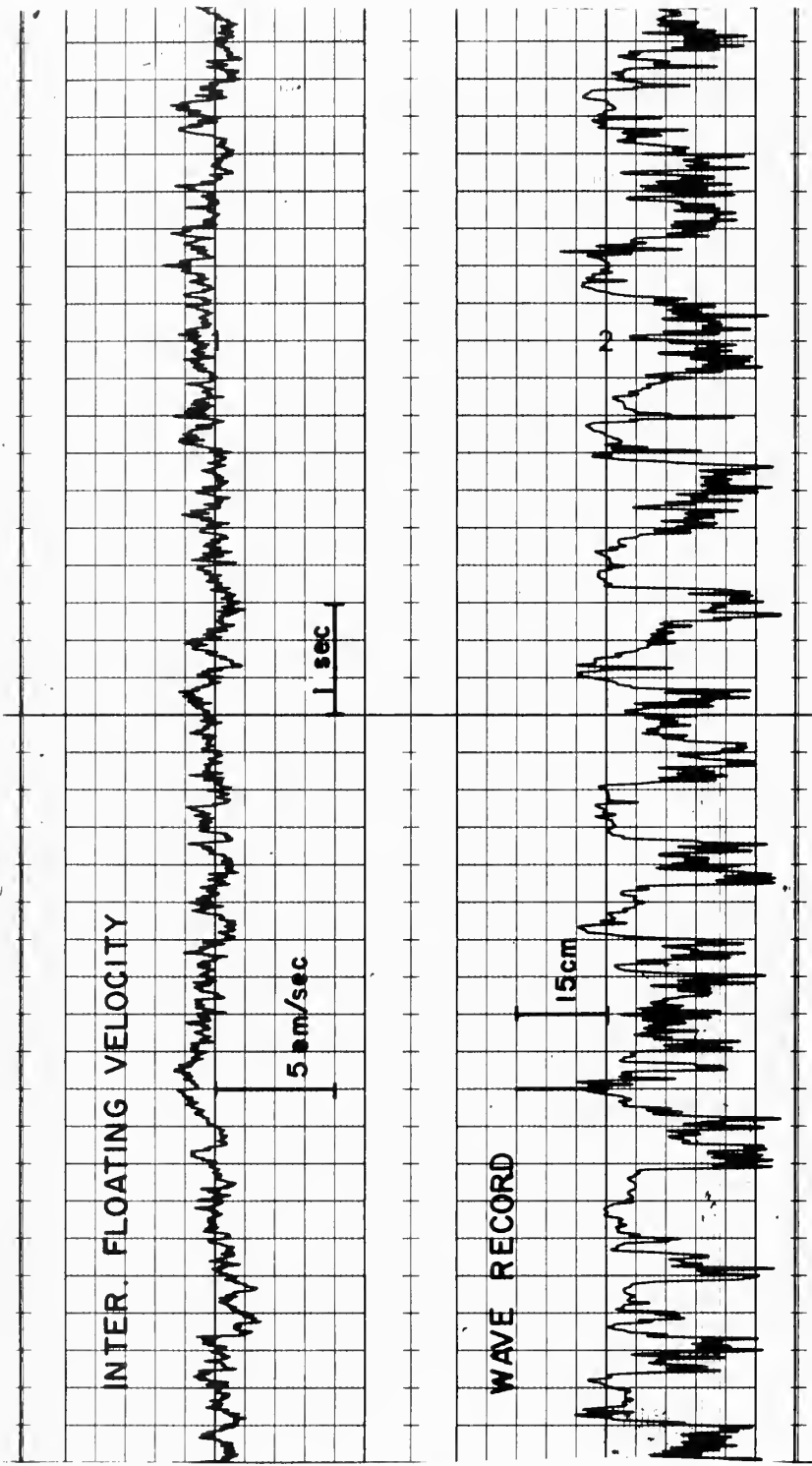


FIGURE-43 SAMPLE RECORD FOR CASE 7



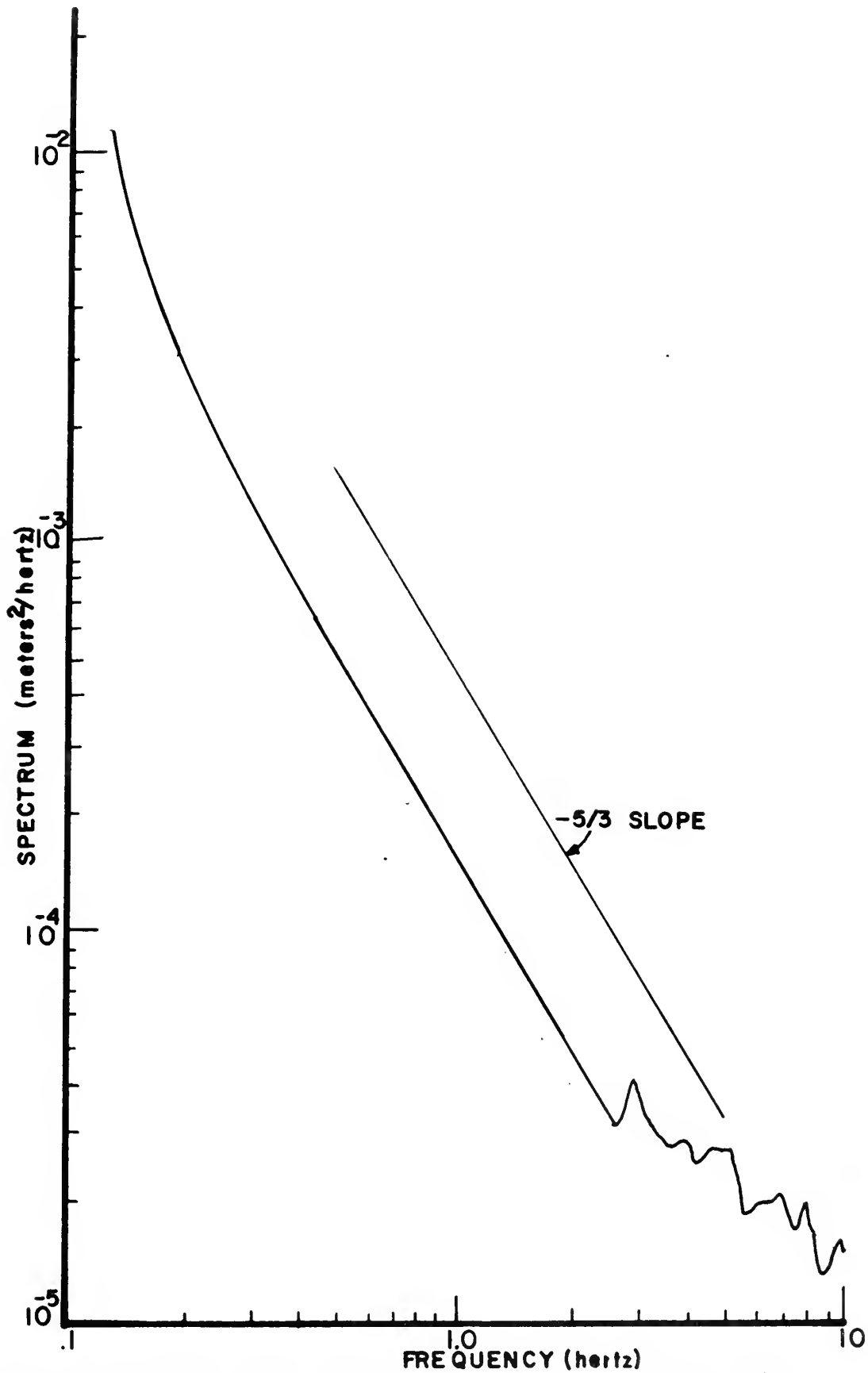


FIG.44 -CASE 7A- SEA SURFACE ELEVATION

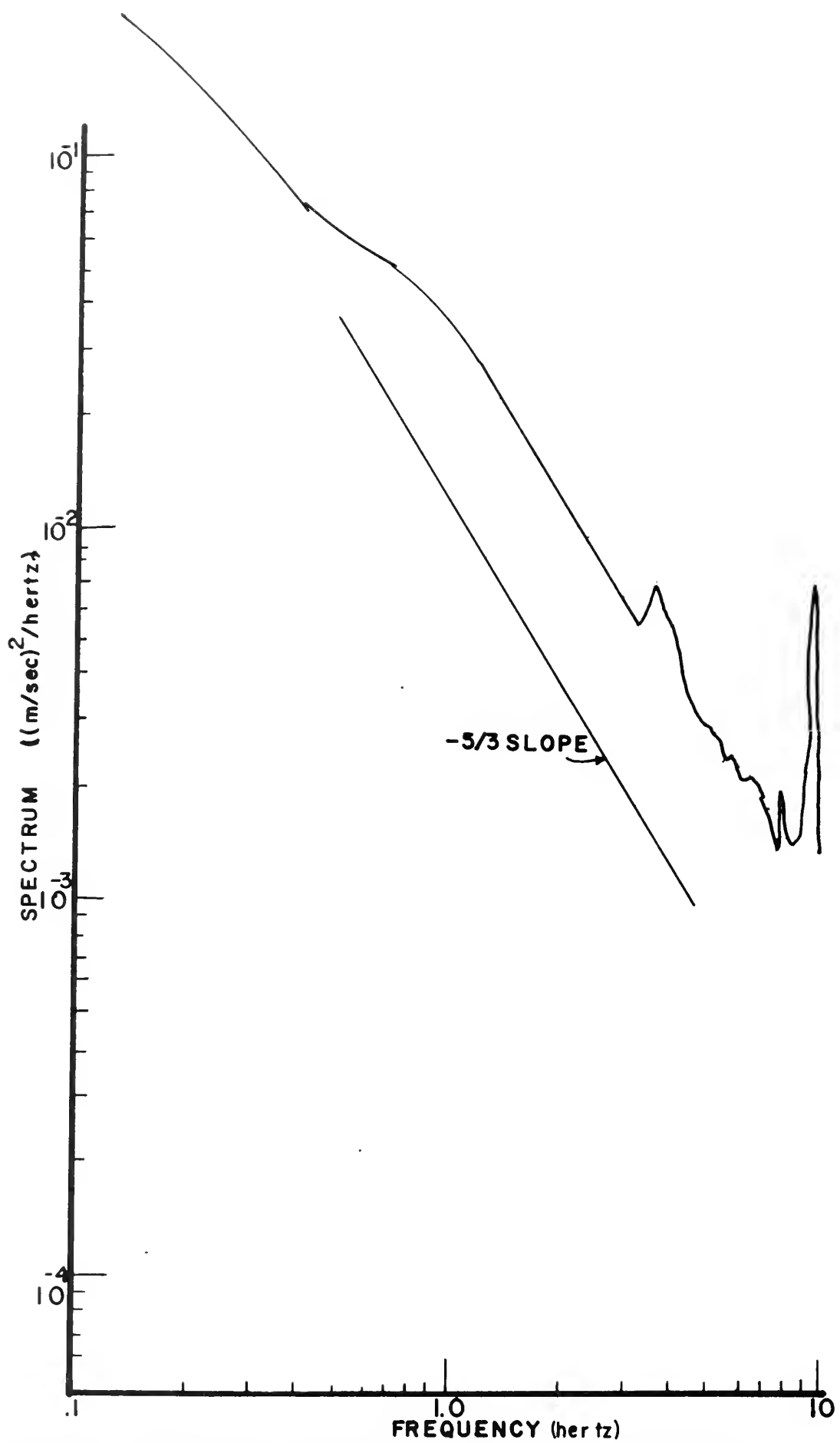


FIG. 45 -CASE 7A- INTER.FLOATING VELOCITY

$\emptyset$  = PHASE ANGLE  
 POSITIVE VALUES MEAN VELOCITY LAGS WAVES

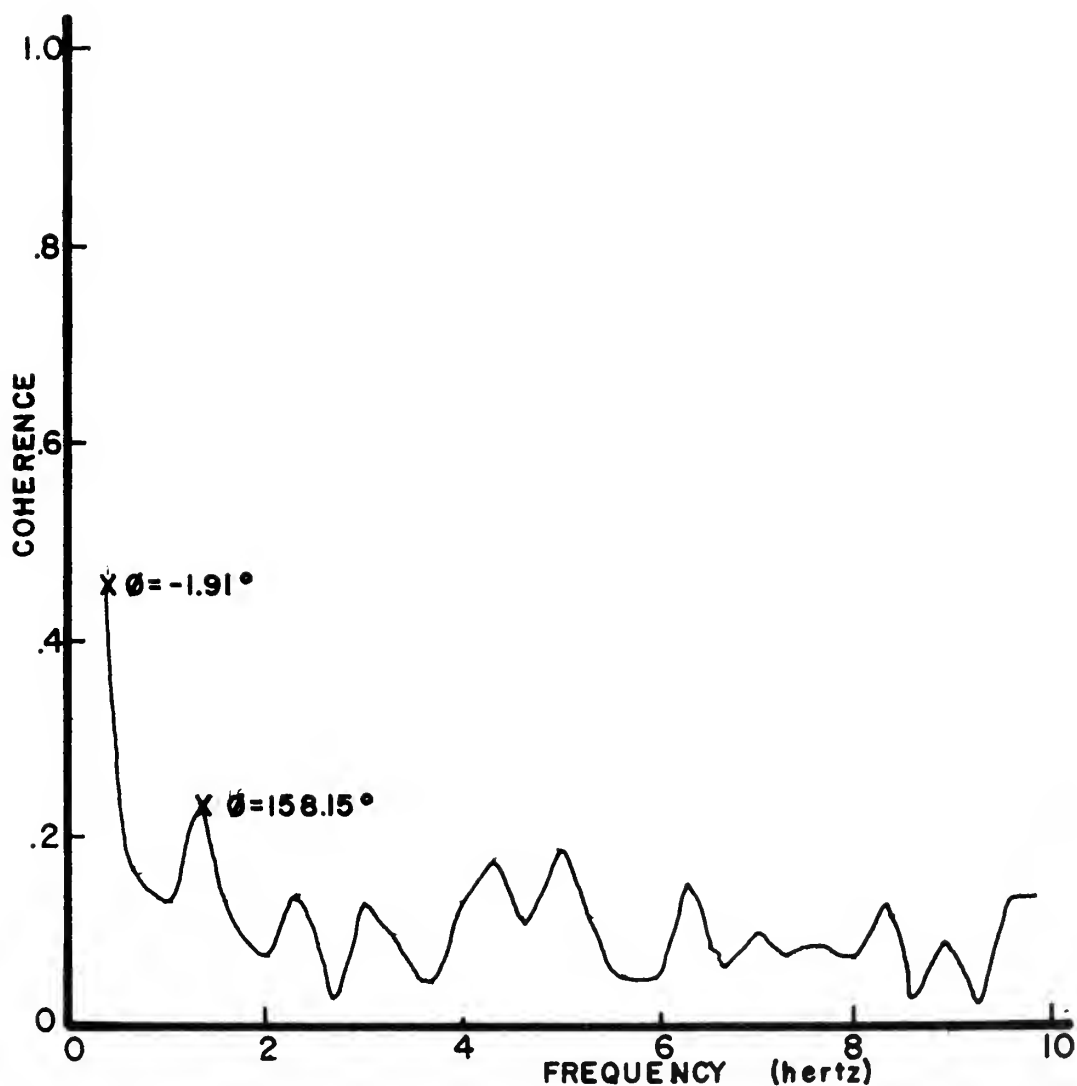


FIG. 46 - CASE 7A- COHERENCE BETWEEN WAVES AND INTER. FLOATING VELOCITY

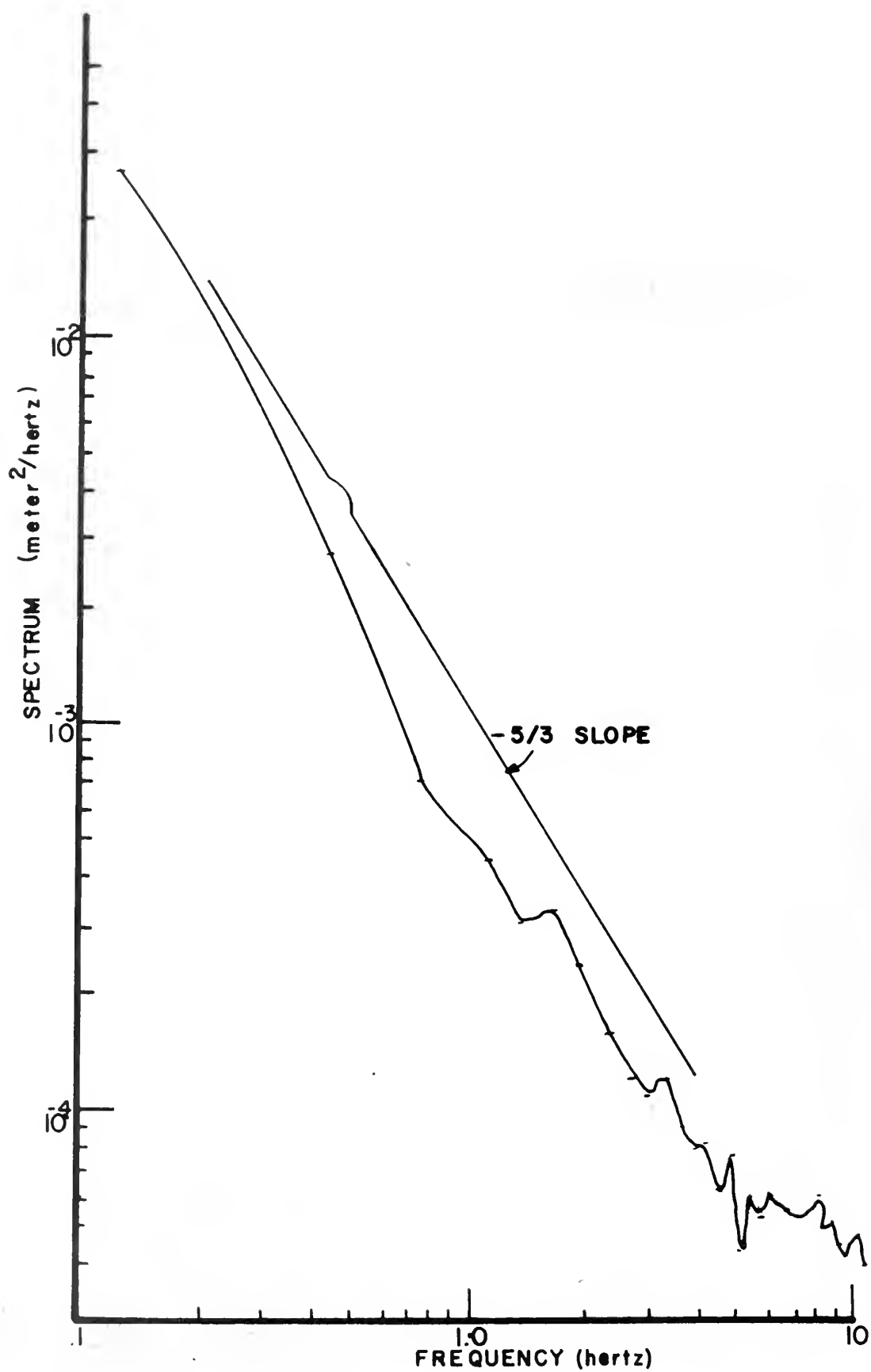


FIG.47 -CASE 7B- SEA SURFACE ELEVATION

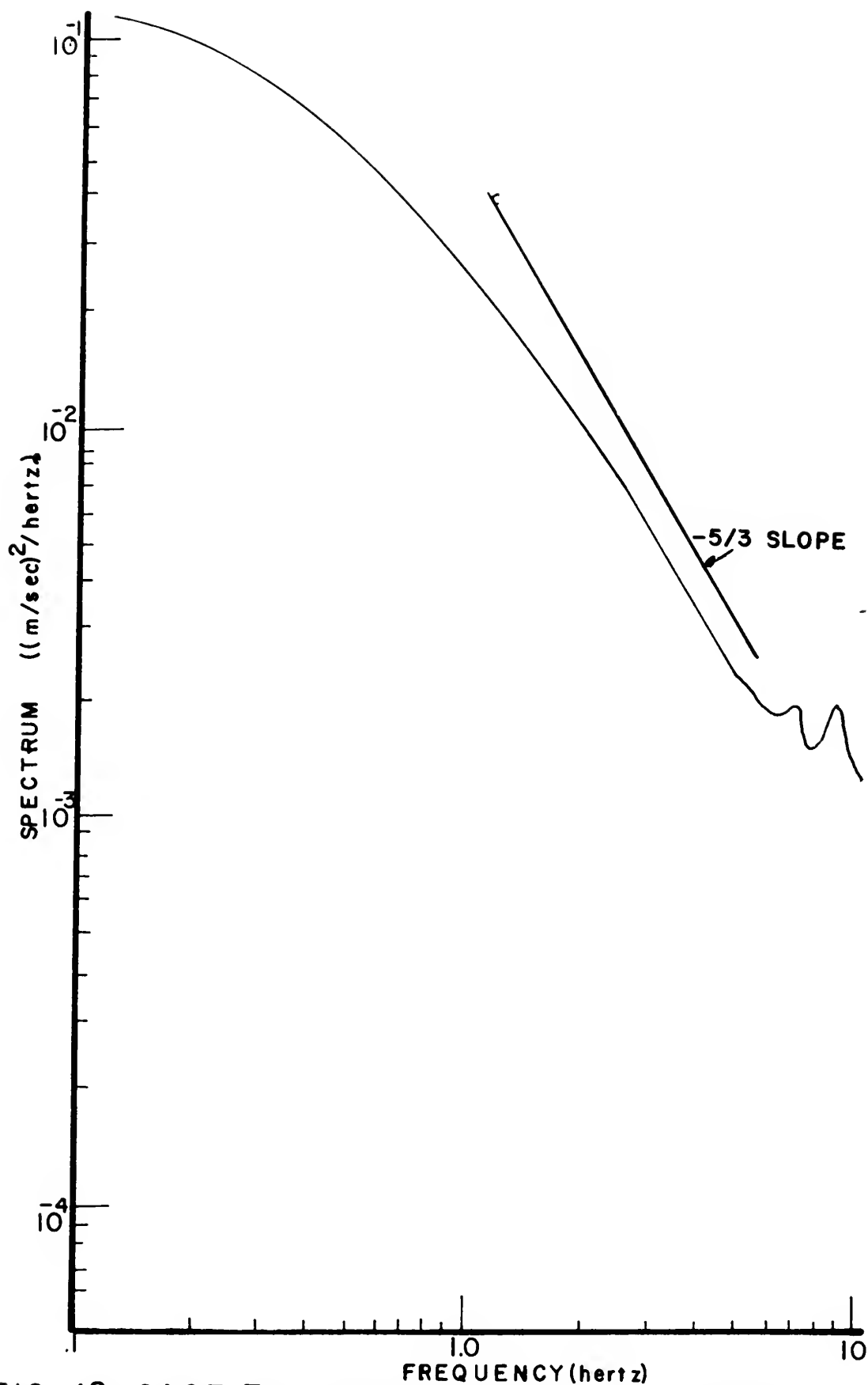


FIG. 48 -CASE 7B- INTER.FLOATING VELOCITY

$\emptyset$  = PHASE ANGLE  
 POSITIVE VALUES MEAN INTER. VELOCITY LAGS WAVES

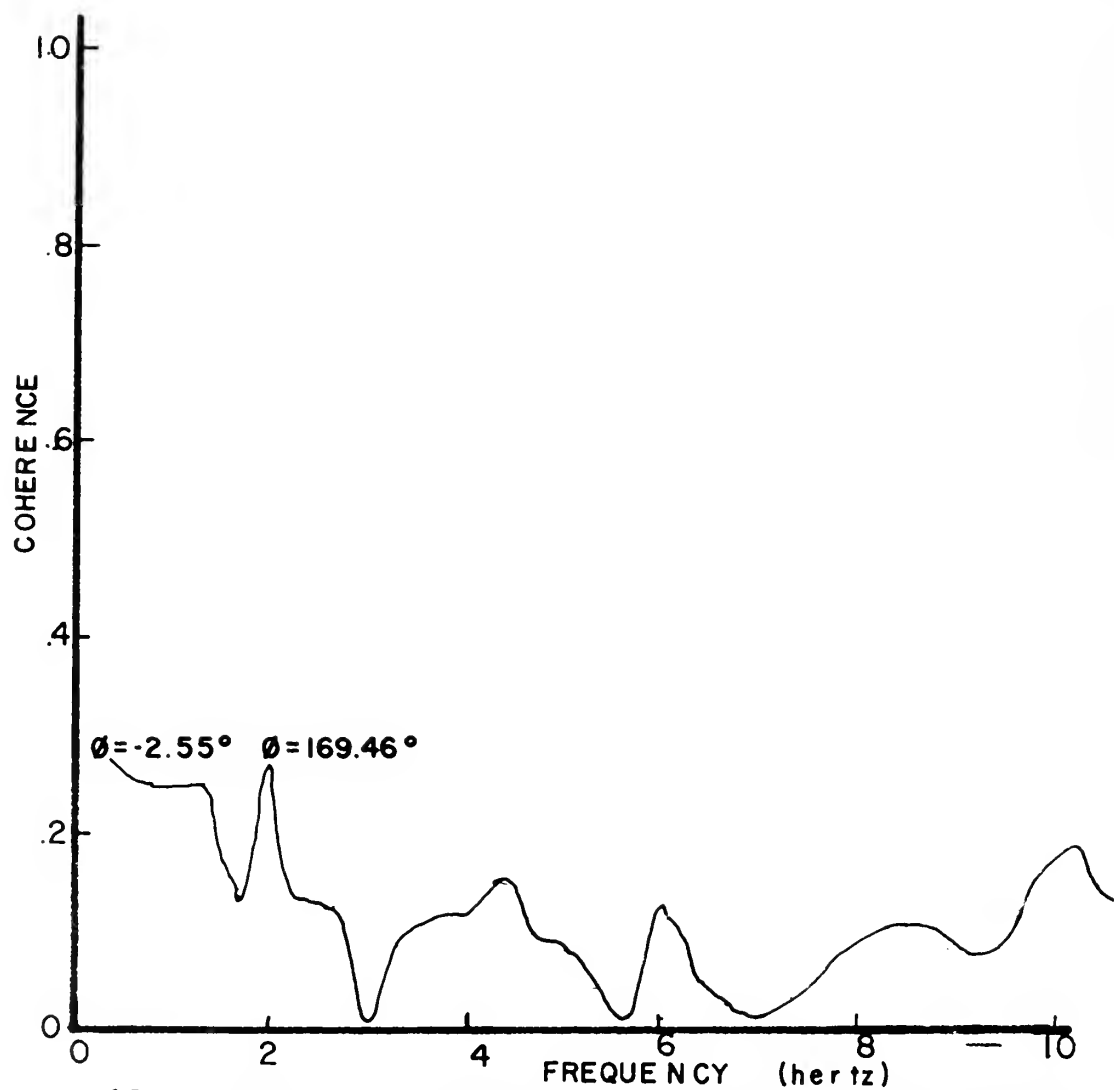


FIG. 49 - CASE 7B- COHERENCE BETWEEN WAVES AND INTER.FLOATING VELOCITY

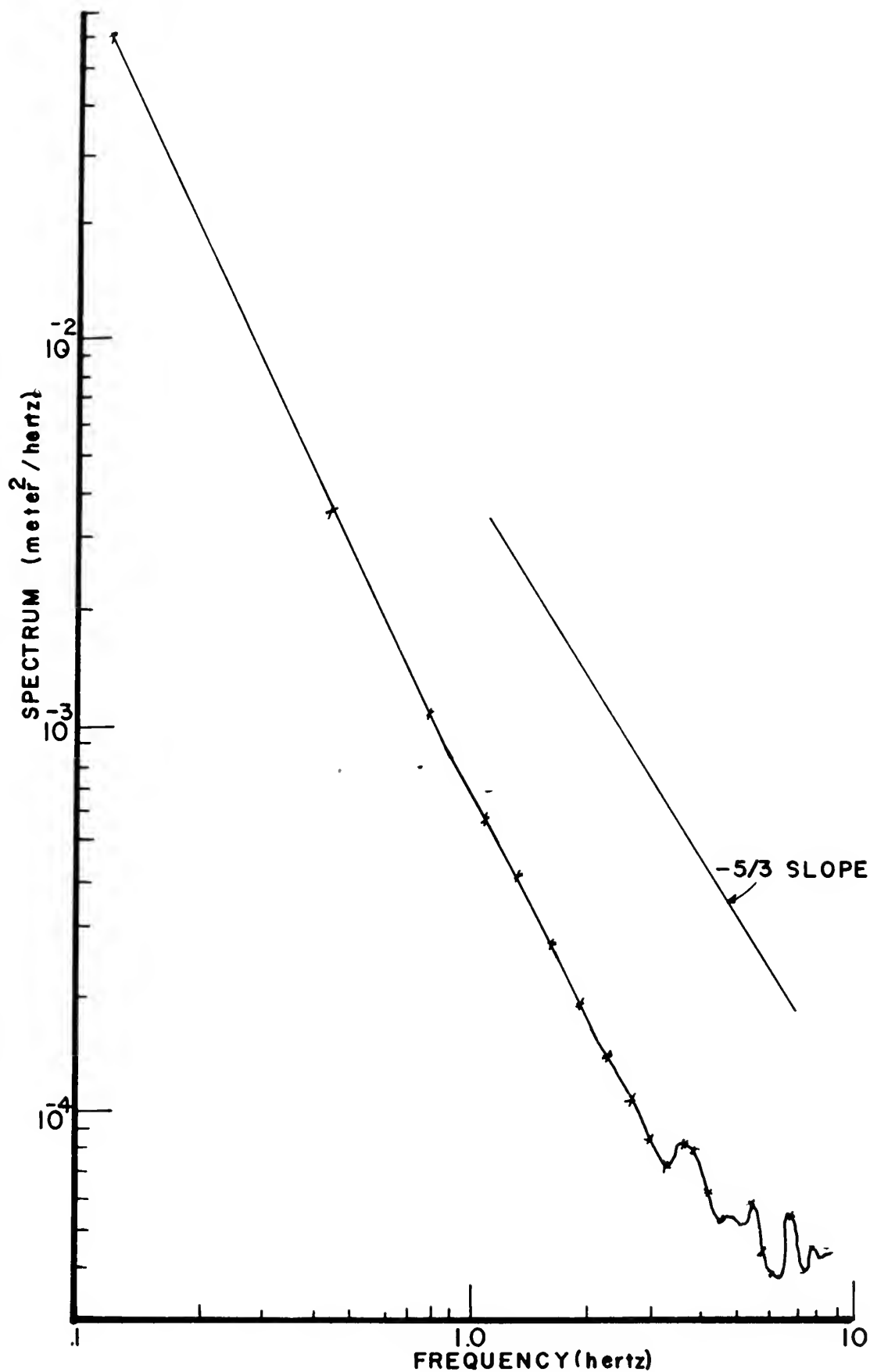


FIG. 50 - CASE 7C - SEA SURFACE ELEVATION

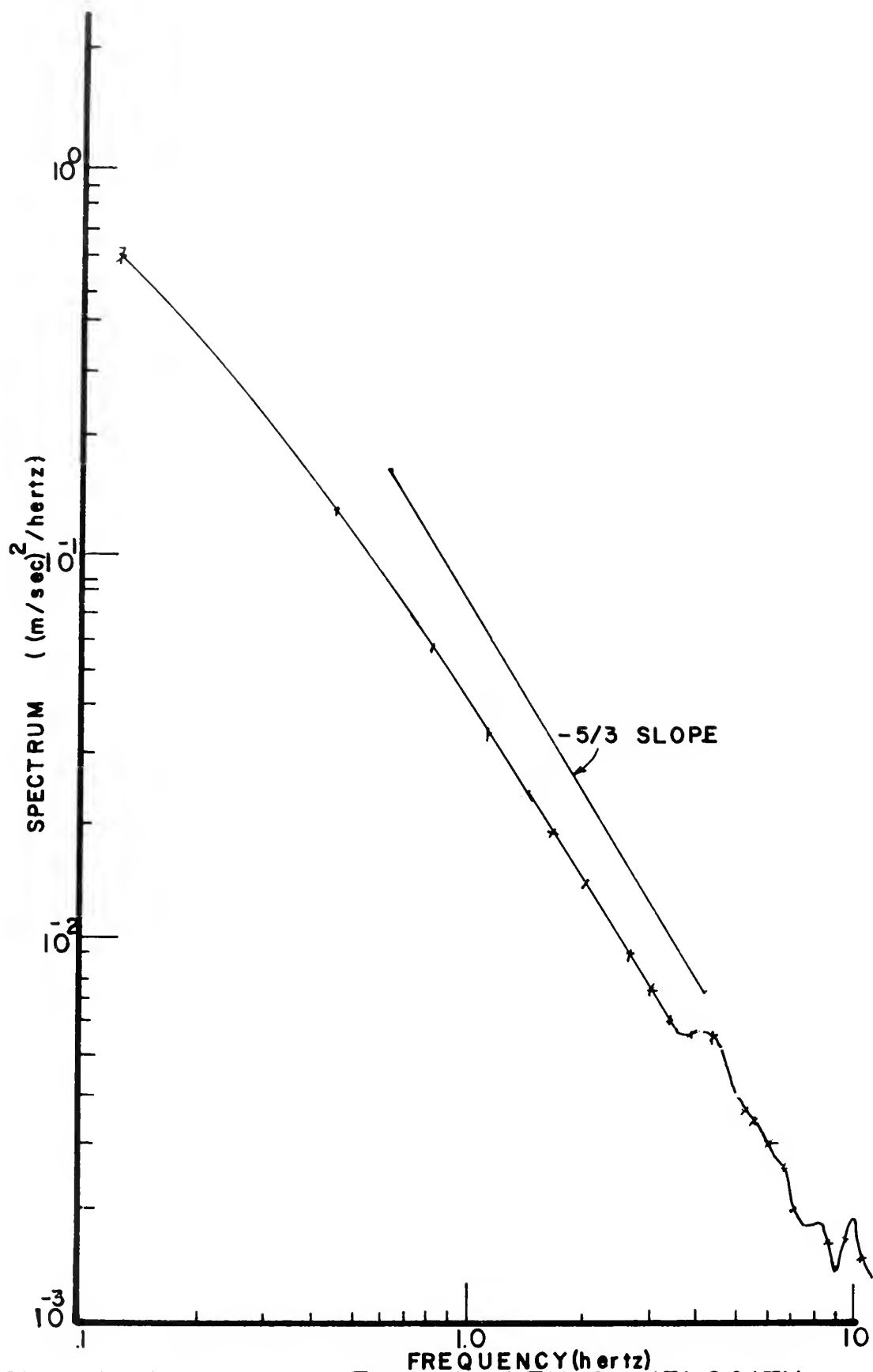


FIG.51 -CASE 7C- INTER. FLOATING VELOCITY



$\emptyset$  = PHASE ANGLE  
 POSITIVE VALUES MEANS VELOCITY LAGS WAVES

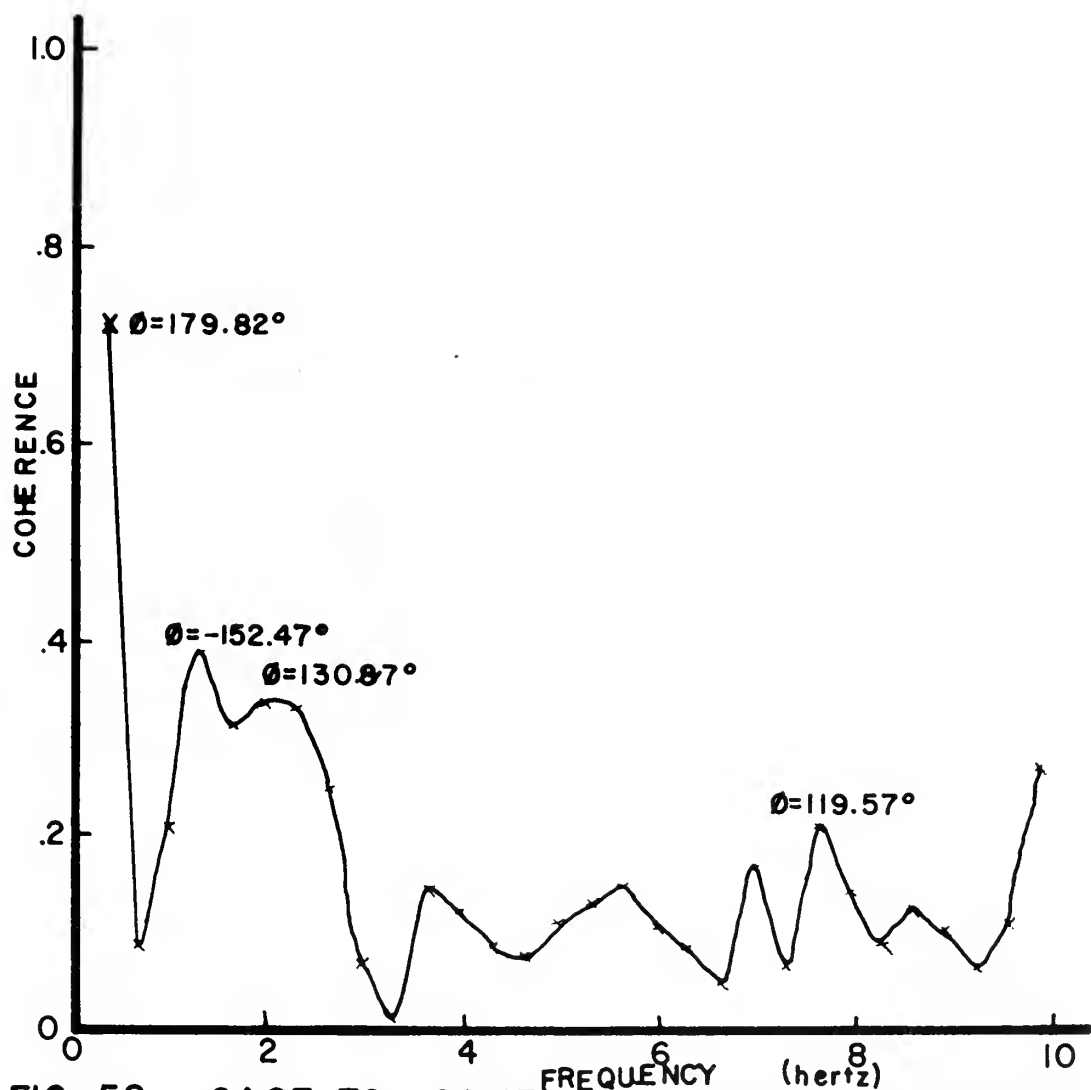


FIG. 52 -CASE 7C- COHERENCE BETWEEN WAVES AND INTER. FLOATING VELOCITY

The environmental information included:

Wind and wave direction  $270^{\circ}$ T

Mean wind speed

1.2 meters above sea surface = 3.57 m/sec

1.5 meters above sea surface = 3.53 m/sec

1.7 meters above sea surface = 3.68 m/sec

2.7 meters above sea surface = 3.80 m/sec

Wet bulb temperature  $16.5^{\circ}\text{C}$

Dry bulb temperature  $18.1^{\circ}\text{C}$

Water temperature  $19.3^{\circ}\text{C}$

Water depth 1.9 meters, tide ebbing

Cloudless sky

Critical height 32.4 cm

As in Case 7, this case (figure 53) confirms the notion that the interaction between wave motion and wind velocity increases at small heights above the sea surface. However, the data does not show a definite break which would be observed if a "cats-eye" was encountered. As in other cases, the velocity spectrum (figures 54 and 55) follows the  $-5/3$  power law, but the wave spectrum slope has become more negative. However, the slope is less negative than expected for the usual wave spectrum. This may be related to wind wave generating conditions that existed during this run.

## I. CASE 9

A hot-film velocity sensor was placed on the wave follower 1 cm above the sea surface. Since splash was considered important, the

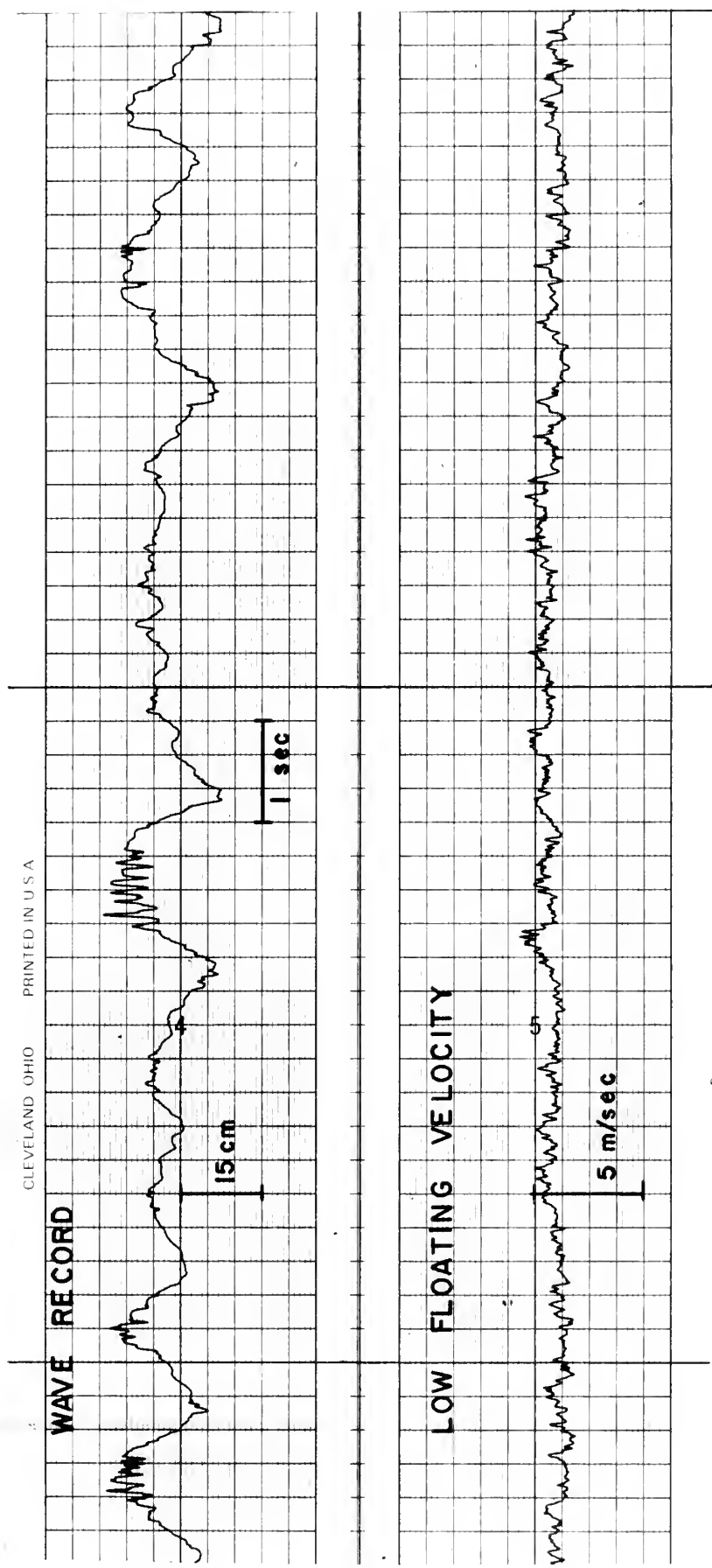


FIGURE-53-SAMPLE RECORD FOR CASE 8

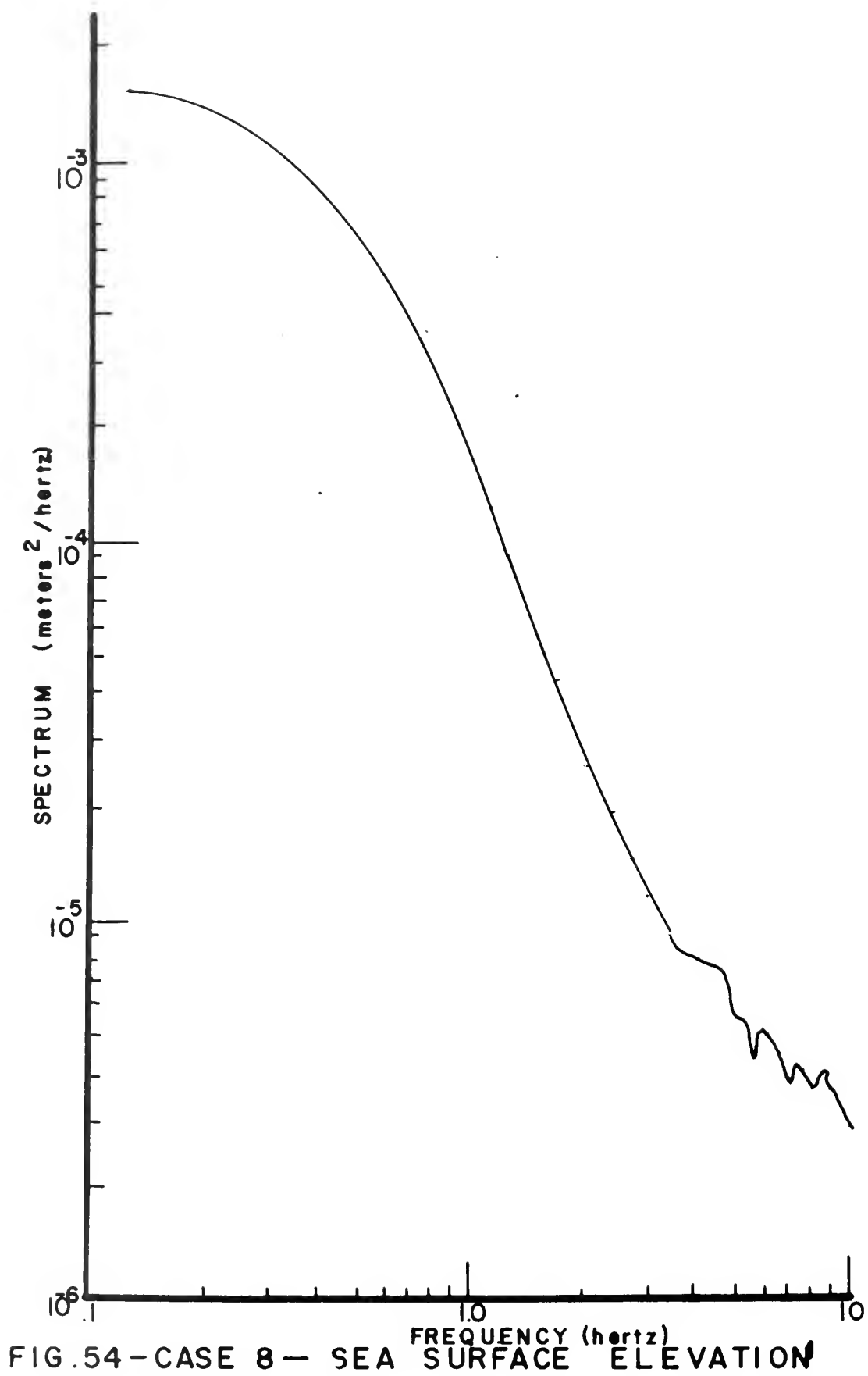


FIG.54-CASE 8-SEA SURFACE ELEVATION

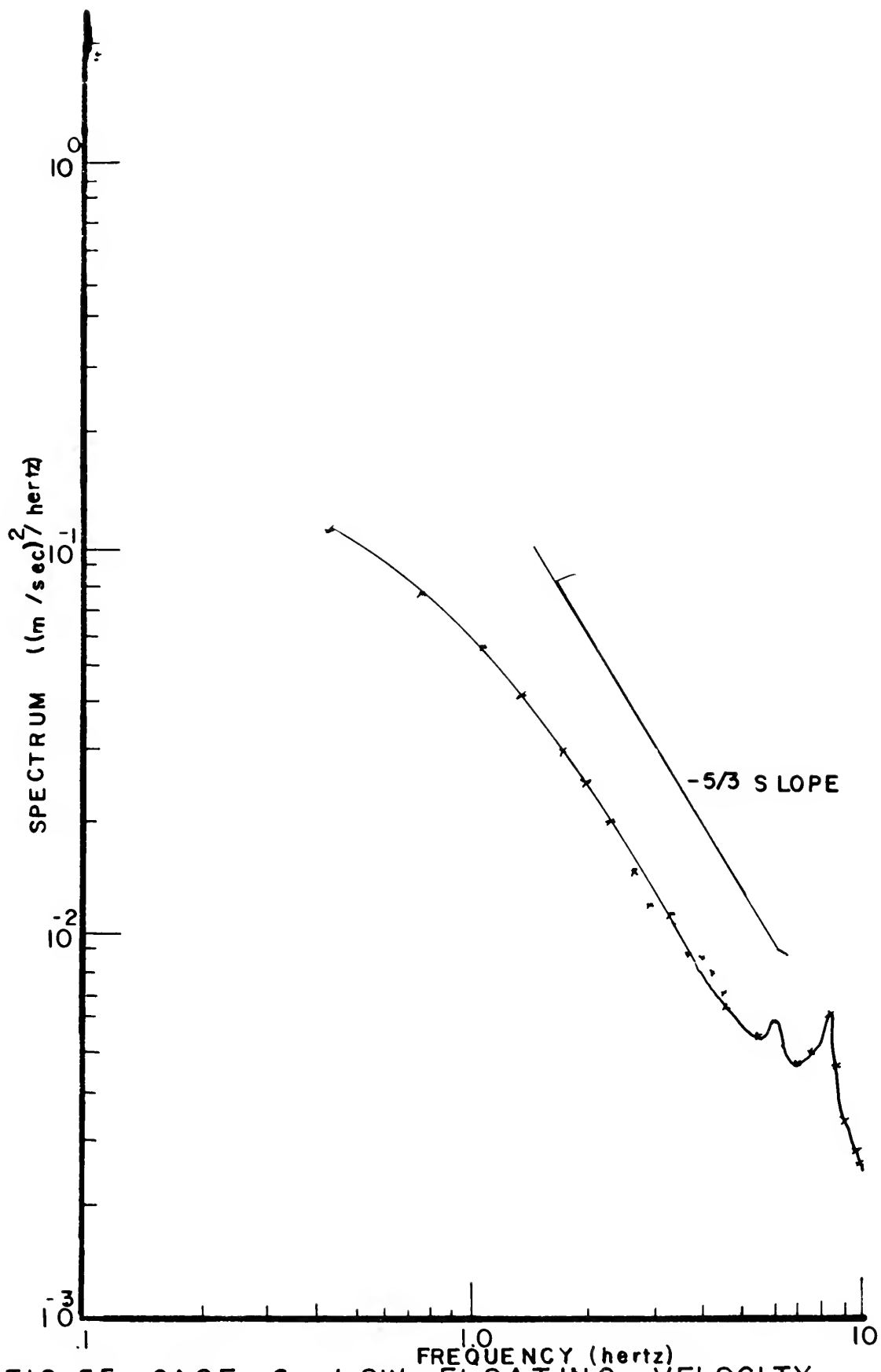


FIG 55 - CASE 8- LOW FLOATING VELOCITY

$\emptyset$  = PHASE ANGLE  
 POSITIVE VALUES MEANS VELOCITY LAGS WAVE

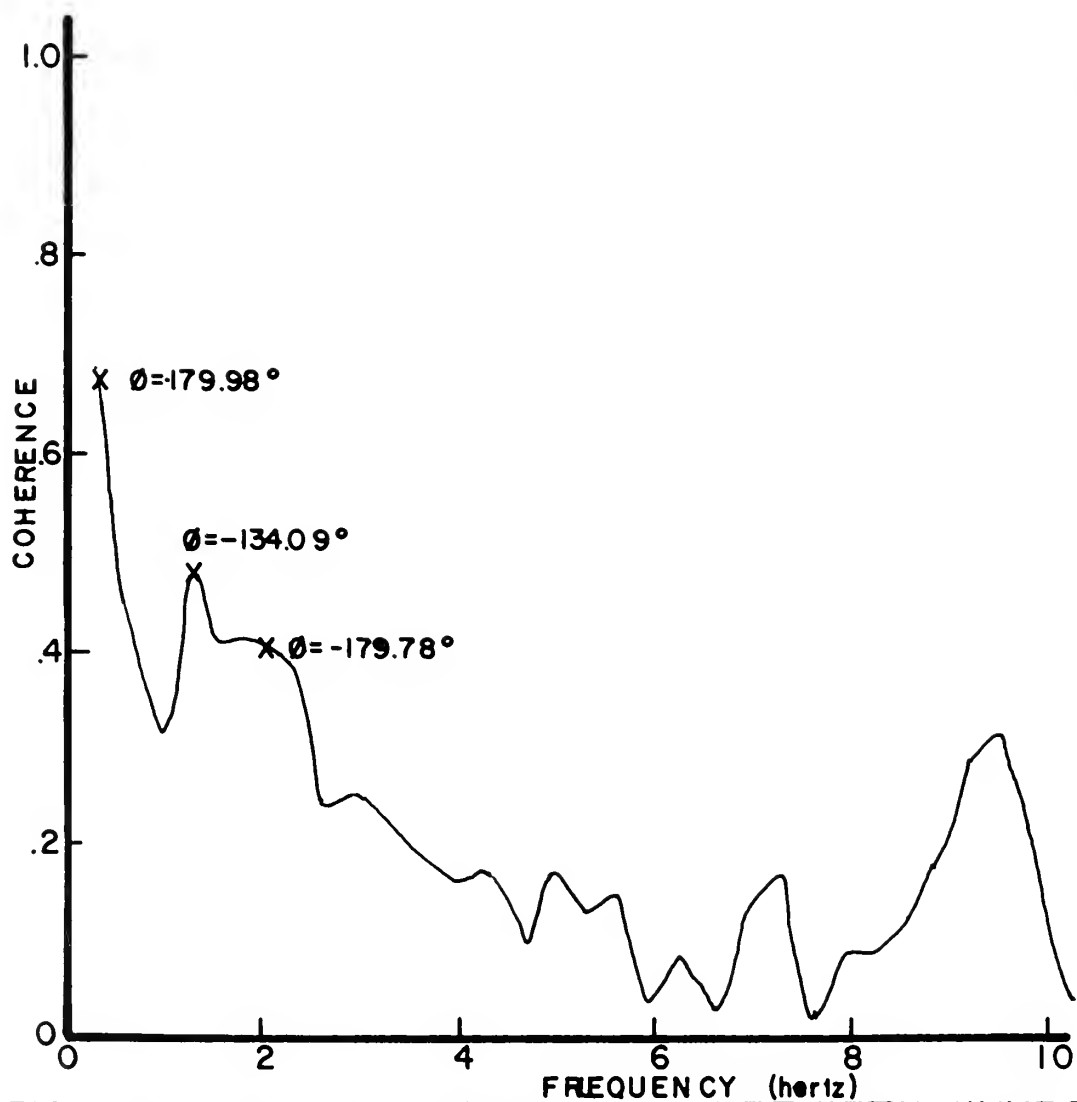


FIG. 56 - CASE 8 - COHERENCE BETWEEN WAVES AND LOW FLOATING VELOCITY

overheat ratio was reduced to one-half the previous value. No breakage problems were encountered. The data for this case were collected between 1232 and 1337 on 23 July 1969. No digital analysis was performed. This case is presented to show that measurements this close to the sea surface can be made successfully.

The environmental information for this case was:

Wind and wave direction 275°T

Mean wind speed

1.2 meters above sea surface = 3.36 m/sec

1.5 meters above sea surface = 3.70 m/sec

1.7 meters above sea surface = 3.50 m/sec

2.7 meters above sea surface = 3.55 m/sec

Wet bulb temperature 17.0°C

Dry bulb temperature 18.6°C

Water temperature 19.7°C

Water depth 1.8 meters, tide ebbing

Clear sky.

Critical height 12 cm above sea surface

Because only analog (P.A.R.) analysis was used, little information was determined from the results produced. Due to the fact that the waves splash the velocity sensor (figure 57), a spike removal routine must be employed if the data is to be digitally or analog analyzed.

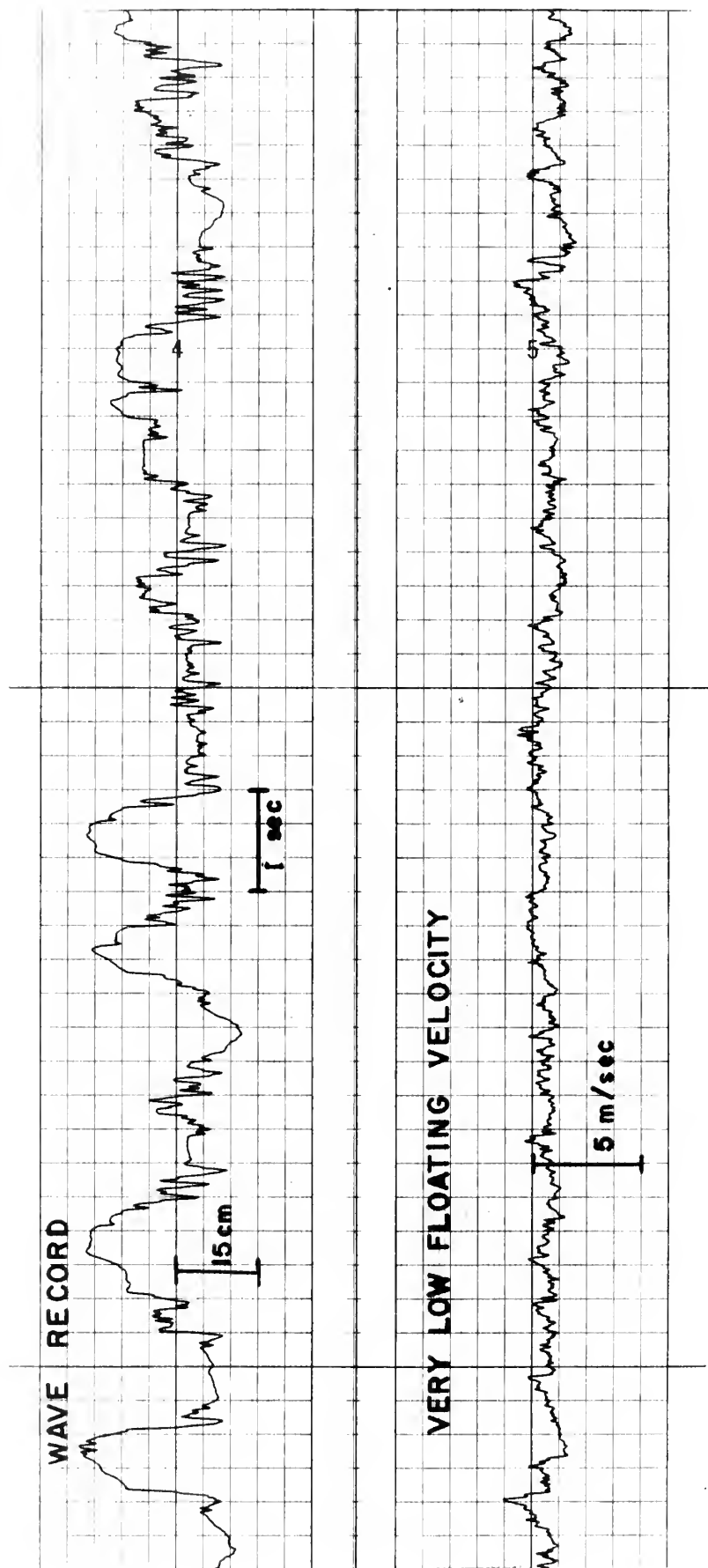


FIGURE-57- SAMPLE RECORD FOR CASE 9



## IX. CONCLUSIONS AND AREAS FOR FUTURE WORK

The results presented in this thesis are of a preliminary nature. Certain features are suggested, but some questions must be answered before any confidence can be placed in them. Perhaps the most puzzling concerns the  $-5/3$  power law behavior of the wave spectrum which was obtained when the wind was actively generating waves. This result is at odds with most theories and almost all observations. The credibility of this result is in question because of the deteriorating signal produced by the follower during these wind wave generation runs. However, a  $-5/3$  power law behavior for the resulting noise would be equally surprising. Clearly, this aspect deserves further attention.

In each case an attempt has been made to estimate a critical height. Ideally, this is the height at which the wave celerity,  $C$ , is equal to the mean wind speed,  $U$ . In fact, the critical height exists only in theory, since for a real sea many wave trains are present causing the critical height to be smeared across the level where  $U$  equals the  $C$  associated with the peak of the wave spectrum. The method used for estimating the critical height was the best that could be obtained for the data that were available. However, it is probably overestimated. F. W. Dobson, working at the same height, has obtained much lower critical heights (private communication). However, if the critical heights reported here are correct, then there seems to be only a weak dependency of the turbulent velocity fluctuations with critical height. This result tends to be in agreement with arguments proposed by Stewart (1967).

In general, the amplitudes of the fluctuations of both temperature and velocity are smaller when these measurements are made at a constant distance from the sea surface (i.e., mounted on the wave follower). The closer measurements are made to the sea surface, the more effect the waves have on them. Clearly, the waves cause appreciable reorganizing the air and temperature fields above the waves.

Whereas the air-sea interaction results of this study are tentative, some definite conclusions can be reached regarding the instrumentation. The outstanding contribution of this study is to show that measurements of turbulent and wave parameters can be made very near the sea surface, specifically at heights less than the wave amplitude above the sea surface. This was accomplished by means of the wave follower. The wave follower used was a preliminary design and as is to be expected, deficiencies became obvious during the Spanish Banks trials. Despite this, usable data were obtained with this instrument. Based on the field experience, an improved design could be used which would improve considerably the quality of both the wave and turbulence data. Such an instrument would open opportunities for a new set of wave-momentum experiments, investigations of momentum and heat flux, and in general investigations of various turbulent exchanges and air-flow occurring very near the sea surface.

The digital analysis was performed on an IBM 360/67 using programs tested and proven by the Institute of Oceanography at the University of British Columbia. The sampling rate was overestimated which limited the extent to which analysis could be extended to low frequencies. If more information is desired at low frequencies, a redigitization of the data at a lower sampling rate would be required.

Since an analog computer was not immediately available, some approximate analyses were attempted with a Princeton Applied Research Fourier Analyzer. The analog data were not entirely suited for this machine. The data records were not long enough and signals were not repeatable (i.e., no tape loops were made). Further, the bandwidth was too small. The spectra produced were not easily interpreted as only a linear plot was possible. The conclusion is that the PAR is not a suitable analog device for the analysis of atmospheric turbulence data or short wave records. A standard analog computer is required.

## BIBLIOGRAPHY

- Batchelor, G. K., "Small scale variations of connected quantities like temperature in a turbulent fluid," Journal of Fluid Mechanics, v. 5, p. 113-133, 1959.
- Bendat and Piersol, Measurement and Analysis of Random Data, Wiley Publications, New York, N. Y., 1966.
- Jeffreys, H., "On the formation of waves by wind," Proc. of the Royal Society, A 107, p. 189-206, 1924.
- Makova, V. I., "Relation between the atmospheric turbulence spectra in the lower levels over the sea and the spectrum of surface waves," OKEANOLOGIA, v. 5, No. 4, p. 592-605, 1963.
- Miles, J. W., "On the generation of surface waves by shear flow," Journal of Fluid Mechanics, v. 3, p. 185-204, 1957.
- Miles, J. W., "On the generation of surface waves by shear flow," Journal of Fluid Mechanics, v. 6, p. 568-582, 1959.
- Miles, J. W., "On the generation of surface waves by turbulent shear flow," Journal of Fluid Mechanics, v. 7, p. 469-478, 1960.
- Miles, J. W., "On the generation of surface waves by turbulent shear flows, Part 4," Journal of Fluid Mechanics, v. 13, p. 433-448, 1962.
- Miles, J. W., "A note on the interaction between surface waves and wind profile," Journal of Fluid Mechanics, v. 22, p. 823-827, 1965.
- Miles, J. W., "A note on the interaction between surface waves and wind profiles, Part 5," Journal of Fluid Mechanics, v. 30, p. 163-175, 1967.
- Phillips, O. M., "On the generation of waves by turbulent wind," Journal of Fluid Mechanics, v. 2, p. 417-445, 1957.
- Pond, S. et. al., "Spectra of velocity and temperature in the atmospheric boundary layer over the sea," Journal of the Atmospheric Sciences, v. 23, p. 376-383, 1966.
- Pond, S., Stewart, S. D., and Burling, R. W., "Turbulent spectra in the wind over waves," Journal of the Atmospheric Sciences, v. 20, No. 4, p. 319-324, 1963.
- Princeton Applied Research Corporation, "Instruction manual for the model 102 Fourier analyzer," Princeton, N. J., 1968.

- Ramzy, J. R. and Young, E. T., "Investigation of temperature fluctuations near the air-sea interface," Unpublished Master's Thesis, Naval Postgraduate School, Monterey, California, December 1968.
- Seesholtz, J. R., "A field investigation of air flow immediately above ocean surface waves," Unpublished Doctor's Thesis, Massachusetts Institute of Technology, Cambridge, Mass., May 1968.
- Smith, S. D., "Thrust anemometer measurement of wind velocity spectra and Reynolds stress over a coastal inlet," Journal of Marine Research, v. 25, No. 3, p. 239-262, 1967.
- Stewart, R. W., "Mechanics of air-sea interface," The Physics of Fluid Supplement, v. 10, p. 547-555, 1967.
- Wilson, R. J., Boston, N. E. J., and Denner, W. W., "Digital analysis of turbulence data on the IBM 360/67 at the Naval Postgraduate School," Naval Postgraduate School publication NPS-58 DW 9071A, 1969.

# INITIAL DISTRIBUTION LIST

	No. Copies
1. Defense Documentation Center Cameron Station Alexandria, Virginia 22314	20
2. Library Naval Postgraduate School Monterey, California 93940	2 1
3. Naval Weather Service Command Washington Navy Yard Washington, D. C. 20390	1
4. Director Naval Research Laboratory Attn: Tech. Services Info. Officer Washington, D. C. 20390	1
5. Department of Oceanography, Code 58 Naval Postgraduate School Monterey, California 93940	3
6. Department of Meteorology, Code 51 Naval Postgraduate School Monterey, California 93940	1
7. Oceanographer of the Navy The Madison Building 732 N. Washington Street Alexandria, Virginia 22314	1
8. Naval Oceanographic Office Attn: Library Washington, D. C. 20390	1
9. National Oceanographic Data Center Washington, D. C. 20390	1
10. Director, Maury Center for Ocean Sciences Naval Research Laboratory Washington, D. C. 20390	1
11. Professor Noel E. J. Boston Department of Oceanography Naval Postgraduate School Monterey, California 93940	10

	No. Copies
12. Professor Warren W. Denner Department of Oceanography Naval Postgraduate School Monterey, California 93940	1
13. Lt.(jg) G. M. Davis, USN Student, Nuclear Power School (Class 69-3) Mare Island Naval Shipyard Vallejo, California	3
14. Dr. R. W. Burling Institute of Oceanography University of British Columbia Vancouver 8, British Columbia Canada	1
15. Mr. David Lindquist Department of Physics University of British Columbia Vancouver 8, British Columbia Canada	1
16. Dr. Russell L. Snyder Institute of Oceanography Nova University Fort Lauderdale, Florida	1
17.. Dr. P. Michael Davis Route 1, Windmill Park Nicholasville, Kentucky 40356	1
18. Mr. Paul G. Davis 2832 N. E. 26th Street Fort Lauderdale, Florida 33305	1





## DOCUMENT CONTROL DATA - R &amp; D

(Security classification of title, body of abstract and indexing annotation must be entered when the overall report is classified)

1. ORIGINATING ACTIVITY (Corporate author)  Naval Postgraduate School Monterey, California 93940		2a. REPORT SECURITY CLASSIFICATION  Unclassified	
3. REPORT TITLE  Measurement of Air Temperature and Wind Velocity from One to Eighty Centimeters Above the Sea Surface		2b. GROUP	
4. DESCRIPTIVE NOTES (Type of report and inclusive dates)  Master's Thesis; October 1969			
5. AUTHOR(S) (First name, middle initial, last name)  Gary Malcolm Davis			
6. REPORT DATE  October 1969	7a. TOTAL NO. OF PAGES  109	7b. NO. OF REFS  19	
8a. CONTRACT OR GRANT NO. NAVORD CONTRACT ORD TASK-03C-005/551-1/UR104-03-01 b. PROJECT NO.		9a. ORIGINATOR'S REPORT NUMBER(S)	
c.  d.		9b. OTHER REPORT NO(S) (Any other numbers that may be assigned this report)	
10. DISTRIBUTION STATEMENT  This document has been approved for public release and sale; its distribution is unlimited.			
11. SUPPLEMENTARY NOTES  Completed under Professors Boston, Denner, and Green under contract to Naval Ordnance Systems Command, Wash., DC		12. SPONSORING MILITARY ACTIVITY  Naval Postgraduate School Monterey, California 93940	
13. ABSTRACT  A wave following mechanism was designed and tested at the field station operated by the Institute of Oceanography of the University of British Columbia.  Separate measurements were made of temperature and velocity fluctuations by sensors attached to the vertically moving follower arm at heights of 1 cm, 5 cm, 24 cm, and 78 cm above the sea surface. These data were analyzed both by analog and digital methods. While the data generally follow the -5/3 power law proposed by Kolmogorov, there are significant departures from existing theories which could prove important.  Since most air-sea interactions take place below 30 cm and few measurements have been made below this level, the wave follower could be a useful tool in investigating near surface phenomena.			

14

## KEY WORDS

## LINK A

## LINK B

## LINK C

ROLE

WT

ROLE

WT

ROLE

WT

oceanography, marine science, air-sea  
interaction, oceanographic instrumentation,  
measurement near the sea surface, random data  
analysis







thesD16958

Measurement of air temperature and wind



3 2768 002 09593 7

DUDLEY KNOX LIBRARY